2015

Drilled Shaft Skin Resistance Design in the Cooper Marl

William J. Gieser
University of South Carolina

DRILLED SHAFT SKIN RESISTANCE DESIGN IN THE COOPER MARL

by

William J. Gieser

Bachelor of Science
Georgia Institute of Technology, 2009

Submitted in Partial Fulfillment of the Requirements

For the Degree of Master of Science in

Civil Engineering

College of Engineering and Computing

University of South Carolina

2015

Accepted by:

Sarah L. Gassman, Director of Thesis

Charles E. Pierce, Reader

Lacy Ford, Senior Vice Provost and Dean of Graduate Studies

DEDICATION

To my grandfather, Herbert P. Gieser, who always believed in hard work and education.

ACKNOWLEDGEMENTS

Throughout the process of research and writing, I have received a lot of help along the way. I would first like to thank all the teachers who have taught me along the way from kindergarten until the last class I took at the University of South Carolina. Every one of you has contributed something that helped in this task. For my time at the University of South Carolina, I would like to thank Dr. Chunyang Liu, Dr. Nathan Huynh, Dr. Nicole Berge, Dr. Michelle Maher, Dr. Charles Pierce, and Dr. Mike Meadows. All of you taught me while I was at the university and I truly appreciate it. In particular, I would also like to thank Dr. Sarah Gassman who was my academic advisor and thesis advisor in addition to a class professor. I really appreciate your patience with me throughout this process and your willingness to answer as many questions as it took for me to learn in the four classes you taught me as well as the thesis work.

In the preparation of this thesis, I would like to thank Zane Abernethy for helping me with the engineering logic and local engineering and construction history, James "Ricky" Wessinger and Dr. Will Doar, III for helping with the geologic research and review, and Chris Gaskins and Jon Sinnreich for providing me with the load test data used in the analysis. Without all of you, this research would not have been possible.

Finally, but not least, I would like to thank my friends and family for their support through the entire graduate school process. Sometimes, someone telling you that you have their support is as important as someone telling you how to solve the problem.

ABSTRACT

As drilled shafts have become a more popular foundation type in the Charleston, South Carolina area, there has been an ongoing goal of optimizing drilled shaft design while maintaining the structural integrity of the foundation. In the Charleston area, the primary bearing stratum for deep foundations is the Cooper Marl, a calcareous Oligocene formation. Research performed from 2002 to 2004 on load test data from drilled shafts constructed in the Cooper Marl and soil properties from three test sites for the Cooper River Bridge explored the relationship between the measured skin resistance and geotechnical properties. In the 15 years since the load tests for the Cooper River Bridge were performed, additional load tests have been performed throughout the Charleston area. Evaluation of this load test data, the Cooper River Bridge load test data, and earlier load test data allows better understanding of drilled shaft skin resistance in the Cooper Marl as well as the ability to use in-situ geotechnical properties to better predict axial capacity when a load test is not performed. Drilled shafts founded in the Cooper Marl are designed primarily for using skin resistance and LRFD design methodologies and load factors.

Using data from 27 drilled shaft load tests at 15 test sites in the Cooper Marl, the relationships between load test measured unit skin resistance and undrained shear strength, overburden pressure, and SPT N-values were evaluated. The distribution of unit skin resistance with elevation was also studied across the Cooper Marl. To derive a design unit skin resistance for use when a load test is not feasible, a statistical method

evaluating the 97.5% confidence interval and the historical load test method were used. Finally, an empirical method was used to verify the LFRD resistance factor currently required for design in the Cooper Marl.

Based on the performed analyses, there is not a correlation between unit skin resistance and SPT N-values. Across the Cooper Marl, the unit skin resistance distribution was found to be constant with depth up to -80 ft-MSL. When evaluating the relationship between undrained shear strength and unit skin resistance, the α-value was found to be 0.85, which is approximately 60% larger than the α values for clay presented in the literature. Based on the load test data, a design unit skin resistance of 3.2 ksf is supported using the historical load test method and a unit skin resistance of 2.88 ksf is supported using the 97.5% confidence interval method for typical sites. Additionally, the current resistance factor for LRFD design of 0.45 is data supported. Finally, although the Cooper Marl is treated as a homogeneous formation, there are known geologic discontinuities that should be accounted for during design.

TABLE OF CONTENTS

LIST OF TABLES

LIST OF FIGURES

LIST OF SYMBOLS

A	Shaft segment surface area
B	Shaft diameter
COV	Coefficient of variation
DL	Dead load
FS	Factor of safety
f_s	Unit skin resistance
f_{SN}	Nominal unit side resistance
LL	Live load
K_r	Ratio of mean value to characteristic value
N_{60}	N-value corrected for hammer energy ratio
P_a	Atmospheric pressure
Q	Total load / allowable working load / factored load
Q_D	Nominal value of dead load
Q_L	Nominal value of live load
Q_i	Unfactored axial load
R^2	Coefficient of determination
R_n	Nominal resistance
R_r	Factored resistance
R_{SN}	Nominal side resistance
S_u	Undrained shear strength

V_r Coefficient of variation for geotechnical resistance

α Skin resistance coefficient

β Reliability index

γ_D Mean of the bias values for the dead load
γ_{DL} Load factor for dead load

γ_i Load factor

γ_{LL} Load factor for live load, mean of the bias values for the live load

γ_R Mean of the bias values for resistance

Δz Thickness of soil layer

η_i Load modifier

θ Separation coefficient

φ Resistance factor

List of Abbreviations

AASHTO .....American Association of State Highway and Transportation Officials

ASD.....Allowable Stress Design

ASTM ..... American Society for Testing and Materials

bpf.....Blows per Foot

CAPWAP..... Case Pile Wave Analysis Program

CPT .....Cone Penetration Test

CSL .....Cross-hole Sonic Logging

FAT ..... First Arrival Time

FHWA.....Federal Highway Administration

ft-MSL.....Feet – Mean Sea Level

GDM .....Geotechnical Design Manual

ksf..... Kips per Square Foot

LRFD .....Load and Resistance Factored Design

pcf .....Pounds per Cubic Foot

psi..... Pounds per Square Inch

PDA..... Pile Driving Analyzer

PIT.....Pile Integrity Test

SCDOT .....South Carolina Department of Transportation

SPT..... Standard Penetration Test

TIP.....Thermal Integrity Profiling

USGS .....United States Geologic Survey

CHAPTER 1

INTRODUCTION

1.1 - Purpose of Research

As drilled shafts have become a more popular foundation type in the Charleston, South Carolina area, there has been an ongoing goal of optimizing drilled shaft design while maintaining the structural integrity of the foundation. An effective method of optimizing drilled shaft length is by performing a drilled shaft load test at the construction site to verify the design parameters used to represent the underlying soils. In the Charleston area, the primary bearing stratum is the Cooper Marl, a calcareous sedimentary deposit. This stratum is an Oligocene age formation that is only found in the coastal plain of South Carolina and is primarily concentrated in the Charleston area.

Currently, the South Carolina Department of Transportation (SCDOT) uses Load and Resistance Factored Design (LRFD) methods for drilled shaft analysis and design. This design method applies a geotechnical resistance factor to the expected shaft resistance to account for geotechnical uncertainty and construction defects. LRFD allows for a reduced geotechnical resistance factor for sites where a load test is performed, as a load test reduces the geotechnical uncertainty. However, as load tests are relatively expensive, this is not a feasible option for smaller bridges. For these smaller bridges, empirical design methods or load test results from similar sites are used to represent design foundation resistance. However, these two methods require the use of a higher geotechnical resistance factor than a site where a load test was performed due to the

additional geotechnical uncertainty. The reduction in the geotechnical resistance factor provided by load testing allows for drilled shafts to be shorter as the load test reduces the uncertainty in the geotechnical resistance. Because of this, knowledge of geotechnical resistance is critical to optimizing drilled shaft design and, in turn, maximizing cost savings.

Existing load test data, geotechnical field investigations, and knowledge of the area geology can be utilized to better define the expected soil behavior for drilled shaft construction. The primary goal of this thesis is to provide design engineers with data and analysis that will help improve the design of drilled shaft supported bridges where load tests are not performed and improve the preliminary design of bridges where load tests will be performed. This will be accomplished by evaluating the relationship between load test measured resistance and its correlation to in-situ testing, compiling load test data to derive data-supported soil resistance values in the Cooper Marl, and seeing if the geotechnical resistance factors that are used for drilled shaft construction, which are based on load tests in many soil formations, are applicable in the Cooper Marl. Some previous research into these topics has been performed, with the majority of the data coming from the Cooper River Bridge test sites. This included research into the effects of construction techniques on skin resistance, the effect of vertical effective stress on skin resistance, and comparing multiple empirical methods for estimating skin resistance to load test measured skin resistance. Currently, the majority of bridge foundation designs in this area that do not involve load testing are based on area specific common engineering practice instead of using empirical design methods.

Previous research conducted by Camp (2004) on the relationship between vertical effective stress and skin resistance, which did not show a direct correlation to unit skin resistance. However, there is limited information regarding the relationship between in-situ testing and unit skin resistance, with most of the relationships being based on testing at the Cooper River Bridge. Additionally, there is little to no published research regarding reasonable geotechnical resistance values in the Cooper Marl or if the resistance factors that are presented in the 2010 FHWA Drilled Shaft Design Guide are applicable to drilled shafts constructed in the Cooper Marl.

1.2 - Research Questions

Based on the available drilled shaft load test data in the Charleston, South Carolina area, this study seeks to answer three primary questions:

1. Is there a relationship between geotechnical in-situ testing/properties and drilled shaft load test measured skin resistance values in the Cooper Marl?
2. Based on the obtained load test results in the Cooper Marl, what would an appropriate drilled shaft unit skin resistance be for sites where a load test is not performed when effects from construction methods, load test type, and depth are taken into account?
3. Based on the obtained load test results in the Cooper Marl, what is an appropriate LRFD resistance factor for sites where a load test is not performed?

1.3 - Document Organization

Following the Introduction in Chapter 1, Chapter 2 will introduce the geology of the Charleston, South Carolina area as well as address the engineering properties of the Cooper Marl. Chapter 3 will address the history of drilled shaft construction, construction methodologies, load testing and load test interpretation, empirical drilled shaft design in clays, and resistance factor development and evaluation. Chapter 4 will present the data that will be used for the analysis and Chapter 5 will discuss the analysis methodology. Chapter 6 will present the analyses of the data. Chapter 7 will summarize the work presented in the thesis and offer conclusions based on this work. Paths for future research will also be proposed.

CHAPTER 2

LOCAL GEOLOGY

2.1 - Introduction

This chapter is a general summary of the area geology for this thesis. Included is historical information regarding the geological history, geological classification, and geographical distribution of the Cooper Marl. In addition, the physical properties are discussed as well as known discontinuities and anomalies in the geologic formation.

2.2 - Cooper Marl Geological History and Geologic Classification

For this study, the Cooper Marl Formation is the formation to be analyzed. The name Cooper Marl is a colloquial term used in early phosphate resource geologic reports (e.g. Rogers, 1913; Malde, 1959; Heron, 1962) to describe what is technically classified as the Ashley Member of the Cooper Group (Duncan et al., 1983). An early agriculture report refers to the formation as the "Marl of Ashley and Cooper Rivers and their Branches" as part of the "Great Carolinian Bed of Marl", which includes formations from the Savannah River to the Pee Dee River area (Ruffin, 1843), and as "Ashley Marl" in an early phosphate resource report (Holmes, 1870). Going further back, a report makes mention of fossils found during the construction of a canal between the Santee River and the Cooper River thought to be phosphoric in nature (Drayton, 1802), which is consistent with the interface between the Cooper Marl and the surficial sediments (Holmes, 1870).

It is important to note the Cooper Marl, while part of the Cooper Group, is not the only geologic formation found in the Cooper Group. Other members include the Ocala Limestone and the Harleyville Member, both of which exhibit different physical properties than the Cooper Marl (Duncan et al., 1983). While no mention of Cooper Marl or any soil sharing its characteristics is specifically found in Drayton's (1802) report, phosphate resources in this area are typically encountered as fossils or nodules that sit between the marl and the Holocene to Miocene age surficial sediments (Malde, 1959). These surficial sediments are considered to be part of the Hawthorne Formation and/or the Waccamaw Formation that overlay the Cooper Marl, which is Oligocene in age (Malde, 1959; Duncan et al., 1983; Weems and Lewis, 2002), but was considered Eocene in age by some early resources (Rogers, 1913; Cooke, 1936). Although the presence of Duplin Marl, another Miocene age formation, is indicated as geologically possibly existing above the Cooper Marl (Malde, 1936), it is not readily encountered or properly identified in the Charleston area. There are only a few sporadic outcrops of Duplin Marl in Berkeley County and Dorchester County, with the majority of it likely being eroded by river meandering as well as regression and transgression of sea levels (Cooke, 1936; Weems and Lewis, 2002).

2.3 - Cooper Marl Geographical Distribution

Cooper Marl, as its name implies, was first encountered in the area around the Cooper River and south to the Ashley River (Ruffin, 1843). The full extent of the Cooper Marl is reasonably well defined by geotechnical investigations and geological explorations. The first extensive range description was by Cooke (1936) and confirmed by Heron (1962), which indicated that Cooper Marl was found in Allendale, Bamberg,

Berkeley, Charleston, Colleton, Dorchester, and Orangeburg Counties. In 1983, full length cross sections of the state were presented, which altered this distribution (Duncan et al., 1983). Based on these cross sections, Cooper Marl was not encountered in Allendale or Bamberg and only found in small parts of Colleton and Orangeburg Counties. What was termed Cooper Marl in these areas was likely marl in the Hawthorne Formation with similar visual characteristics, but different mineralogy or fossil composition or other members of the Cooper Group.

In terms of thickness, as with most coastal plain formations, the Cooper Marl dips and increases in thickness as it approaches the Atlantic Ocean. At its thickest, the Cooper Marl is estimated to be 250 to 300 feet thick based on deep well logs (Ruffin, 1843, Malde, 1959) and deep geologic borings (Duncan et al., 1983). Extensive geological borings around the Charleston area, presented by Weems and Lewis (2002), support the general area distribution described by Duncan (1983). Figure 2.1 is an excerpt from one of the full length cross sections performed by Duncan (1983). In this cross section, the dipping of the Cooper Group as it approaches the Atlantic Ocean can be seen. The cross section in Figure 2.1 is the portion of the Lexington to Charleston cross section that spans from Moncks Corner to the Charleston Medical Center (Duncan et al., 1983).

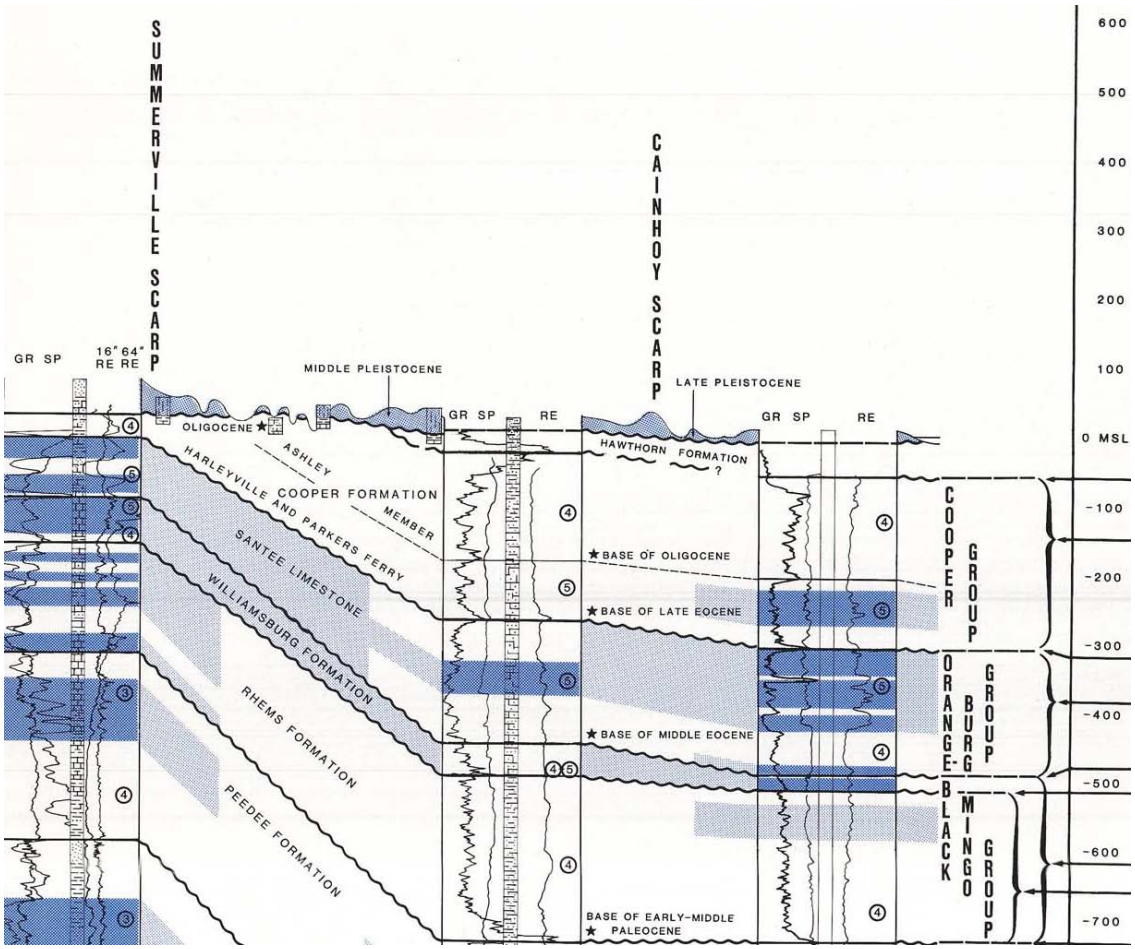

Figure 2.1 – Excerpt of Cross-Section C-C' from Lexington to Charleston (After Duncan et al., 1983)

Rogers (1913) noted some concern with the marl thickness determinations as well as formation distribution of the Ashley Member based on observations from a marl mine 15 miles north of Charleston. His hypothesis was that some of what was being mined was Cooper Marl and some was an underlying formation. Based on the deep borings with gamma ray, resistivity, and spontaneous potential logs (Duncan et al., 1983), the underlying Harleyville Member and Parkers Ferry Member of the Cooper Group that are located between the Charleston Air Force boring and the Summerville Scarp show similar geophysical logging and relative porosity to the Cooper Marl, with the cross section stratigraphy showing the Cooper Marl pinching out before reaching the Summerville

Scarp. But, the boring at the Charleston Medical Center shows the Harleyville Member and Parkers Ferry Member as having a high relative porosity, which is not a characteristic of the Cooper Marl.

An adjacent cross section going from Kiawah Island to Saluda County shows Cooper Marl extending 50 miles inland to a deep boring in St. George with the underlying Harleyville Member showing different geophysical log results from the Cooper Marl in the same borehole for all three logs varieties (Duncan et al., 1983). However, on the cross section between Lexington and Charleston shown in Figure 2.1, Duncan (1983) did not have a deep boring showing good definition between the Ashley Member and the Harleyville Member / Parkers Ferry Member. More recent geotechnical borings in the area show a layer of soil classified as Cooper Marl between the surficial sediments and the Santee Limestone (F&ME, 2008), which is the formation that underlays the Harleyville Member and Parkers Ferry Member in the Charleston area according to Duncan (1983).

A later Cooper Marl characterization for engineering purposes addressed these discontinuities in the Ashley Member, Harleyville Member, and Parkers Ferry Member in the vicinity of the Cooper River Bridge (Camp, 2004). This characterization found that all three members can be treated as Cooper Marl so long as the soil samples and tests show the general engineering properties of typical Cooper Marl (see Section 2.4) even though the typical Cooper Marl only refers to the Ashley Member. No discussion was made regarding the engineering properties of other Cooper Group Members that exist outside the Charleston area.

From a geologic perspective, the most current Cooper Marl distribution map and geologic description was presented by Weems and Lewis in 2002. It was based on a compilation of geologic borings performed in 43 USGS quadrangles around the Charleston area. The information collected in these borings enabled a more detailed geologic map of the area to be built. Additionally, Weems and Lewis refer to the Ashley Member, Parker Ferry Member, and Harleyville Member of the Cooper Group as defined by Duncan (1983) as their own formations (Ashley Formation, Parkers Ferry Formation, and Harleyville Formation). Figure 2.2 presents the general geology map of the Charleston area showing the geologic formations that directly underlie quaternary cover, which are the surface sediment deposits that are less than 2.5 million years old. By removing the quaternary cover, the location of Pliocene, Miocene, Oligocene, and Eocene formations can be observed. This allows the distribution of the Ashley Formation, Parkers Ferry Formation, and Harleyville Formation (Cooper Group members by Duncan, 1983) to be observed as well as the Santee Formation, which underlies the former Cooper Group soils.

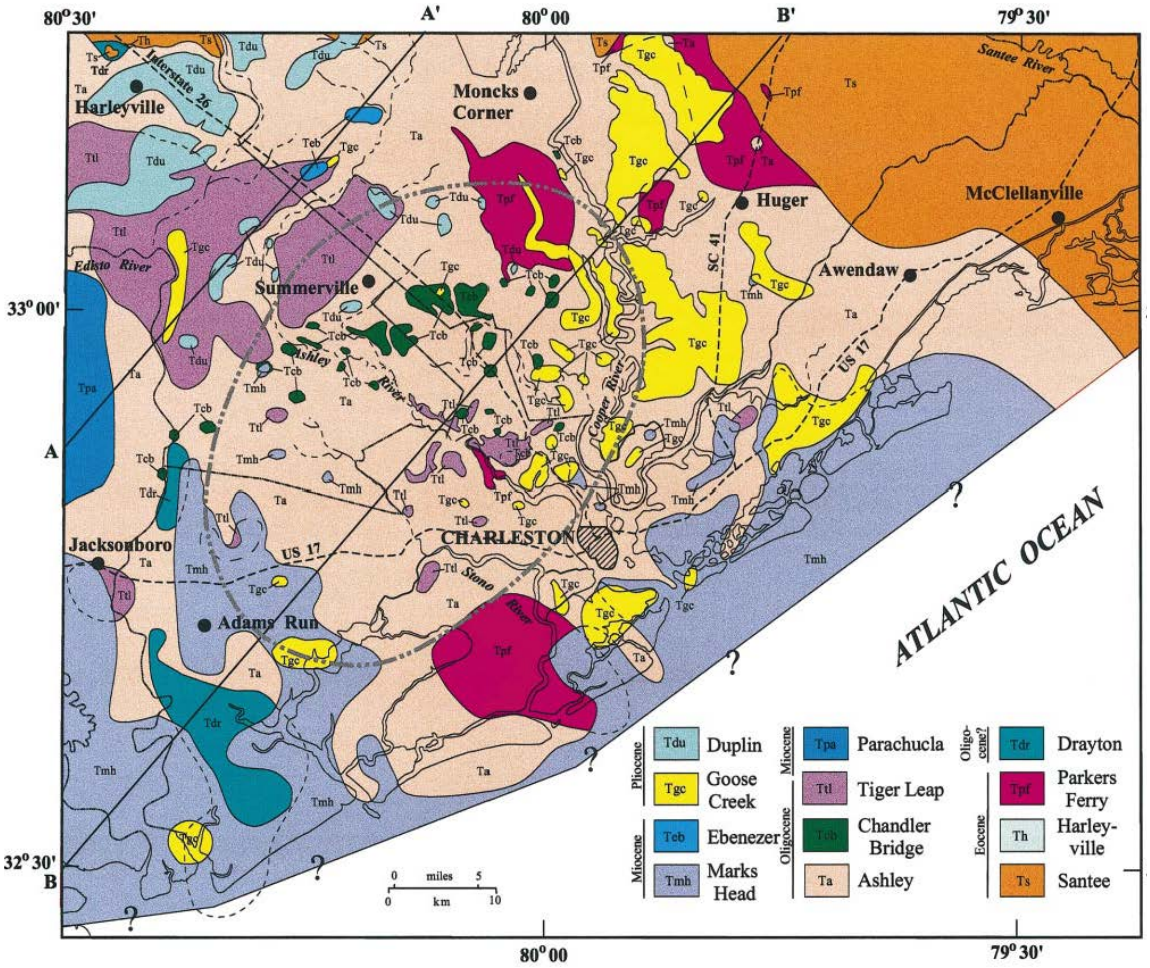

Figure 2.2 – Stratigraphic Units Directly Underlying Quaternary Cover in the Charleston, SC Region (After Weems and Lewis, 2002)

As can be seen in Figure 2.2, the Ashley Formation (Ta) directly underlies quaternary cover in the majority of the Charleston area where the Cooper Marl is encountered. Some outcrops of the Parkers Ferry Formation are also indicated, which would be areas where the Ashley Formation was not encountered. Figure 2.2 does not specify the presence of the Ashley Formation beneath the Pliocene and Miocene formations encountered. However, Weems and Lewis (2002) also presented a contour map of the base of the Ashley Member, which can be used to estimate the base elevation of the formation as well as the geographical distribution and is presented as Figure 2.3.

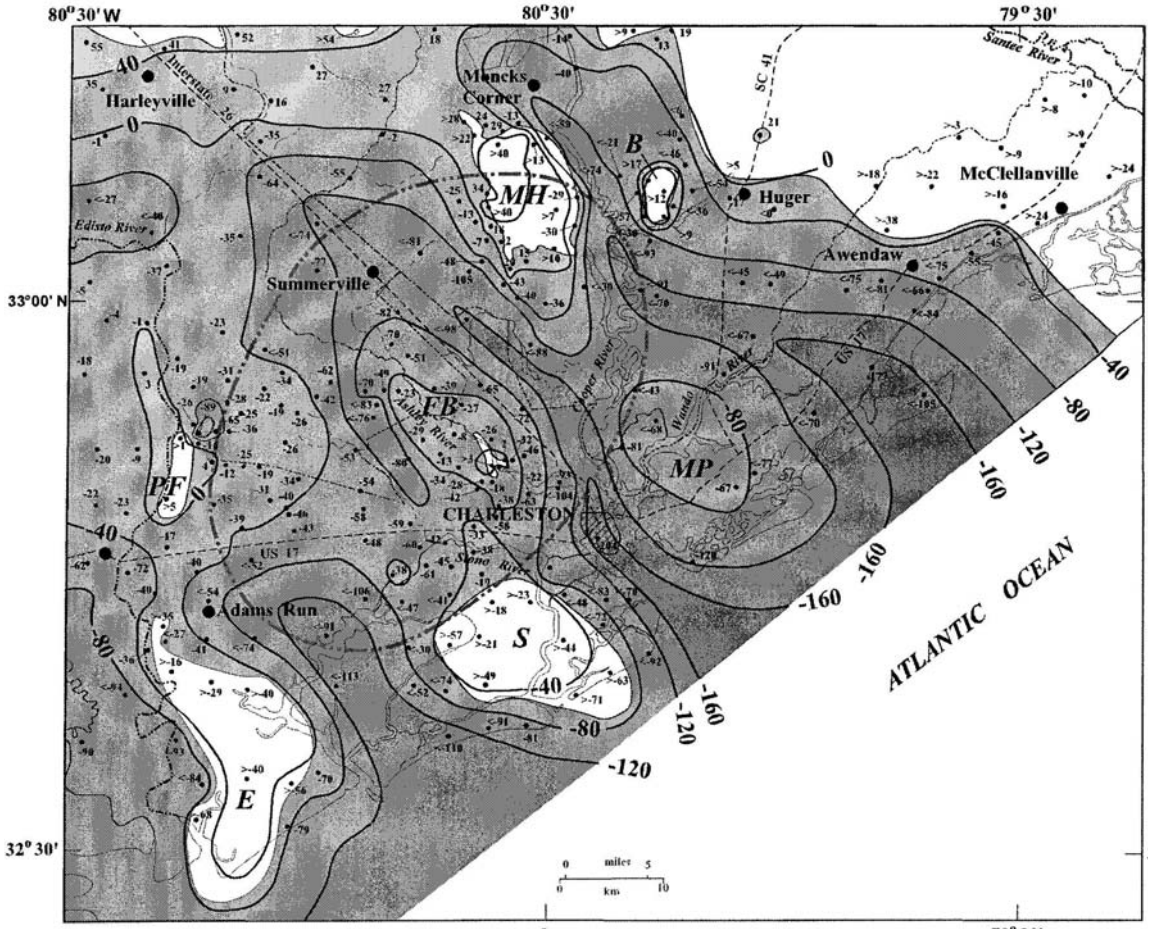

Figure 2.3 – Contour Map of the Base of the Ashley Formation in the Charleston, SC Region (After Weems and Lewis, 2002)

2.4 - Cooper Marl Physical Properties

Even in early descriptions of the Cooper Marl, the reported physical characteristics are consistent. The marl is described as grayish-green to olive green silt with some sand, moist, and slightly plastic when moist (Rogers, 1913; Malde, 1959; Heron, 1962). Munsell coloring was noted as 5Y 5/3 (Olive) or 5Y 6/2 (Olive Gray) when fresh (Malde 1959). From an engineering perspective, the most detailed Cooper Marl description is based on the site characterization program for the Cooper River Bridge (Camp, 2004). Based on that program, the Cooper Marl is defined as being composed of 60% to 80% calcium carbonate, fines content generally in excess of 60%, a USCS classification of MH or CH, liquid limit generally between 40 and 90, plasticity

index between 15 and 60, natural moisture content generally between 40% and 60%, and an average undrained shear strength of 4 ksf (Camp et al., 2002; Camp, 2004). Figure 2.4 presents the shear strength data from the geotechnical testing at the Cooper River Bridge.

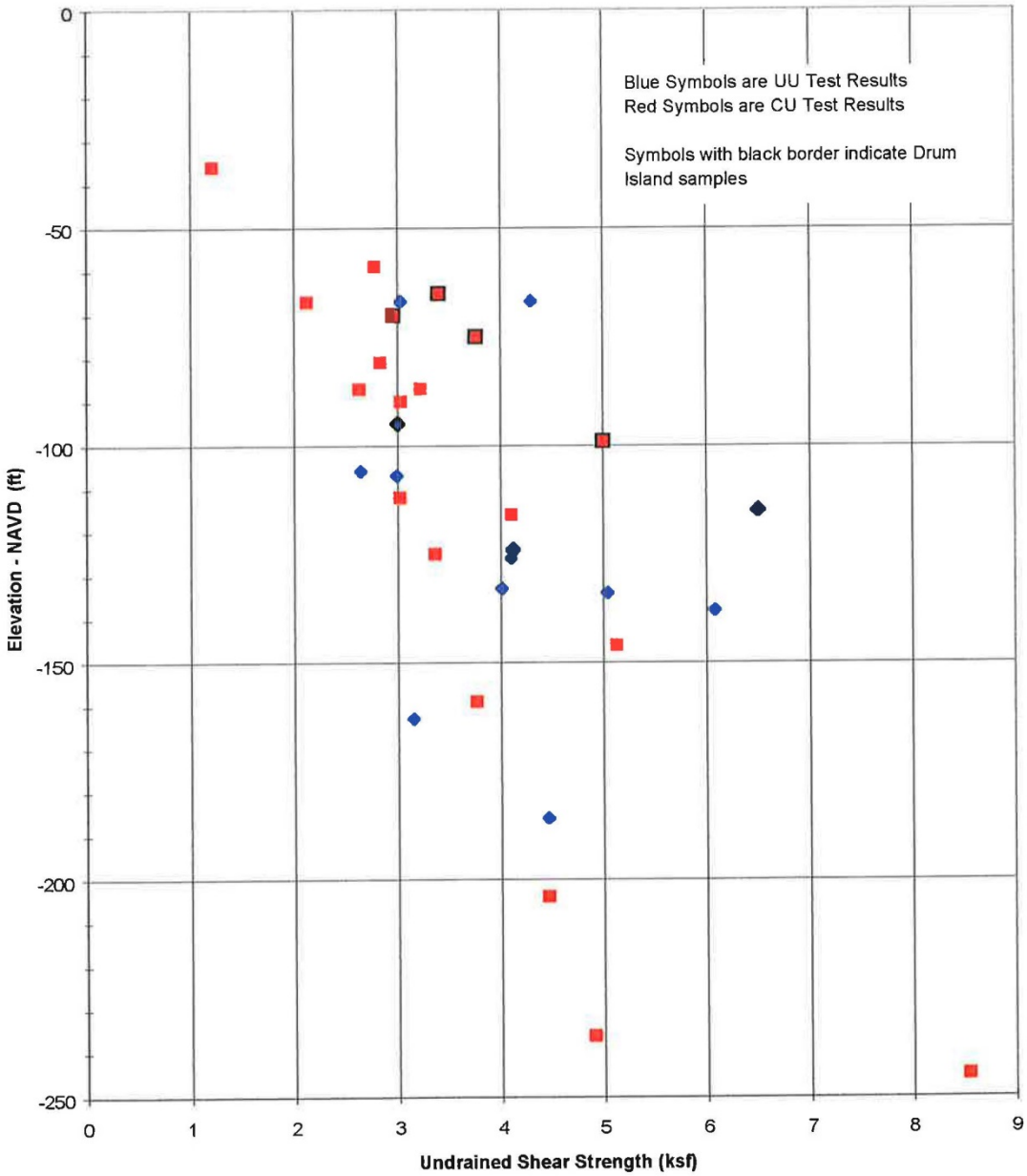

Figure 2.4 – Undrained Shear Strength of the Cooper Marl at the Cooper River Bridge (After S&ME, 2001)

As it pertains to density, the average standard penetration test (SPT) N-value observed was 15 blows per foot (bpf), the observed void ratio ranged between one and

two with a maximum preconsolidation pressure of approximately 16 ksf (Camp, 2004). It should be noted that while the Cooper Marl is not a soft rock it is similar in chemical composition to limestone based on calcium carbonate content and in many cases meets the chemical composition requirements to be considered a limestone formation and not a marl formation (Heron, 1962).

2.5 - Cooper Marl Discontinuities and Anomalies

It is important to note that while the Cooper Marl is considered to be a homogeneous formation from an engineering perspective, there are some variations and disconformities within the formation. One of the commonly noted variations in the Cooper Marl is the existence of cemented lenses (Camp, 2004; F&ME, 2013). Based on the chemical composition of the Cooper Marl, these lenses are hard carbonate lenses that are generally a maximum of a few inches in thickness (Cooke, 1936). From an engineering perspective, these lenses should not be used to define the site as a whole as they may not be contiguous across the site. Additionally, what may appear to be a cemented layer based on a soil test boring SPT, may be a shell, gravel piece, or fossil embedded in the marl even though these items do not appear in high frequency within the marl at depth (Drayton, 1802, Holmes, 1870, Cooke, 1936, Malde, 1959).

Phosphate lag deposits on the top of the marl are also common. These deposits are the phosphate rocks that were originally mined for fertilizer and exist as nodules of cemented microfossils (Holmes, 1870). Generally, these lag deposits are not cemented in layers like other varieties of lag deposits, such as ironstone deposits that are found between surface sediments and Kaolin Beds in the upper coastal plain of South Carolina (USBM, 1996).

Some instances of bedding aside from cemented layers have been noted. One of these instances was a tunneling project near Daniel Island in Charleston County where a sand seam up to 30 feet in thickness was found in the Cooper Marl. In this case, a water tunnel was being constructed through the marl. During construction, cracking in the tunnel casing as well as saturated sand was encountered at a depth below the deepest geotechnical boring. Additional geotechnical investigation revealed a sand seam in the marl that caused the construction issues (Brainard et al., 2009). A boring log for a drilled shaft load test approximately three miles from Daniel Island at the I-526 Bridge over the Cooper River also indicated the presence of a sand seam at a similar depth (S&ME, 1988).

More recently, during the geotechnical investigation for the SC 41 Bridge over the Wando River, a sand seam was discovered across the entirety of the site (ICA, 2014). Based on provided boring elevations, the seam at this site exists at approximately the same elevation as reported by Brainard (2009). Drilled shaft load testing was performed at this site, but the shaft did not extend into the sand layer (GRL Engineers, 2014).

An additional consideration regarding construction in the Cooper Marl is the presence of the Marks Head Formation. This is a Lower Miocene formation in age and occurs directly above the Ashley Formation in some areas (Weems and Lewis, 2002). The geographical distribution and base elevation contours are presented in Figure 2.5. The significance of the Marks Head Formation is that while being an entirely different geologic age, it has similar visual characteristics to the Ashley Member. The Marks Head Formation is visually described as grayish olive to moderate olive brown, but is generally classified as sand (Weems and Lemon, 1985). As this formation is not as well

studied as the Cooper Marl, the engineering properties are not well defined. Because of this, confusion or misidentification within the two formations could lead to improperly designed formations.

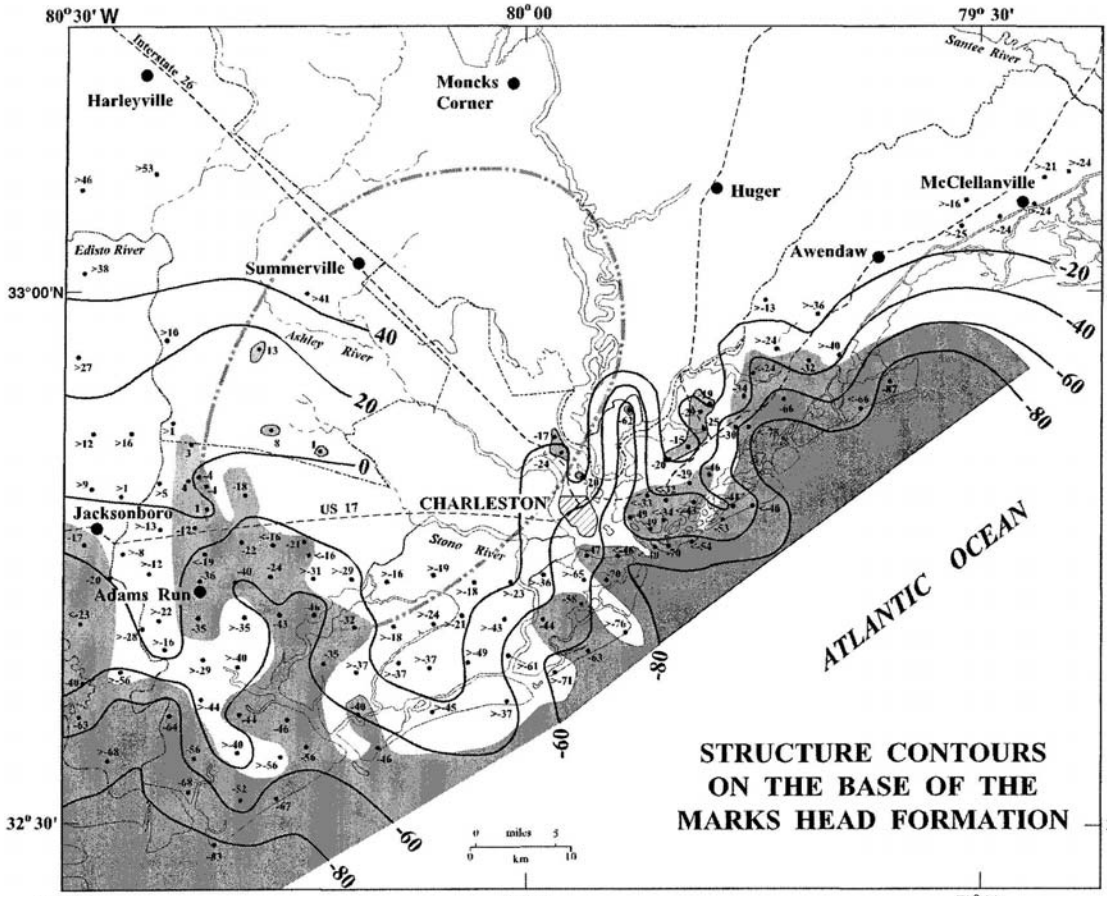

Figure 2.5 – Contour Map of the Base of the Marks Head Formation in the Charleston, SC Region (After Weems and Lewis, 2002)

CHAPTER 3

BACKGROUND

3.1 - Introduction

This chapter presents the engineering background information associated with this thesis. Included is a history of drilled shaft usage, drilled shaft construction and verification testing, effects of defects on axial capacity, drilled shaft load testing, and LRFD design.

3.2 - History of Drilled Shaft Usage

Drilled shafts, also known as drilled piers, while not a recently developed foundation type, have increased in prominence since their initial use in 1869 for a bridge in St. Louis (McCullough, 1972). In South Carolina, drilled shafts have become more popular since the 1980's due to the challenges in constructing pile footings underwater as well as increased lateral seismic loads in the Lowcountry (SCDOT, 2008). In addition, there has been a shift away from using spread footing foundations in the Upstate where seismic lateral loads are lower than the Lowcountry, but competent rock is too shallow for a driven pile foundation to achieve required lateral fixity. Drilled shafts also excel as a foundation type in areas with limited access, areas with high axial capacity needs, and sites requiring scour resistance (Brown, 2012).

The first SCDOT owned bridges constructed utilizing drilled shafts were in Berkeley County near the town of St. Stephen in 1982 (Abernethy, 2014). While the

Cooper Marl was not encountered at these bridge sites, marl does exist in Berkeley County (F&ME, 2008) and the bearing stratum was the Santee Limestone (Farr, 1983), which is overlain by the Cooper Marl in the Charleston area (Duncan et al. 1983, F&ME, 2008). In this area, three static drilled shaft load tests were performed on 42-inch diameter shafts and were denoted as Highway 52, Highway 35, and Highway 45 (Farr, 1983). Based on a map of the area, these three bridges are the US Highway 52, SC Highway 45, and North State Highway 35 (now known as S-8-35) over the Lake Moultrie rediversion canal. This canal connects Lake Moultrie to the Santee River and should not be confused with the diversion canal that connects Lake Marion to Lake Moultrie. These shafts were loaded to 1000 tons for testing the axial capacity and achieved this capacity with 0.4 inches to 3 inches of settlement. This was the maximum capacity of the load testing apparatus and may not have been the maximum capacity of the shafts (Farr, 1983).

Based on a discussion with one of the geotechnical engineers who worked on the bridge projects, drilled shafts were proposed as a value engineering option to the planned design option of pile footings. For construction of a pile footing at these sites, where the foundations are in a body of water, the construction of a cellular cofferdam would have been necessary. At the St. Stephen sites, the Santee Limestone is overlain by silty sand with clay seams, which could make keeping water out of the cofferdam challenging (Farr, 1983; Abernethy, 2014). Drilled shaft construction removes the need for a cellular cofferdam and the need for dewatering of the cell. As of 2014, two of the three original rediversion canal bridges are still in service, with the US 52 Bridge being replaced in 1998, likely due to the widening of US 52. Based on the most recent FHWA bridge

inventory records, the SC 45 Bridge was assigned a sufficiency rating of 98.7% and the S-8-35 Bridge was assigned a sufficiency rating of 99.1% with both having a substructure rating of "good" (FHWA, 2012).

3.3 - Drilled Shaft Construction

The construction of drilled shafts can be divided into two categories – the wet construction method and the dry construction method. In most cases, regardless of using the wet or dry method, a steel casing is installed where the shaft is to be built either by using a vibratory pile hammer or by twisting it in using the drilled shaft rig itself. Generally, the casing is installed to a depth below the water table, to the top of competent rock, or, as is the case for many shafts constructed in the Cooper Marl formation, the casing is installed so that it is a foot or two into the marl (AFT, 2013; GRL, 2012; Loadtest, 2000). After installation of the casing, an auger is used to bore the shaft hole. Depending on the soil conditions, drilling slurry may be needed to maintain borehole stability. In situations with sand layers below the casing, drilling slurry is needed while in cases with cohesive soils below the casing, the need for slurry is determined by the diameter and depth of the shaft to protect against bottom failure. When drilling slurry is used, the shaft is considered to be constructed using the wet method. If no slurry is used, the shaft is constructed using the dry method. In cases where artesian water is present, drilling slurry must be used and the use of an oversize surface casing may be necessary to overcome the artesian water pressure and maintain a stable borehole (FHWA, 2010).

After the shaft drilling is complete, a steel reinforcing cage is placed in the hole and concrete is pumped into the hole. If the wet construction method is used, a tremie pipe is lowered to the bottom of the shaft and concrete is pumped from the bottom. To

minimize slurry contamination of the concrete, the end of the tremie pipe is kept below the concrete and a foam plug known as a pig is placed in the tremie pipe ahead of the concrete. The pig displaces the slurry in the tremie as the initial concrete is placed to minimize concrete contamination. If the dry method is used, the concrete can be placed using a tremie pipe or it can be free-falled as long as the drop distance is less than 75 feet (SCDOT, 2007).

There is some discussion as to whether or not the use of slurry during drilled shaft construction changes the axial capacity of the drilled shaft (Brown, 2002). In 2002, multiple drilled shaft load tests were performed at the Auburn University National Geotechnical Experimentation Site. A total of eleven shafts were built using the dry construction method and the wet construction method using various drilling slurries, including bentonite and polymer slurry. The research showed that the test shafts built using the wet construction method showed a lower axial resistance due to the presence of a slurry film between the drilled shaft and the soil. However, the study hypothesized that the effect of reduced axial capacity may be lessened in soils with a lower hydraulic conductivity.

In a similar study, as part of the US 17 over the Cooper River Bridge replacement project, twelve test shafts were built at three different test sites, all of which used the Cooper Marl as the bearing strata (Camp et al. 2002). These shafts were built using five different methods: dry construction, fresh water as a drilling fluid, bentonite slurry, and two different polymer slurry mixes. Based on the load test results, the construction method and drilling fluid did not significantly affect the axial capacity in the Cooper Marl.

3.4 - Drilled Shaft Verification Testing

Another important aspect in the construction of drilled shafts is the evaluation of in-place foundation construction quality. Unlike a driven pile foundation where the foundation element can be inspected before installation and can be verified during installation using various methods, such as a pile driving analyzer (PDA) or a wave equation bearing chart, there is some degree of uncertainty with drilled shafts. There are many factors impacting construction quality of drilled shafts, such as the concrete quality, the ability of concrete to fully flow around and through the reinforcing cage, and the maintenance of borehole stability throughout the concrete pour (Brown, 2004).

Currently, the method for acceptance testing in South Carolina is the use of cross-hole sonic logging (CSL) for every drilled shaft (SCDOT, 2007). To perform CSL testing, one and a half to two inch steel pipes are attached to the entire length of the reinforcing cage and filled with water before concrete is poured. Typically, there is one CSL tube per foot of shaft diameter equidistantly spaced around the reinforcing cage. After the concrete has cured for a minimum specified duration and to a specified strength, CSL testing may be performed. In South Carolina, CSL testing is to be performed between 72 hours and 15 days of the end of the concrete pour and once the concrete has reached a minimum compressive strength of 3000 psi (SCDOT, 2007). The CSL test itself is governed by ASTM Specification D6760 and consists of lowering a probe down two of the installed tubes. As the probes are raised so that they are at roughly the same elevation, one of the probes emits a sonic signal while the other is a receiver. Based on the engineering value of the material wavespeed of concrete, the measured distance between the two tubes, and the known energy of the emitted pulse, the crosshole analyzer

can determine the first arrival time (FAT) of the pulse as well as the energy loss through the shaft (ASTM, 2008; Likins et al., 2012; Rausche et al., 2010). Based on air voids or pockets of drilling slurry having a slower material wavespeed, a delay in the FAT can indicate a void or defect. Defects can be confirmed non-destructively by performing a CSL tomography which creates a 3D model of the shaft to quantify and delineate the defect (Likins et al., 2004), or in some cases using low-strain integrity testing (PIT) and comparing the wave reflection of the shaft in question to a shaft with no noted defect in the CSL data (Likins et al., 2012). When non-destructive test methods have been exhausted, coring and compressive strength testing of a shaft may be necessary.

One drawback of CSL testing is that the test can only verify the area inside the reinforcing cage between the CSL tubes. Research and testing on thermal integrity profiling (TIP) are currently ongoing (Mullins et al., 2010; Likins et al., 2012; Piscsalko et al., 2013). The process can be performed by using a shaft with tubes similar to the CSL tubes and a temperature sensing probe or by installing temperature sensitive cables that record the concrete hydration heat over time. By using temperature probes, measurements can be taken in all directions and data can be collected from outside the reinforcing cage to analyze the sides of the shaft. While currently not used for shaft acceptance verification in South Carolina, TIP testing has been used in comparison testing on some bridge projects in South Carolina. However, TIP testing does have the potential to remove some of the uncertainty in CSL drilled shaft verification. Early TIP case studies are also showing promising results at detecting defects that the CSL testing consistently detects as well as defects outside the range of CSL testing (Piscsalko et al., 2013; Sellountou et al., 2013).

3.5 - Effects of Drilled Shaft Defects on Axial Performance

Since the geotechnical resistance factor in LRFD is used to account for construction defects of the drilled shafts, it is important to take the strength loss of the shaft into account when determining if it is acceptable to make the resistance factor less conservative. To evaluate the effects of shaft defects on axial performance, load testing on scale models of drilled shafts in a laboratory setting has been performed (O'Neill et al., 2003). These model shafts simulated cross-sectional loss of 15% of the total shaft area in two different modes: a loss of area outside the reinforcing cage and a loss of cross-sectional area in a wedge shape starting from the center of the shaft. These samples were then tested in flexural loading, axial loading, and combined loading. The results showed structural strength losses of up to 20% of the control samples (O'Neill et al., 2003). It is important to note though that this testing was of the shaft material itself and not of the interaction of a shaft with an anomaly with in-situ soils. Also, defects this large would likely be identified by verification testing and could be repaired using methods such as pressure grouting, which would ensure solid contact between the soil and shaft.

Full scale tests of a similar variety have also been performed. A large-scale drilled shaft test program consisting of twenty shafts at four test sites in California and Texas was completed in 1993. In this program, drilled shafts were constructed with various types of defects, such as necking, soft bottom defects, and shaft bulging. These defects in cross-sectional area impact affected up to 70% of the shaft and were created using sandbags. Control shafts were also constructed as a basis of comparison. Load testing on these shafts with defects indicated that the axial capacity determined by dynamic testing was not greatly affected by the defects with the caveat that the capacity

controlling material for a drilled shaft in soil is the soil, not the shaft itself (FHWA, 1993). Even with these results, it should be noted that this study did not address the long-term effects of shaft defects on axial capacity nor the moment capacity of defective shafts.

3.6 - Drilled Shaft Load Testing Information

The following review of drilled shaft load testing is primarily based on information from the 2010 Federal Highway Administration (FHWA) Drilled Shaft Design Manual. At the publication date of this document, this design guide is the most recent drilled shaft design guide issued by the FHWA. Additional data sources used to supplement this document will be specifically annotated.

Drilled shaft load testing is a method of verifying drilled shaft capacities and determining if the empirical design methods were appropriate or if changes need to be made to the drilled shaft design. Drilled shafts can be tested both laterally and axially using static and dynamic methods depending on which test information is critical. There are two varieties of drilled shaft load tests: pre-construction load tests and proof tests.

The most common variety of load testing in South Carolina is a pre-construction load test. For a pre-construction load test, a dedicated test shaft is constructed for the sole purpose of load testing. This shaft is then loaded to failure or to a design test load, and the load transfer properties of the shaft are analyzed and compared to the anticipated design values. Based on the differences between the anticipated design values and the load test results, changes to the drilled shaft design can be performed if necessary. This shaft is not incorporated into the bridge structure.

While not often performed in South Carolina, proof testing of drilled shafts is also a test option. This consists of loading a production shaft to a certain load above its design load, without loading the shaft to failure, as a means of confirming post-construction shaft integrity. Proof testing is generally performed on a percentage of the total number of production shafts in conjunction with a pre-construction load test and can be used to justify the use of a less conservative resistance factor.

One use of proof testing that does have an appreciable cost-to-benefit ratio is the verification of drilled shaft defect remediation. An example of this in South Carolina is the SC Highway 247 Bridge over the Saluda River on the Anderson/Greenville County line. This bridge was supported by 54 in. drilled shafts with 48 in. rock sockets founded in weathered gneiss. The bridge design was based on the shaft achieving ultimate resistance in a combination of end bearing and skin friction (AFT, 2001). CSL testing performed on the shaft indicated the presence of a major defect at the toe of the shaft approximately two to three feet in thickness in multiple shafts across one of the bent lines (GRL, 2001). These drilled shafts were then full-depth cored to verify the anomaly. The coring verified the presence of sand in the bottom of the drilled shafts that may have negatively affected the axial capacity of the shaft (F&ME, 2001). Based on the core results, a remediation plan was developed that encompassed cleaning out the bottom of the drilled shafts, pressure grouting the toe voids, and performing a statnamic proof test of twice the design load on the shaft that had the worst core results (F&ME, 2001). After grouting, the proof test verified the required capacity (AFT, 2001) and the shaft was accepted by the geotechnical designer of record, preventing a more expensive option such as removing and replacing the shaft (F&ME, 2001).

3.7 - Types of Drilled Shaft Load Tests

Axial load testing can be split into two main groups: static load testing and dynamic load testing. Static load testing is comprised of tests where a static load is incrementally applied and maintained on the drilled shaft for a set duration and the drilled shaft response is measured for each load increment until the design test load or maximum axial shaft displacement is achieved. The required load can be applied in a number of ways depending on the location of the shaft, required capacity, and the local resources. Examples of this type of test are the Conventional Method static load test, Kentledge Method, and Osterberg Cell load test. Dynamic load tests are tests where the design test load is rapidly applied in a single stage and the shaft response is measured as the shaft moves. Primary examples of dynamic tests are the Statnamic load test and High-Strain Dynamic Testing. As the primary focus of this research is the axial capacity of drilled shafts, lateral testing methods will not be discussed.

3.7.1 - Static Load Test – Conventional Method

The Conventional Method (see Figure 3.1) is governed by ASTM Specification D 1143. To perform this test, the design test load is calculated from empirical methods and the test shaft is constructed. Based on the test load, reaction piles are designed and then constructed around the test shaft. The sum of the uplift resistance of these reaction piles must be greater than the design test load to be applied to the test shaft. If the resistance of the reaction piles is insufficient, the reaction piles could come out of the ground before the full test load is applied. Once the reaction piles are installed, a reaction beam is placed on the reaction piles. This beam is centered over the test shaft and used to transfer the load to the reaction piles.

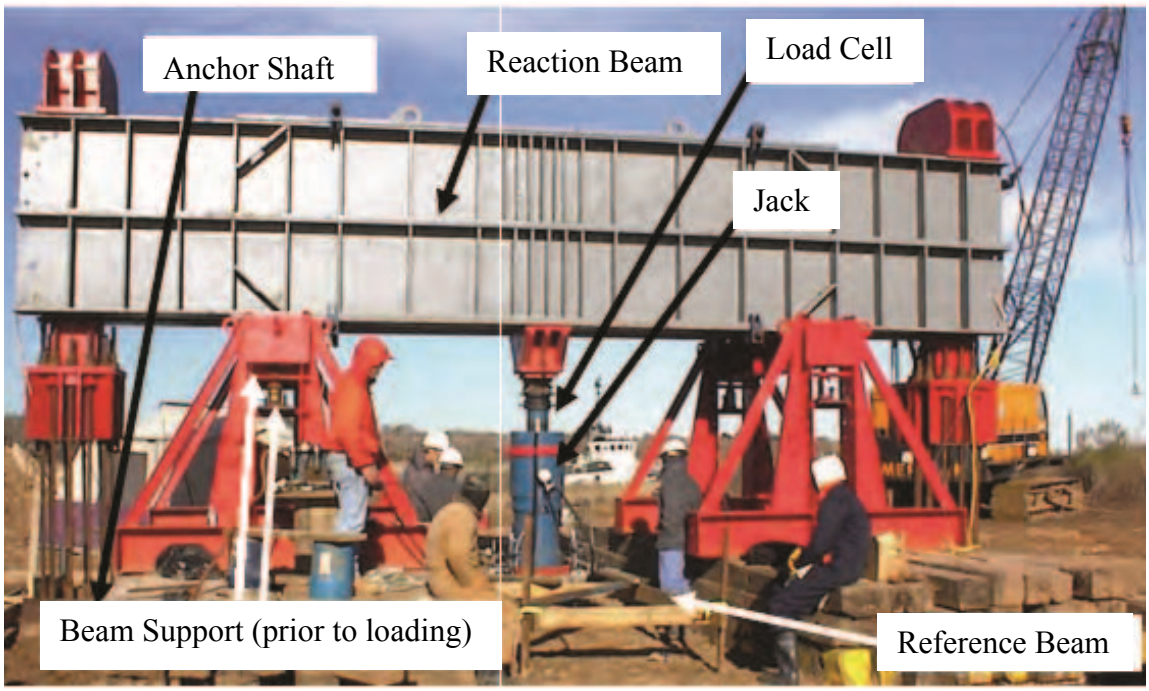

Figure 3.1 – Conventional Method Load Test (After FHWA, 2010)

Between the reaction beam and the top of the test shaft, a hydraulic jack is inserted to apply load to the test shaft. A load cell is placed between the reaction beam and hydraulic jack to measure the applied load. A reference beam is also installed and used to measure the vertical deflection of the top of the shaft as the load is applied. Once the reaction system and shaft are constructed and calibrated, the test load is incrementally added to the top of the shaft using a hydraulic jack. Once a load increment is applied, it is held for a set duration for the shaft creep to be measured, if any is present. Measurements of the strain and deflection at the shaft head and along the shaft body are recorded, and then the load is increased. Increments are added until the design test load is achieved, shaft plunge occurs, or the reaction piles are lifted out of the ground.

To measure the strain behavior and the deflection of the shaft at depth, the shaft is instrumented with strain gauges and telltale bars at various depths. The strain gauges are used to measure the strain of the shaft under load. The telltale bars are steel rods that are

anchored at a certain shaft depth and run up a pipe to the surface of the shaft. They are used to determine the vertical movement at depth of the drilled shaft. The movement of the top of the shaft as well as the telltale bars is measured using surveying equipment. Data from both instruments is used to obtain strain versus load behavior and develop the load transfer curves used to determine the shaft capacity.

3.7.2 - Static Load Test – Kentledge Method

The Kentledge Method is similar to the Conventional Method in terms of the shaft instrumentation and test sequencing. The primary difference is the method in which the load is applied. In the Kentledge Method, dead weight is directly placed on the top of the shaft. In most cases, large concrete blocks and steel plates are stacked on a bearing plate, which replaces the reaction beam and reaction pile system. For load tests that are performed over water, large ballast tanks with water pumped from the local waterway can be used as the load. This method is generally used only when there are no other methods available due to cost and safety concerns. An example of this kind of situation is when the maximum test load exceeds that which can be applied with the conventional method. This can occur when the surrounding soil is insufficient to provide the necessary uplift resistance for the reaction piles (FPS, 2006).

3.7.3 - Osterberg Cell Load Test

A more recent version of the static load test is the Osterberg cell load test (O-Cell), which is shown in Figure 3.2. This test was developed in 1984 (Hayes, 2012) based on early experimental work in the 1970's (Horvath, 1980). Like the standard static load test, this test method is also governed by ASTM Specification D 1143. The O-Cell is a pressure cell that is built into the test shaft and is then loaded (Osterberg, 1998).

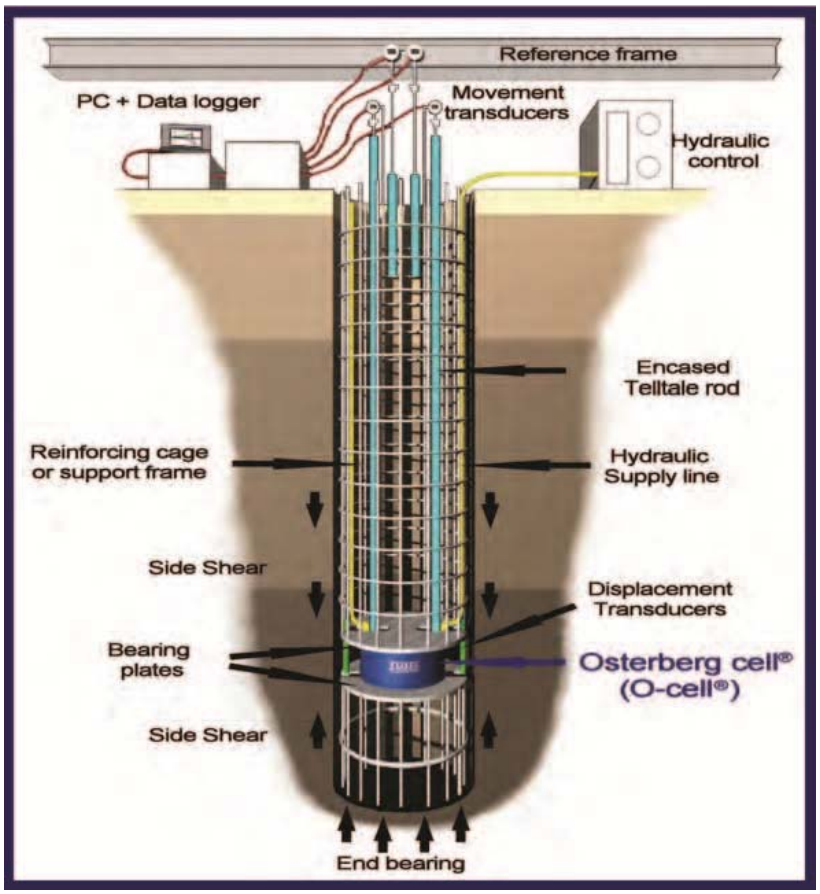

Figure 3.2 – Typical Osterberg Cell Setup (After FHWA, 2010)

The early experimental tests of this nature were test shafts setup with pressure jacks set in recesses beneath rock sockets then pressurized (Horvath, 1980). This idea of internal loading was taken further with the creation of the O-Cell. Unlike the initial work, the O-Cell can be used in any soil type. The goal is to place the cell at the balance point between the available capacity below the cell and above the cell. The test shaft itself is instrumented with strain gauges and telltale bars in the same manner as a static load test, but no reaction system is needed. A reference frame, as shown in Figure 3.2, can be used but is not necessary. The cell is then slowly pressurized, splitting the shaft into two pieces. The load increments are increased until the design test load has been applied to the shaft (Osterberg, 1998).

Since the O-Cell test is the only axial load test that does not use top-down load application, issues can arise if the load capacity above and below the cell are not balanced. If the bottom section of the test shaft has significantly more resistance that the top, the load test will not be able to fully mobilize the resistance in the bottom portion of the shaft (Hayes, 2012; Loadtest, 2014). Likewise, if the top portion has more capacity than the bottom or if the bottom of the shaft is not fully cleaned, the bottom of the shaft can plunge without fully mobilizing the skin friction of the top portion (Osterberg, 1998; Loadtest, 2013). These concerns can be mitigated by adding a second O-Cell to the test shaft, but this is not necessarily a fool-proof method (Loadtest, 2014).

The main advantages to the O-Cell versus standard static load test methods is the speed of testing, space required, and lack of external disturbance required for the test. The O-Cell is installed when the shaft is poured. And, while installation is more time consuming than a production shaft, it takes less setup time than standard static load testing or any of the dynamic methods. Also, since the cell is contained in the shaft and is loaded with a hydraulic pump, this type of load test can be performed in tight areas where there is a lack of staging area or difficult access, such as a test over water and in areas where construction vibrations must be kept to a minimum (Osterberg, 1998). O-Cell testing is also capable of achieveing test loads in excess of 36,000 tons – loads which would likely require Kentledge static load testing (Hayes, 2012).

3.7.4 - Statnamic Load Test

Statnamic load testing is one of the two types of common dynamic testing. This test was developed in 1989 (Middendorp et al., 1992; Brown, 1994) and is governed by ASTM Specification D 7383-08. As Figure 3.3 shows, a load cell is placed on top of the

shaft. The load piston and reaction mass are then lowered onto the load cell within the catch mechanism. Fuel is loaded in a cavity behind the piston during this step. When the shaft is ready to be tested, the fuel is ignited, the piston is forced against the load cell/test shaft, and the reaction mass is forced upward and caught by the catch mechanism. The statnamic load test is based on measuring equal and opposite forces to determine the shaft response. The test shaft is instrumented with strain gauges to measure the compression of the shaft under the test load and accelerometers to measure the energy at different shaft levels.

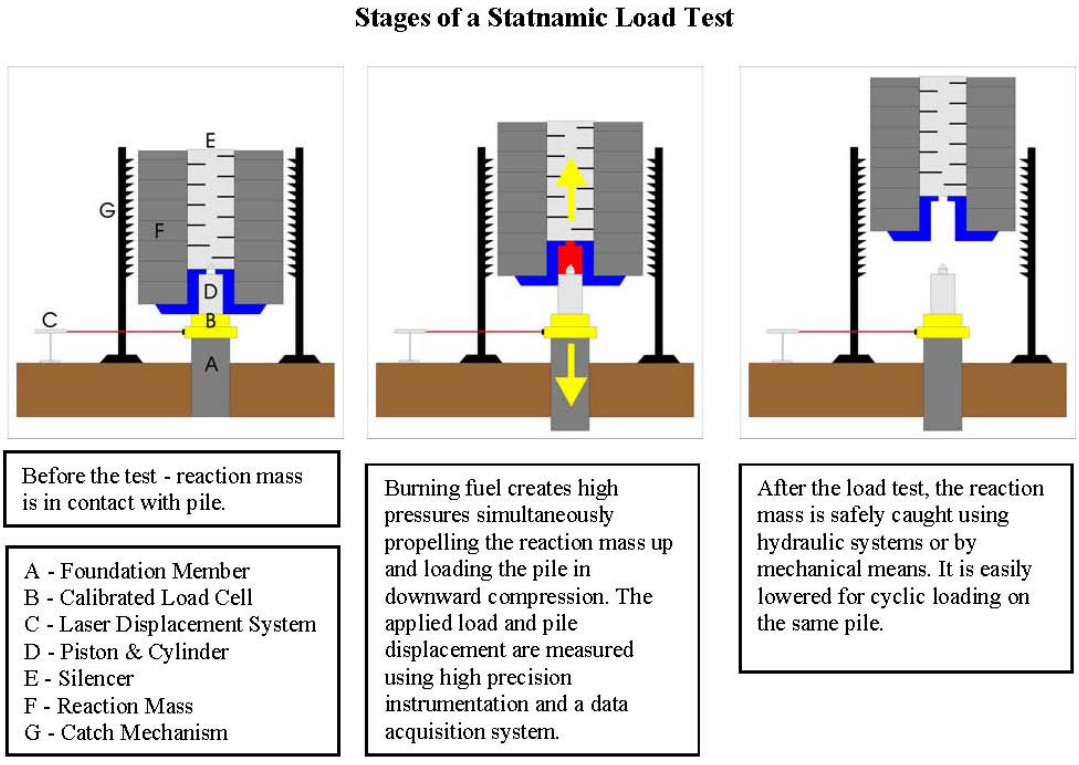

Figure 3.3 – Statnamic Load Test Setup and Sequence (After AFT, 2014)

Statnamic load testing has some of the advantages and disadvantages of both standard static load tests and O-Cell tests, but also has some factors to account for thatare unique to dynamic testing. Since statnamic testing is a top-down test, there is no load

section balancing as needed for an O-Cell while also taking less space and setup time than a static load test. Additionally, the statnamic load test does not rely on reaction piles. The primary challenges with the statnamic testing are the noise, vibration, and loading rate factors (Brown, 1994).

3.7.5 - High Strain Dynamic Load Test

High strain dynamic testing, also known as an APPLE test, is a fast and relatively inexpensive load test type that is becoming more often used (Conroy et al., 2010). This test method is governed by ASTM Specifications D 4945-12 and D 7383-10. Unlike the other three axial load tests, the APPLE test is performed on a drilled shaft with no internal instrumentation. For this method, the capacity is determined using the CAse Pile Wave Analysis Program (CAPWAP) method (Seidel et al., 1984).

The basic premise of the test is to treat the drilled shaft as a driven pile being tested with a PDA. First, a test shaft is constructed for the purpose of testing that has between five and ten feet of the shaft above ground. Then, a large dead drop hammer is built around the test shaft. To measure the forces in the shaft, strain gauges and accelerometers are attached below the top of the drilled shaft as they would be installed on a driven pile. To test the shaft, the hammer is dropped from increasing heights which in turn increases the applied energy. Pile head elevation heights are measured between each drop to measure the shaft displacement. The end of the test is taken either when the design test load is applied or once the shaft resistance does not further increase (Rausche et al., 1984; Hussein et al., 1992).

High strain dynamic testing has the benefits of cost and speed. Because there is no requirement for shaft instrumentation, such as strain gauges or telltale bars, the

material cost is less than other drilled shaft test methods. Also, because no internal shaft instrumentation is required, it is a good test method for proof testing or on sites where multiple tests are required (Conroy et al., 2010). The primary concern regarding high strain dynamic testing is that the capacity and load distribution is based on a wave equation and not an instrumented shaft.

3.7.6 – Correlation Testing between Load Test Types

Although all four types of load tests discussed are test styles that are used in practice, there are certain considerations that need to be taken into account to ensure that the correct resistance is found in the dynamic tests (Brown, 1994). Unlike the static axial test methods, the statnamic load test relies on an explosion to generate the test load, which causes significant noise, ground vibration, and can cause flying debris. From an engineering standpoint, the rate at which the load is applied is one of the primary concerns of dynamic load testing. Loading the shaft too fast can cause the soil to appear to have a higher capacity that a static load test would indicate. To account for this, the FHWA Drilled Shaft Design Manual (FHWA, 2010) provides a rate factor table based on soil type.

Correlation testing between high strain dynamic testing and other testing, such as Osterberg and Statnamic load tests, have shown that the prediction of the load by APPLE testing varies, especially when looking at the unit skin resistance. Test shafts at the National Geotechnical Experiment Sites in Amherst, MA and Opelika, AL showed a variation between the APPLE test and other load test methods with the APPLE test generally under predicting the shaft capacity (Robinson et al., 2002). But, the shafts that were tested had been load tested before, possibly affecting the capacity of the shafts.

Comparison tests on a drilled shaft project in Las Vegas, NV and on an auger grouted pressure displacement pile in Los Angeles, CA showed ultimate capacities within 2% of an O-Cell test in Las Vegas (Mackiewicz et al., 2012) and within 4% of a strain gauge instrumented dynamic test in Los Angeles (Alvarez et al., 2006). However, unit skin resistances varied by up to 58% in a single increment for a single shaft increment in Las Vegas (Mackiewicz et al., 2012) and an overall shaft side resistance differential of 20% in the Los Angeles test (Alvarez et al., 2006). This limitation should be taken into account when using high strain dynamic testing for design and determining skin resistance for a geologic formation or construction site.

3.8 - Load Test Interpretation

To evaluate the drilled shaft skin resistance characteristics based on a load test, two graphs are required: load versus shaft head displacement and load versus depth. Additionally, if information regarding the end bearing is required, graphs for the tip displacement versus bearing pressure will be required. As this thesis focuses on skin resistance, the tip displacement versus bearing pressure graph will not be discussed in depth.

3.8.1 - Static Load Test Data

As shown in Figure 3.4, the graph of load versus displacement summarizes the movement of the pile head as each load increment is applied to the top of the pile. This graph was created using data directly measured during the load test – the load information from the pressure exerted by the jack in parallel with the pressure measurements from the load cell and the shaft displacement by measuring the change in the shaft height as compared to the reference beam.

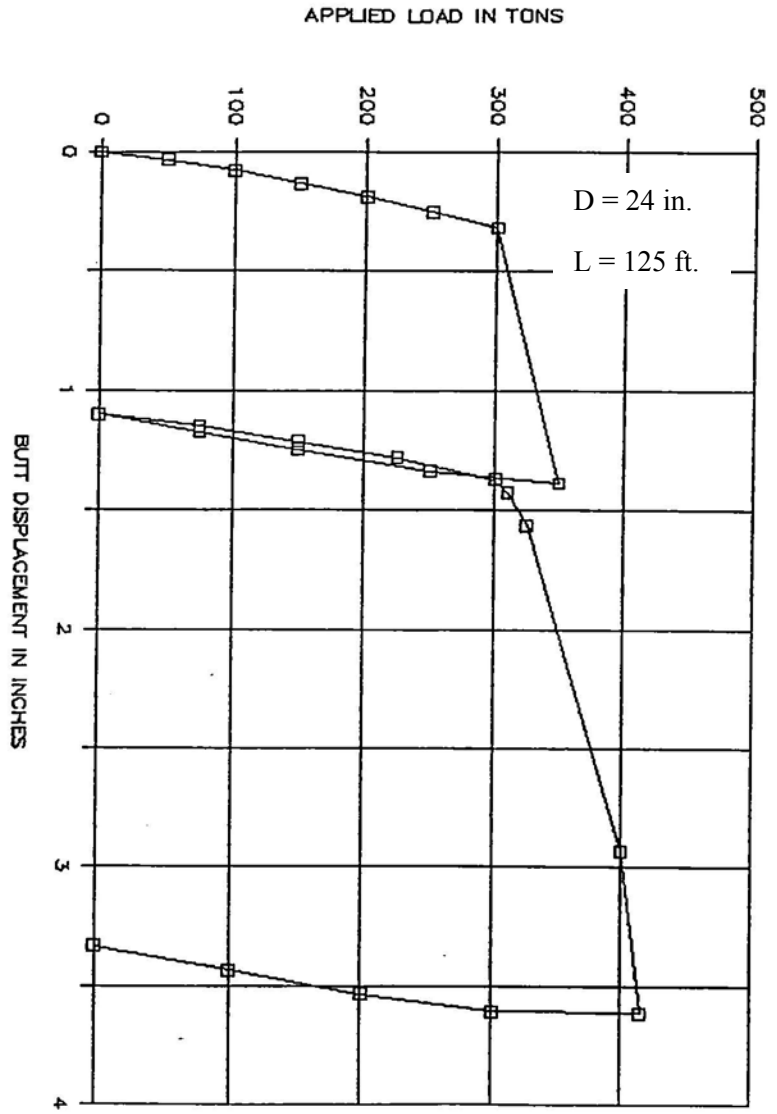

Figure 3.4 – Example of a Load versus Displacement Graph (After LAW Engineering, 1991)

The load versus displacement graph serves two main purposes. First, this graph can be used to determine when the drilled shaft failed based on a plunging failure condition in the load test. In Figure 3.4, the shaft displaces in a relatively linear manner as the loads are applied up to 300 tons. When the 350 ton load increment was applied, the overall displacement of the shaft approximately tripled to a displacement of approximately 1.4 inches. This indicated to the operator of the load test that the shaft was

nearing failure or had failed. At this point, an unload cycle was applied to determine the permanent shaft displacement and if there was any residual shear strength loss. Following the unload cycle, the shaft was reloaded past the initial failure point to 400 tons, at which time the shaft plunged 3.6 inches, indicating complete failure.

Second, the load versus displacement graph can be used to determine allowable shaft loading based on a maximum shaft head deflection. For example, based on the data shown in Figure 3.4, if the test shaft was built like the planned production shafts and the maximum allowable shaft head deflection as specified by the structural engineer was 0.25 inches, the maximum allowable load would be 250 tons.

The load versus depth graph serves a related purpose. Figure 3.5 shows a set of load versus depth curves from the same test shaft as the load versus displacement graph in Figure 3.4. Load versus depth graphs are used to determine the unit resistance properties from the load test. As mentioned previously, the maximum allowable load is determined based on the maximum allowable deflection. Based on the maximum allowable load, the corresponding curve is selected from the load versus depth graph. Based on this curve, the load transfer can be determined for each section of the shaft, with a shaft section being the part of the shaft between two strain gauges. The locations of the strain gauges are indicated by the points shown on each curve. For example, using the 350 ton curve in Figure 3.5, the unit skin resistance at the failure load in each segment at that load can be determined.

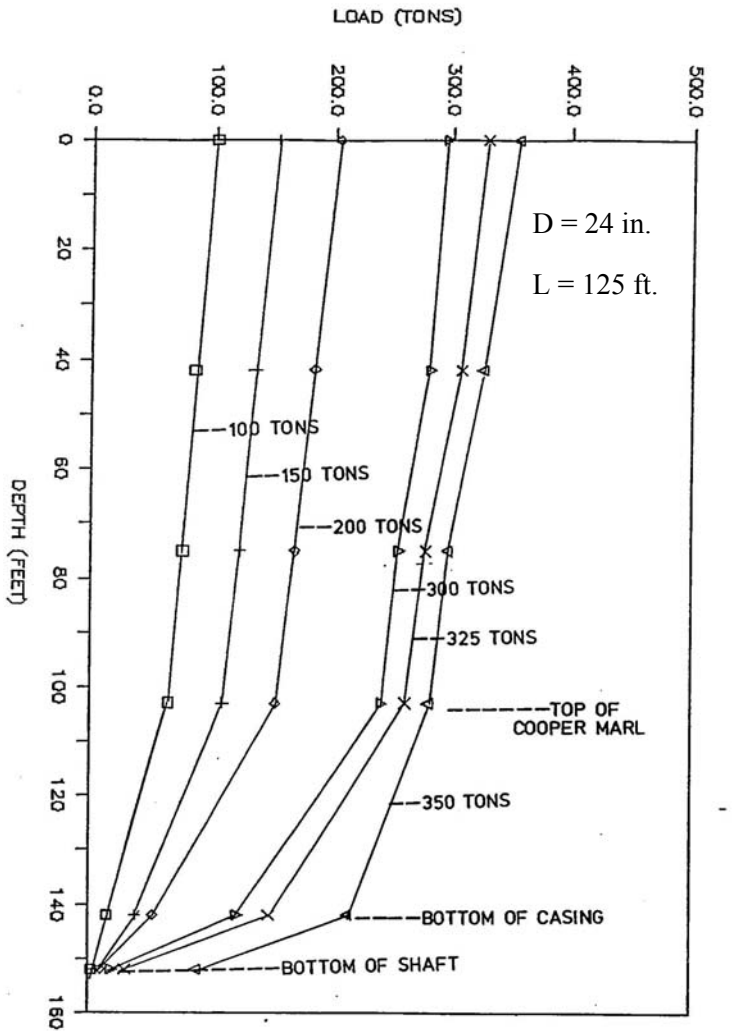

Figure 3.5 – Example of a Load versus Depth Graph (After LAW Engineering, 1991)

The section between the top of the Cooper Marl and the bottom of the casing is approximately 40 feet long. To determine the load carried in this section, the load at the top of Cooper Marl is subtracted from the load at the bottom of the casing. In this case, the load at the top of the Cooper Marl is approximately 290 tons and the load at the bottom of the casing is 210 tons, showing that the load carried in that segment is 80 tons total. The unit skin resistance can be found from the following equation:

$$f_s = \frac{Q}{A} \tag{3-1}$$

where f_s is the unit skin resistance, Q is the total load, and A is the shaft segment surface area.

In the load test report (LAW Engineering, 1991), the shaft is stated to be 24 inches in diameter. Over a 40 foot section, this equates to a segment surface area of approximately 250 square feet, thus, an average skin friction of 0.32 tons per square feet is found from Equation 3-1.

3.8.2 - Osterberg Cell Load Test Data

Load test data from O-Cell load tests is collected for each segment of the test shaft, as the shaft is split into segments between the Osterberg cells, instead of the shaft as a whole. The strain and displacement data from each segment is combined to determine the equivalent behavior to a shaft that is loaded from the top.

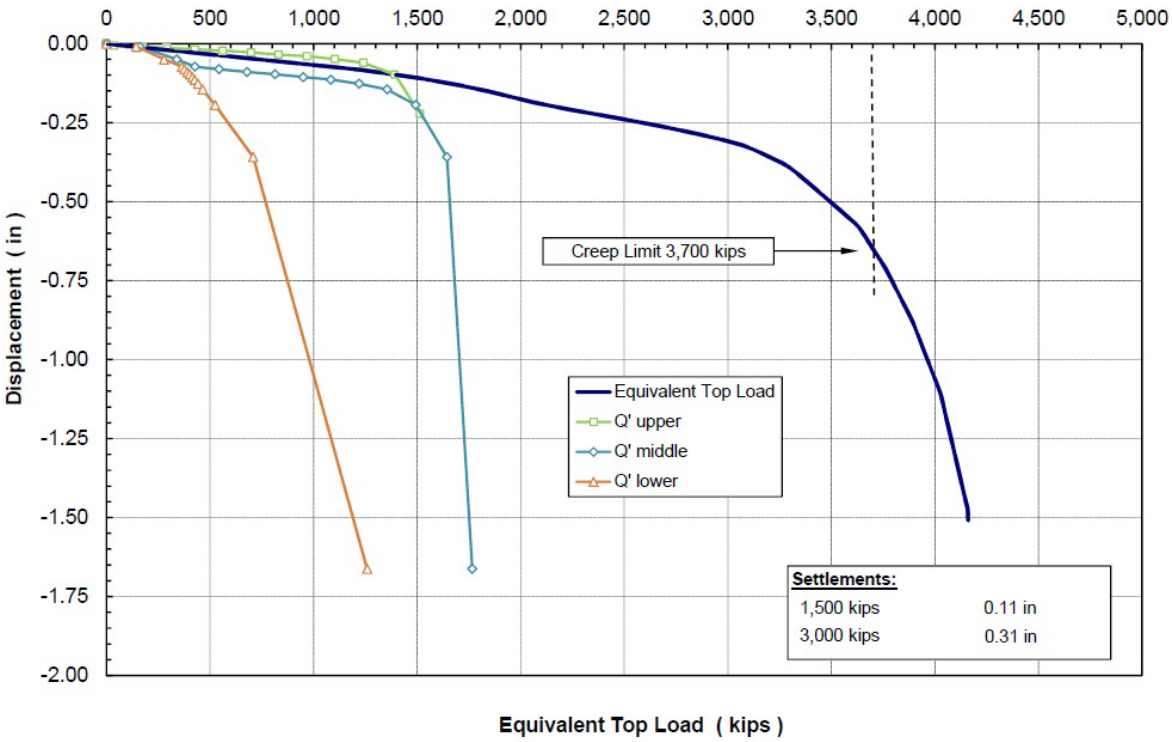

Figure 3.6 – Example of an Osterberg Equivalent Top Load-Displacement Graph (After Loadtest, 2014)

Figure 3.6 is an example of a load versus displacement graph from a two-cell Osterberg test. Load versus displacement curves for each of the three test shaft segments are noted as the Q' upper, Q' middle, and Q' lower. Since the segments moved in different directions (when the top segment moved up, the bottom segment moved down), the displacement is normalized to the same direction. Then, the three segment curves are combined to form the equivalent top load curve, which is the curve on the far right of Figure 3.6. This curve is interpreted in the same manner as the static load test load versus displacement graph presented in Figure 3.4.

To evaluate the unit skin resistance, the same methodology discussed in Section 3.8.1 is used. One factor to take into account is that for a multi-cell O-Cell load test, there will be a graph of load versus depth for each load stage, as both cells are generally not pressurized simultaneously.

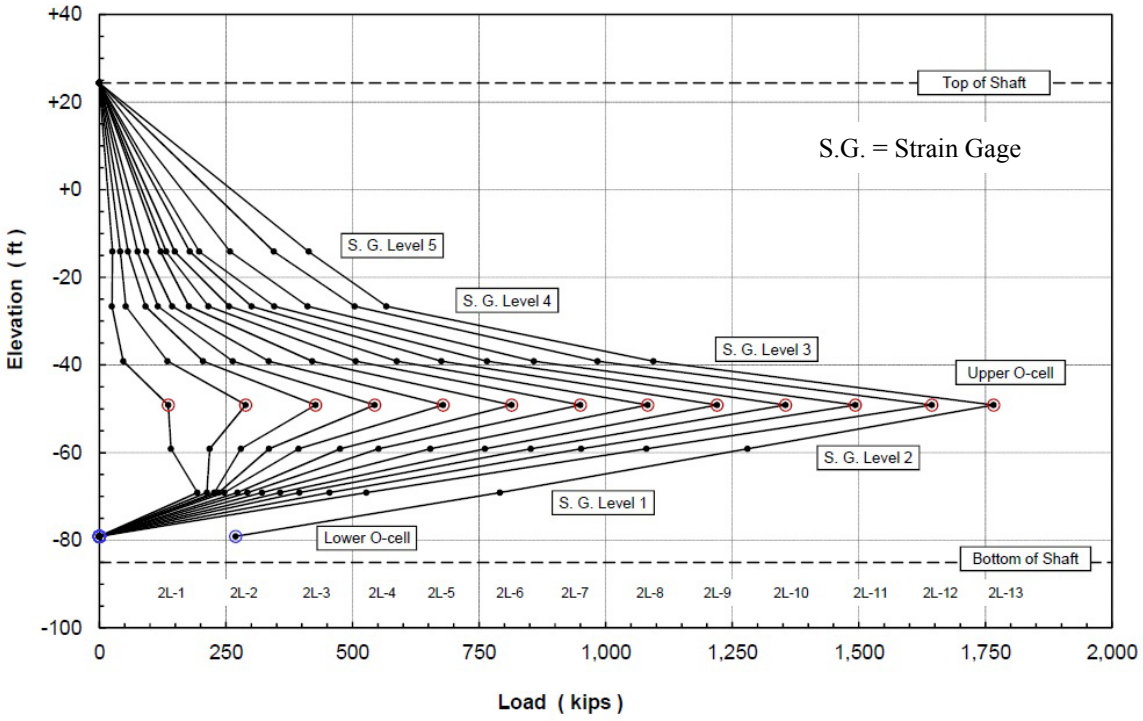

Figure 3.7 – Example of an Osterberg Load Test Load versus Depth Graph (After Loadtest, 2014)

Figure 3.7 shows the load versus depth curves for the upper O-Cell, which was pressurized as the second load stage for the example load test. A similar curve would be generated for the pressurization of the lower O-Cell, which would have been the first stage. In some cases, a third stage of both O-Cells being pressurized simultaneously is performed to evaluate the elastic modulus of the test shaft.

The primary difference between determining the unit skin resistance from an Osterberg load test (Figure 3.7) and a static load test (Figure 3.5) is that the direction of the load curve is indicative of the loading orientation, not the capacity orientation. For example, load increment 2L-13 from Figure 3.7, the load between the strain gauge at Level 2 and strain gauge at Level 1 decreases. This does not indicate that the shaft loses capacity in this increment, but rather the direction of the resistance.

3.8.3 - Statnamic Load Test Data

As a Statnamic load test applies the load in a single step, the data gathered has a time component. By rapidly measuring the load and deflection behavior as the load is applied, a load versus displacement graph, such as shown in Figure 3.8, can be developed using Statnamic load testing. Since the load is applied in a single step, the load versus displacement graph is also generated in a single step. This data is gathered by the load cell that is placed on the top of the shaft measuring the pressure from the Statnamic load rapidly and correlating that information with head displacement values that are measured at the same rate.

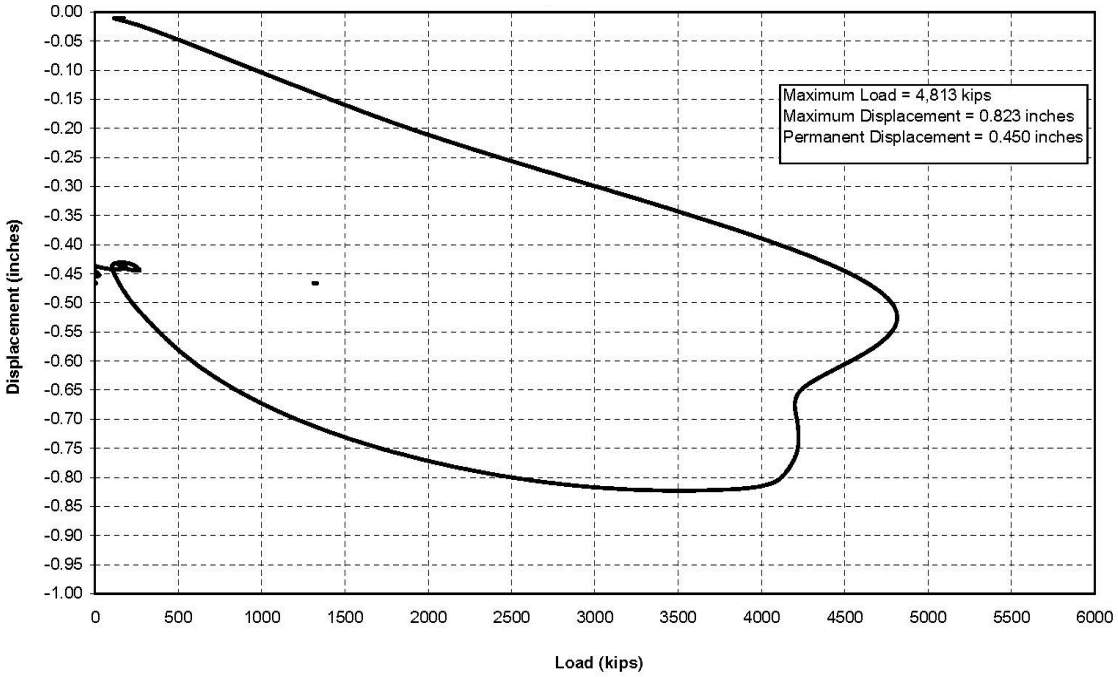

Figure 3.8 – Example of a Statnamic Load versus Displacement Graph (After AFT, 2013)

The presentation of the load versus displacement data for a Statnamic load test is presented on a segment by segment basis, which is different from the static load test and the O-Cell load test. Additionally, the Statnamic load test report generally presents a unit side shear versus displacement, as shown in Figure 3.9, instead of a load versus depth chart. However, the data presented could be used to create the same graphs shown in Figure 3.5 and Figure 3.7.

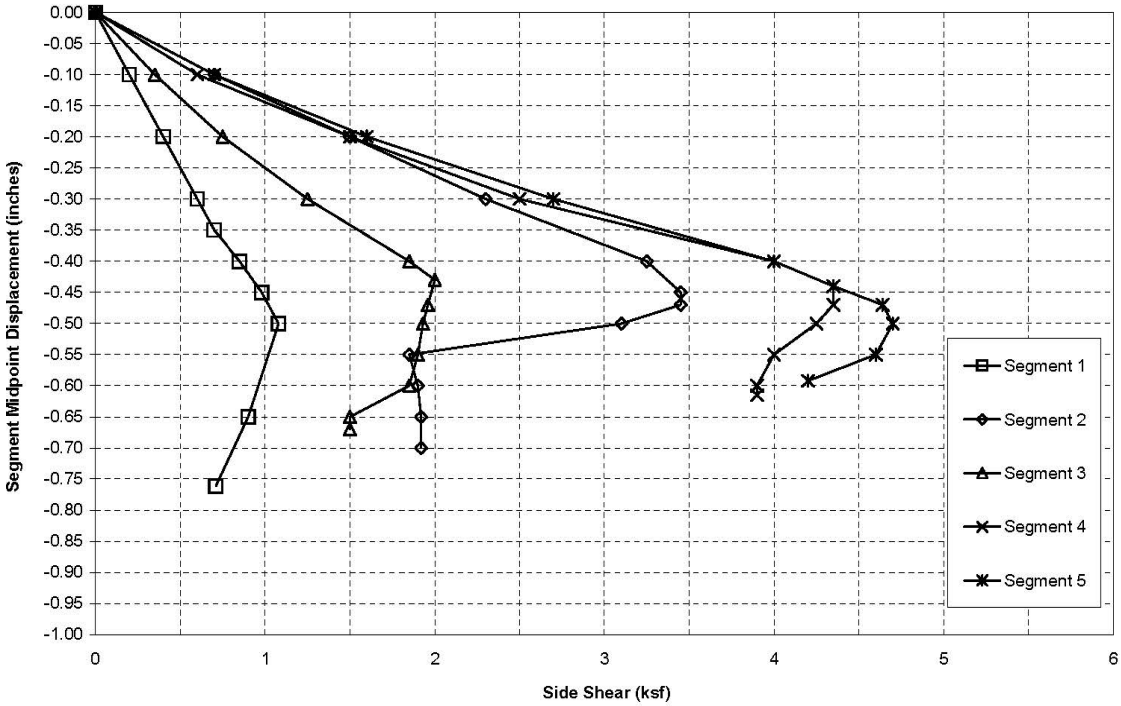

Figure 3.9 – Example of a Unit Side Shear versus Displacement Graph (After AFT, 2013)

The unit skin resistance is directly found by using the side shear values presented on the graph for each shaft segment based on that segment's midpoint displacement. The primary benefit of this graph is that it presents a good visual representation of the ultimate unit skin resistance values as well as the residual unit skin resistance values. To evaluate the unit resistance based on a given load, the displacement from the topmost segment can be compared to the shaft head deflection to approximate the load at the top of the shaft.

3.8.4 - High Strain Dynamic Load Test Data

To build the load versus displacement graph for the APPLE test, as shown in Figure 3.10, the top of the shaft is surveyed before and after each load application to determine the top elevation of the shaft before and after each load is applied. The elevations are used to determine the permanent pile displacement.

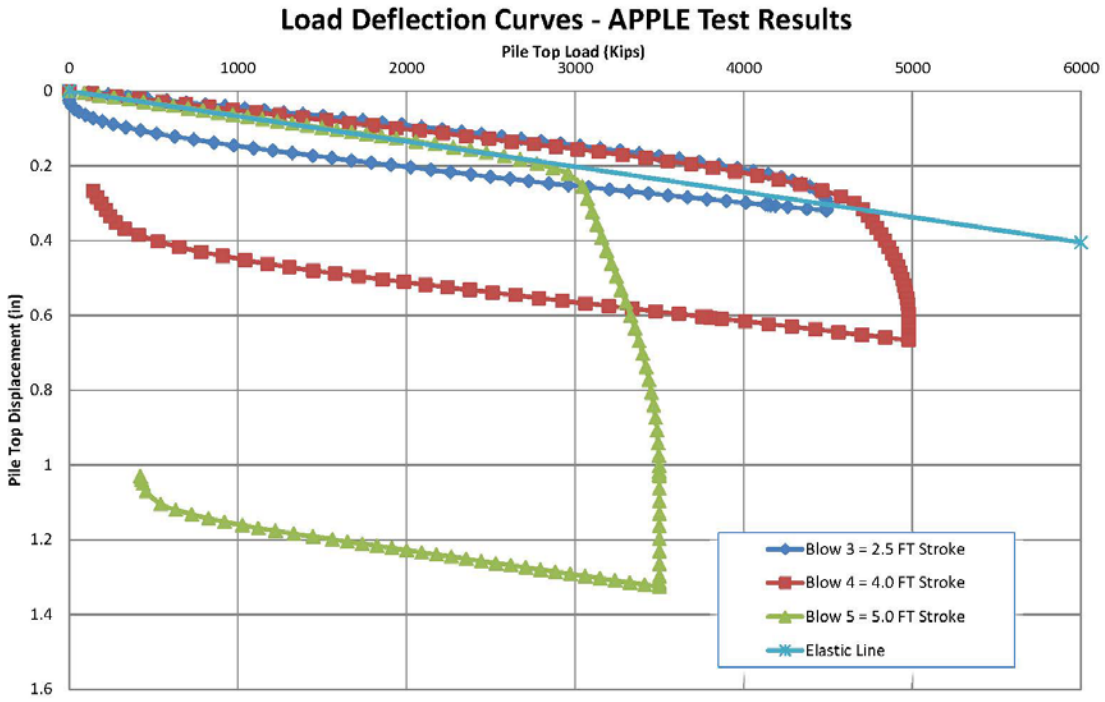

Figure 3.10 – Example of a Load versus Displacement Graph for an APPLE Test (After GRL, 2014)

The CAPWAP analysis (Hussein et al., 1992) is used to determine the load transferred to the top of the shaft as well as the slope and profile of the load versus deflection curves. The applied load is based on strain and wave acceleration measured by the strain gauges and accelerometers connected to the shaft. The load transfer is not a directly measured load throughout the length of the shaft as the test shaft is not instrumented with strain gauges below the ground surface.

The unit skin resistance values are obtained within the CAPWAP analysis based on the wave behavior in the shaft. Since the analysis is based on a signal matching methodology, the analysis is all internal to the CAPWAP software. When the shaft is loaded, the strain gauges and accelerometers measure the wave that goes down the pile as well as the wave that comes back up. The CAPWAP analysis then breaks the wave into

terms of shaft segments and determines what resistance values, damping values, and quake values would best mimic the observed wave based on soil conditions and the engineer's experience (Rausche et al., 2010).

3.9 - Drilled Shaft Axial Design

The current AASHTO bridge design methodology is the Load and Resistance Factor Design (LRFD) design method (AASHTO, 2012). This method was adopted as an alternative to the Allowable Stress Design (ASD) method in 1994 and has been used almost exclusively for bridge design since 2003. The change from ASD to LRFD was made to account for the differences in loading variability of different load types and the desire to take a more statistical approach to bridge design. In the ASD methodology, the nominal resistance, R_n, is divided by a factor of safety, FS, to determine the allowable working load, Q:

$$Q \leq \frac{R_n}{FS} \tag{3-2}$$

The primary concern with the ASD method is that all loads are weighted with the same load factor (i.e. FS) when in actuality, some load effects are more variable than others. LRFD was developed to include the addition of load modifiers and load factors to account for the statistical variation of the design loads as well as resistance factors to account for the reliability of the soil to structure interaction and of the soil consistency. The formula used to determine the factored resistance, R_r, for LRFD design is as follows:

$$Q = \Sigma \eta_i \gamma_i Q_i \leq \varphi R_n = R_r \tag{3-3}$$

where Q is the factored load, Q_i is the unfactored axial load, η_i is the load modifier, γ_i is the load factor, R_n is the nominal resistance, and φ is the resistance factor.

The purpose of the load modifiers, $\eta_{i,}$ is to account for structural global variables such as foundation redundancy, structural ductility, and operational importance of the structure from a transportation systems standpoint. In terms of foundation redundancy, a structure with more foundation elements is considered a more redundant system. For example, in a redundant system, if there was a defect in one element the other elements could support the extra load more easily. Structural ductility is based on the relative ductility of the foundation and is more a concern with lateral loading than axial loading. The operational importance is a factor of the use and location of the structure. For example, a bridge on a rural two-lane road with many detour options is not as operationally important as a bridge on a two-lane road that is the only route off of an island or a major interstate bridge.

Load factors, $\gamma_{i,}$ serve the purpose of accounting for the statistical load predictability of a certain type of load. These factors were developed based on different service loading, strength loading, and extreme loading cases. Each case considers a different set of loads to simulate a different combination of loads. These cases were developed to take into account the probability of multiple events occurring simultaneously. For example, ice loadings and hurricane wind loadings are not applied in the same load case as it would be unlikely both would occur at the same time.

In general, unfactored loads, load modifiers, and load factors are not directly dependent on the discrete geological formation in which the foundation is constructed or the applicable resistance factors. Because the scope and purpose of this thesis is to study nominal resistance and resistance factors, this thesis will focus on the right side of the

equation presented in Equation 3-3, to include nominal resistance, R_n, factored resistance, R_r, and resistance factors, φ.

3.9.1 - Nominal Shaft Resistance

Nominal resistance, R_n, is the amount of axial resistance generated by the selected foundation system. It is composed of two pieces: side resistance, also known as skin friction, and tip resistance. To predict drilled shaft axial resistance, the method of analysis is based on the soil classification of the bearing stratum for both the side resistance and tip resistance. For drilled shafts founded in the Cooper Marl, the primary design methods used in South Carolina are the alpha method (α-Method) and historical load test data method. Other methods, such as the beta method (β-Method) (Kulhawy et al., 1983), could also be used. There are also analysis methods specific to CPT data such as the LCPC Method (Bustamante and Gaineselli, 1982), Takasue Method (Takesue et al., 1998), and Eslami & Fellenius Method (Eslami and Fellenius, 1997). However, as the resistance factors were developed by AASHTO for use with the α-Method and historical load test method, the primary focus will be on those two methods. As the scope of this thesis is limited to the side resistance design, the design methodology for end bearing shafts will not be discussed.

3.9.1.1 - The α-Method

The α-Method is a total stress analysis method for evaluating the drilled shaft capacity in clays. This method was primarily developed and presented by Skempton (1959) based on observation of drilled piles in the London Clay, which is a river-deposited Eocene age clay. Prior work by Meyerhof (1951) on driven piles as well as drilled pile research by Meyerhof and Murdock (1953) and Golder and Leonard (1953)

indicated that the skin resistance of drilled and driven piles was less than the undrained shear strength for foundations built in the London Clay. There was a difference of opinion between Meyerhof and Murdock (1953) and Golder and Leonard (1953) as to the proper constant that should be used to account for the difference between the shear strength and the skin resistance for design. Skempton (1959) compiled the load test data from both previous sets of load tests with shear strength data obtained at those sites to obtain a method to relate soil shear strength to skin resistance and which he referred to as α. Early development assigned an α value of 0.45.

The equation for determining the skin resistance portion of the axial capacity using the α-Method is given by the following equation:

$$R_{SN} = \pi B \Delta z f_{SN} = \pi B \Delta z (\alpha S_u) \quad (3\text{-}4)$$

where R_{SN} is the nominal side resistance, B is the shaft diameter, Δz is the thickness of the soil layer over which the resistance is calculated, S_u is the average undrained shear strength for soil interval Δz, α is the skin resistance coefficient related to the undrained shear strength, and f_{SN} is the nominal unit skin resistance.

Note that this equation is used to calculate the total side resistance of a single drilled shaft. To calculate the design nominal unit side resistance, f_{SN}, Equation 3-5 can be simplified to give the following equation:

$$f_{SN} = \alpha S_u \quad (3\text{-}5)$$

The undrained shear strength of the soil layer is measured by undrained triaxial shear laboratory testing or found from correlations of shear strength to CPT or SPT values.

The presented value for the α-value has changed as further research has been performed. These changes were based on additional load test data and observations as well as proposed solutions based on numerical analysis. Since Skempton (1959) based his α-value on foundations in a single clay formation, revisions to the α-value occurred as his methodology was applied to additional soil formations and further research and observation was performed. Table 3.1 presents an overview of the α-values that have been proposed:

Table 3.1 – Methods for Evaluating the α-Value

α-Value	Source	Limitations
$\alpha = 0.45$	Skempton (1959)	Value based on a single clay formation.
$\alpha = 0.55$	O'Neill and Reese (1999)	Value does not account for different soil strengths or types.
$\alpha = 0.4\left[1 - 0.12*\ln\left(\frac{S_u}{P_a}\right)\right]$	Salgado (2006)	Clay fraction must be >50% and OCR between 3 and 5
$\alpha = 0$ from a depth of 0 to 5 feet $\alpha = 0.55$ when $\frac{S_u}{P_a} \leq 1.5$ $\alpha = 0.55 - 0.1\left(\frac{S_u}{P_a} - 1.5\right)$ where $1.5 \leq \frac{S_u}{P_a} \leq 2.5$ where P_a is atmospheric pressure.	FHWA (2010)	Soil must have a shear strength < 5.3 ksf

After the initial analysis by Skempton (1959), the next major update to the α-value was by O'Neill and Reese (1999). This update was presented in the 1999 FHWA Drilled Shaft Manual. The change in the suggested value was based on the addition of load test data from other clay types. With this additional load test data, the α-value was

revised to 0.55. The method proposed by Salgado (2006) was developed based on curve fitting the α-value with the intent of offering a statistical method of determining the α value , rather than the approach taken in the 1999 FHWA Drilled Shaft Manual which assigned a blanket value of 0.55 for α (FHWA, 1999) or the α of 0.45 proposed by Skempton (1959), which as discussed, was based on drilled shafts in a single soil formation.

The α-Method is the AASHTO designated method for determining the axial capacity of drilled shafts in silts and clays and is the specified method for evaluating axial resistance in conjunction with the AASHTO resistance factors (AASHTO, 2012). This method is a total stress analysis method. Use of the α-Method is laid out in the 2010 FHWA Drilled Shaft Design Manual (FHWA, 2010). The α-Method is limited for clays with shear strength less than 5.3 ksf, as the undrained shear strength to atmospheric pressure ratio is greater than the specified limit of 2.5 and is based on the normalized undrained shear strength (i.e. the ratio of the undrained shear strength to atmospheric pressure) and the depth of seasonal moisture change (FHWA, 2010).

Other methods of evaluating the α parameter have been researched using drained conditions and finite element analysis to evaluate the total stress analysis method and investigate the α parameter with effective stress analysis method results. These tests have shown variability between the drained and undrained α parameter of less than 10%, which supports the use of undrained parameters (Chakraborty et al., 2013).

3.9.1.2 - Historical Load Test Method

Prior to the development of the empirical resistance formulas or the in-situ correlation methods, common engineering practice for designing drilled shafts was based

on load tests at every site or basing a design by load tests at similar sites. These design practices eventually lead to the development of the α-Method.

More recently, the SCDOT GDM specifies a performance based method based on load tests performed in the design bearing stratum (SCDOT, 2010). Since the Cooper Marl is the primary bearing strata in many of the areas where the marl is present (Camp, 2004), the use of historical load test data could be applicable in the Cooper Marl. To use this method, the SCDOT GDM (2010) requires a minimum of five load tests in the bearing stratum to be used and a site comparison of the load test sites to the design sites to determine applicability.

3.9.1.3 - Predicted Versus Measured Skin Resistance

To complement design methodologies, studies have been performed in many geologic formations, including the Cooper Marl to assess the usage of empirical methods as compared to load test results. These studies include load testing performed in sands and gravels (Rollins et al., 2005), alluvial clays (Mackiewicz et al., 2012), and coastal plain sediments (Pizzi, 2007) to include the Cooper Marl Formation (Camp et al., 2002; Brown et al., 2008). In these studies, different empirical methods within and outside the standard methods in the AASHTO LRFD Bridge Design Specifications (AASHTO, 2012) are used and correlated back to drilled shaft load test data. Generally, the goal is to determine the appropriate α-value and/or unit skin resistance in a given formation or to determine which empirical methods are most effective in a given formation. Table 3.2 summarizes the results of some of these studies.

Table 3.2 – Predicted Skin Resistance Compared To Measured Skin Resistance

Study	Predicted Resistance	Measured Resistance	Percent Difference	Design Method	Soil Type
Camp et al. 2002	2.07 ksf	3.98 ksf	63	α-Method	Cooper Marl
Camp et al. 2002	2.94 to 4.41 ksf	3.98 ksf	10 to 30	β-Method	Cooper Marl
Camp et al. 2002	1.92 ksf	3.98 ksf	70	LCPC Method	Cooper Marl
Camp et al. 2002	0.80 ksf	3.98 ksf	134	Eslami & Fellenius	Cooper Marl
Camp et al. 2002	5.36 ksf	3.98 ksf	30	Takesue et al.	Cooper Marl
Rollins et al. 2005	10 to 187 kips	15 to 315 kips	40 to 51	β-Method	Sand and Gravel
Pizzi 2007	2380 to 4375 kips	2490 kips	5 to 55	β-Method	Sand and Gravel
Mackiewicz et al. 2012	234 to 1219 kips	1560 to 2580 kips	72 to 148	α-Method	Clay
Mackiewicz et al. 2012	334 to 936 kips	1560 to 2580 kips	94 to 129	LCPC Method	Clay

As it pertains to the Cooper Marl, the primary study regarding predicted versus measured axial capacity values was performed at the site of the Cooper River Bridge (Camp et al, 2002). At the Cooper River Bridge site, the average undrained shear strength as measured by triaxial testing was 4 ksf. Ten load tests consisting of both Osterberg and Statnamic load tests were performed at three test sites along the project corridor in conjunction with the bridge design. The average results of these load tests were compared with six empirical methods for determining the skin resistance, including the α method using an α of 0.5. Based on the results from this study, the α-Method under predicted the axial capacity at these test sites by approximately 90%. Under prediction was specifically noted in the FHWA report on the development of the geotechnical resistance factors, with the α-Method design being on average 10% below the actual

capacity for clays with undrained shear strength above 3 ksf based on an α value of 0.55 (FHWA, 2005).

3.9.2 - Resistance Factors

The change from ASD design to LRFD design necessitated the need for the development and calibration of resistance factors. For the basic foundation design parameters put forth by SCDOT, the resistance factor can be taken as the inverse of the factor of safety (SCDOT, 2010). The development of the resistance factors took a statistical approach based on the factors of safety in the ASD design. Two different methods were used in the development of the resistance factors: the calibration by fitting to the ASD factor of safety and the reliability theory calibration (FHWA, 2005).

Resistance factors, φ, are the rough equivalent of the ASD factor of safety. Their purpose is to account for the geotechnical and construction uncertainty. Selection of a resistance factor is based on the foundation type, material in which the foundation is constructed, and foundation redundancy. Other site and design variables, such as load testing, can alter the required resistance factor. Table 3.3 presents the geotechnical resistance factors for use in South Carolina.

Table 3.3 – Drilled Shaft Resistance Factors, φ (After SCDOT, 2010)

Performance Limit		Limit States			
		Strength		Service	Extreme Event
		Redundant	Non-Redundant (1)		
Nominal Resistance Single Drilled Shaft in Axial Compression in Clay	Side	0.55	0.45	N/A	1.00
	Tip	0.50	0.40	N/A	1.00
Nominal Resistance Single Drilled Shaft in Axial Compression in Sand	Side	0.65	0.55	N/A	1.00
	Tip	0.60	0.50	N/A	1.00
Nominal Resistance Single Drilled Shaft in Axial Compression in IGM	Side	0.70	0.60	N/A	1.00
	Tip	0.65	0.55	N/A	1.00
Nominal Resistance Single Drilled Shaft in Axial Compression in Rock	Side	0.60	0.50	N/A	1.00
	Tip	0.60	0.50	N/A	1.00
Nominal Resistance Single Drilled Shaft in Axial Compression with Static Load Testing		0.70	0.70	N/A	1.00
Nominal Resistance Single Drilled Shaft in Axial Compression with Statnamic Load Testing.		0.65	0.65	N/A	1.00
Nominal Resistance Single Drilled Shaft in Axial Uplift Load (Side Resistance)	Clay	0.45	0.35	N/A	1.00
	Sand	0.55	0.45	N/A	1.00
	IGM	0.55	0.45	N/A	1.00
	Rock	0.50	0.40	N/A	1.00
Nominal Resistance Single Drilled Shaft in Axial Uplift with Static Load Testing		0.60	0.60	N/A	1.00
Drilled Shaft Group Block Failure (Clay)		0.55	N/A	N/A	1.00
Drilled Shaft Group Uplift Resistance		0.45	N/A	N/A	1.00
Single or Group Drilled Shaft Lateral Load Geotechnical Analysis (Structural Capacity)		N/A	N/A	1.00	1.00
Single or Group Drilled Shaft Lateral Load Geotechnical Analysis (Lateral Displacements)		N/A	N/A	1.00	1.00
Single or Group Drilled Shaft Vertical Settlement		N/A	N/A	1.00	1.00

(1) If foundation is a hammerhead (one shaft and one column) reduce the non-redundant resistance factor by 20 percent.

The most basic method for deriving resistance factors is fitting them to the ASD factors of safety. This method takes into account the ratio of the live load to the dead load as well as the live load and dead load LRFD load factors to determine the resistance factor (FHWA, 2005). The equation used by FHWA (2005) for the resistance factor φ is:

$$\varphi = \frac{\gamma_{DL}(DL/LL)+\gamma_{LL}}{\left((DL/LL)+1\right)FS} \tag{3-6}$$

where DL is the dead load, LL is the live load, γ_{DL} is the load factor for the dead load and γ_{LL} is the load factor for the live load.

Using this method, with a given live load to dead load ratio and specified load factors from the AASHTO LRFD Bridge Design Specifications (2012) or the SCDOT GDM (2010), Equation 3-6 can be reduced to a single-variable generalized with the factor of safety as the sole input. However, this method does not take into account the probability or variability inherent in loading conditions and soil types, which make this a good method for approximation of the order of magnitude for a resistance factor without needing to perform a statistical analysis (FHWA, 2005).

To achieve a more statistically based set of resistance factors, the reliability theory method of determining resistance factors was developed and adopted by AASHTO and in turn FHWA (FHWA, 2005; Becker et al., 2005). The reliability theory method is based on a statistical analysis of the frequency of a particular load occurring, a particular resistance being achieved, the loading conditions, and the ASD factor of safety. These factors are used to determine the reliability index (β), given in Equation 3-7, which is then used in part to determine the resistance factor (Paikowsky et al., 2004; FHWA, 2005).

$$\beta = \frac{LN\left[\frac{\lambda_R FS(Q_D/Q_L+1)}{\lambda_D Q_D/Q_L+\lambda_L}\sqrt{\frac{1+COV_R^2+COV_{QD}^2+COV_{QL}^2}{1+COV_R^2}}\right]}{\sqrt{LN\left[(1+COV_R^2)(1+COV_{QD}^2+COV_{QL}^2)\right]}} \quad (3\text{-}7)$$

where,
β = the reliability index
Q_D = nominal value of the dead load
Q_L = nominal value of the live load (Q_D/Q_L is the dead load to live load ratio)
λ_R = mean of the bias values (measured/predicted) for the resistance
λ_D = the mean of the bias values (measured/predicted) for the dead load
λ_{LL} = the mean of the bias values (measured/predicted) for the live load
FS = the factor of safety used in ASD
COV_{QD} = the coefficient of variation of the bias values for the dead load
COV_{QL} = the coefficient of variation of the bias values for the live load
COV_R = the coefficient of variation of the bias values for the resistance

From a design standpoint, the target reliability index for drilled shafts is taken as 2.5 to 3.0 based on Equation 3-7 and the resistance factor is calibrated thusly (FHWA, 2005). The data sets used to calibrate the reliability indices has varied as more data has become available. The initial calibration was weighted toward the ASD factors of safety with the thought that given the success of ASD, too many changes were not necessary (Barker et al., 1991). More recently, a larger and more geographically widespread data set of load tests has been used to look at the true variability of resistances to determine the reliability index from field testing (Paikowsky et al., 2004; Abu-Farsakh et al., 2013).

Once the target reliability index is chosen, there are multiple ways of finding the correlating resistance factor. One method, assuming that the FS in Equation 3-7 is the same as Equation 3-6, would be to use Equation 3-7 to back calculate the factor of safety based on a target reliability index and then use that value to solve for the resistance factor using Equation 3-6. Another semi-empirical method presented by Becker (2005) for determining the resistance factor is presented in Equation 3-8:

$$\varphi = k_r e^{-\theta\beta V_r} \quad (3\text{-}8)$$

where k_r is the ratio of mean value to characteristic value (commonly 1.0 or 1.1 by Becker, 2005), θ is the separation coefficient (taken as 0.75 by Becker, 2006), and V_r is the coefficient of variation for the geotechnical resistance.

The other method commonly used to determine resistance factors is a fully statistical method which treats the foundation loads and resistance as random variables that are normally distributed (Paikowsky et al., 2004; Roberts et al., 2011). Based on the frequency of occurrence of a load compared to a resistance, the failure probability can be determined based on the occurrence of an overlap in the resistance and load curves from a Monte Carlo simulation. This method can be calibrated using load testing data to give a more realistic resistance distribution since soil resistances are generally more variable than a normal distribution (Abu-Farsakh et al., 2013).

3.9.2.1 - Regional and Site Specific Resistance Factors

In selection of an appropriate resistance factor, there is a caveat that higher regionally specific resistance factors can be developed by using "substantial statistical data combined with calibration or substantial successful experience" (AASHTO, 2012). Multiple states have undertaken statewide projects to determine the appropriateness of the resistance factors for those states using statistical and performance based approaches.

The State of Louisiana (Abu-Farsakh et al., 2013), when performing a statewide evaluation of resistance factors, adopted the statistical approach to evaluating resistance factors. A total of 34 load tests throughout the state and from Mississippi were used to determine the resistance distribution as well as to determine the difference between the

predicted and tested shaft resistance for both the toe and skin resistance. Using this data, the coefficient of variation was determined and used in conjunction with a target reliability index to evaluate the resistance factors and make recommendations on increasing or decreasing them. Based on their work, the recommendation was made for decreased resistance factors rather than increased ones. The recommendations for this study proposed a φ of 0.26 for skin resistance with a β of 3.0 in Louisiana. As a note, this study was based on load tests performed in multiple soil types and geologic formations.

The State of Colorado in its analysis adopted a performance based approach (Abu-Hejleh et al., 2003). The goal of their study was focused on the design of rock sockets in weak rock and mudstone based on field testing values and Osterberg load tests from four test sites. Then, the load test data was aggregated and compared with the predicted resistance from the soil test borings, pressuremeter tests, and unconfined compression tests. Based on the reliability and predictability of these field tests as compared to the measured resistance, the validity of the resistance factors was evaluated as well as a determination of minimum socket lengths. Based on the analysis of the data, the resistance factors were not revised as the resistance factors in use were supported by the performed analyses.

3.9.2.2 - Resistance Factor Usage in South Carolina Foundation Design

Currently, the SCDOT (SCDOT, 2010) specifies the geotechnical resistance factors separate from the AASHTO LRFD Bridge Design Specifications (AASHTO, 2012). These resistance factors were developed based on the LRFD analyses that are state specific, such as a fixed global modifier, and load combinations that are more common to the state as the AASHTO LRFD Bridge Design Specifications is applicable

nationwide. The main differences between the AASHTO resistance factors and the SCDOT resistance factors for axial capacity are that AASHTO does not use a different resistance factor for redundant versus non-redundant systems nor does it specify a resistance factor for statnamic / dynamic load testing. For all non-redundant and non-tested foundation systems, AASHTO and SCDOT use the same resistance factor. For drilled shafts in the Cooper Marl, the resistance factors for clay are used.

CHAPTER 4

DATA

4.1 - Load Test Data

Axial load test data from fifteen drilled shaft load test sites in the Charleston, SC area, marked on the map shown in Figure 4.1, were used to evaluate the unit skin resistance properties in the Cooper Marl. The majority of the load test data was acquired from the SCDOT by request. Additionally, some load test data was provided by request from the companies that provided the load testing services, when permissible. All of the load test data was obtained from load tests performed for public bridge projects. There are likely load tests that have been performed in the area for private projects that were not included due to data availability. These sites include tests from Charleston and Berkeley Counties. Although Cooper Marl exists in other counties, load tests could not be found in these areas that had significant amounts of Cooper Marl represented in the test shaft. Additional load testing was not performed for this thesis.

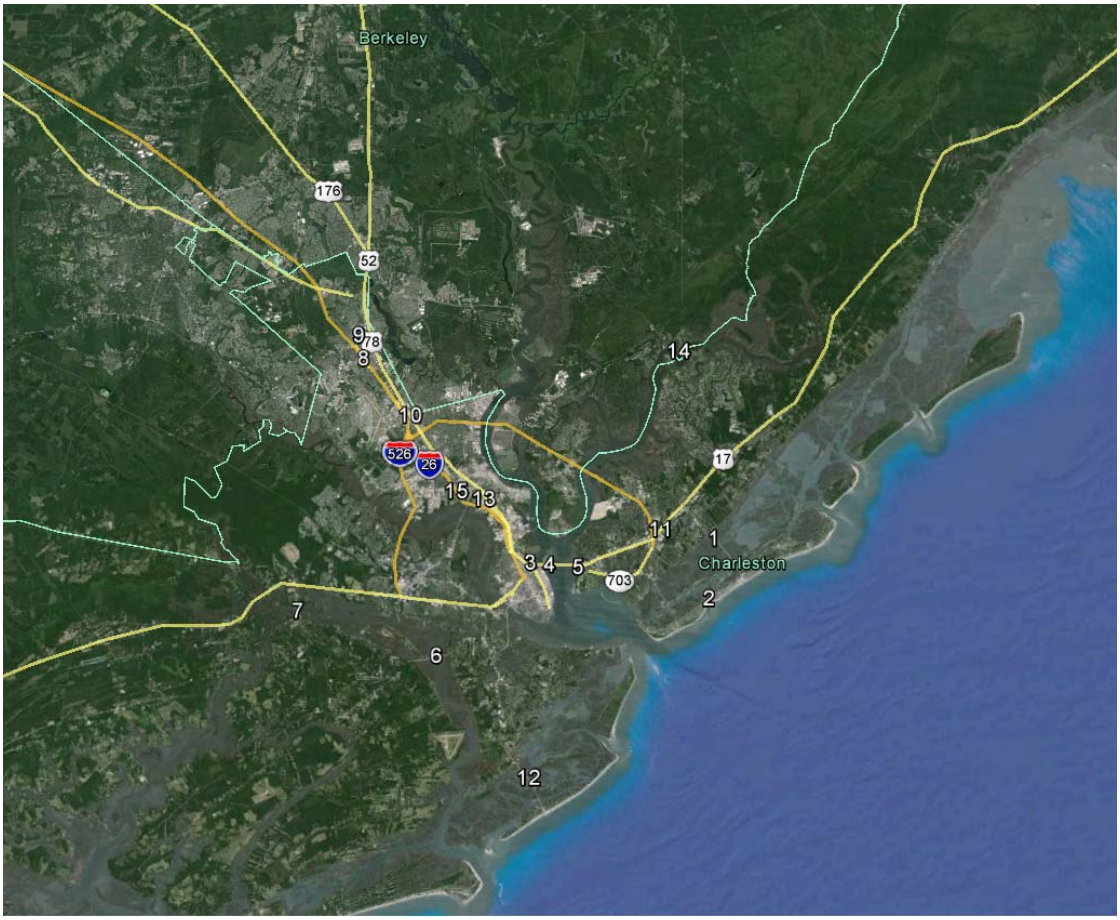

Figure 4.1 – Location Map of Load Tests (Mapping with Google Earth, 2014)

Table 4.1 summarizes the available load test data. A full list of the citations for the load test data is included in the Appendix. This data is based on a review of the drilled shaft construction logs and submitted load test reports. For each test shaft, construction information includes the test location, year tested, type of load test, shaft diameter, shaft length, depth to marl, and uncased shaft length in marl. The availability of boring logs and lab test data is also noted as well as the average mobilized unit skin resistance for the test shaft.

Table 4.1 – Summary of Available Drilled Shaft Load Test Data

Test Site	Location	Year Tested	Type of Axial Load Test	Shaft Diameter (in)	Shaft Length (ft)	Depth to Marl (ft)	Uncased Length in Marl (ft)	Boring Log Available	Lab Testing Available	Mobilized Unit Skin Resistance in Marl (ksf)
1A	Isle of Palms Connector (SC 517) - TS-1	1991	Static	24	153	101	10	Yes	Yes	3.66
1B	Isle of Palms Connector (SC 517) - TS-2	1991	Static	24	140	101	23	Yes	Yes	3.39
2	SC 703 over Breach Inlet	2000	Osterberg	48	144.4	58.4	86	Yes	Yes	1.34
3A	US 17 over the Cooper River - Charleston - C-1	2000	Osterberg	96	157.3	63	89.2	Yes	Yes	4.74
3B	US 17 over the Cooper River - Charleston - C-2	2000	Osterberg	96	157.5	63	88.6	Yes	Yes	3.99
3C	US 17 over the Cooper River - Charleston - C-3	2000	Osterberg	96	111.3	54.9	43.3	Yes	Yes	3.78[1]
3D	US 17 over the Cooper River - Charleston - C-4	2000	Osterberg	72	110.1	67.1	32.9	Yes	Yes	3.22[1]
3E	US 17 over the Cooper River - Charleston - C-3	2000	Statnamic	96	111.3	54.9	43.3	Yes	Yes	3.08
3F	US 17 over the Cooper River - Charleston - C-4	2000	Statnamic	72	110.1	67.1	32.9	Yes	Yes	8.55[2]
4A	US 17 over the Cooper River - Drum Island - DI-1	2000	Osterberg	96	158.5	57	85.5	Yes	No	3.45
4B	US 17 over the Cooper River - Drum Island - DI-2	2000	Osterberg	72	115.1	57	43.1	Yes	No	3.81
5A	US 17 over the Cooper River - Mount Pleasant - MP-1	2000	Osterberg	96	158.1	37	100.8	Yes	Yes	3.95
5B	US 17 over the Cooper River - Mount Pleasant - MP-2	2000	Osterberg	96	157	37	84	Yes	Yes	4.35
5C	US 17 over the Cooper River - Mount Pleasant - MP-3	2000	Osterberg	96	109	38	37.5	Yes	Yes	3.43
5D	US 17 over the Cooper River - Mount Pleasant - MP-4	2000	Osterberg	72	106.4	38	37.8	Yes	Yes	2.97[1]
5E	US 17 over the Cooper River - Mount Pleasant - MP-3	2000	Statnamic	96	109	38	37.5	Yes	Yes	2.93
5F	US 17 over the Cooper River - Mount Pleasant - MP-4	2000	Statnamic	72	106.4	38	37.8	Yes	Yes	5.28
6	Maybank Highway (SC 700) over the Stono River	2001	Osterberg	78	84.9	22.3	50.2	Yes	No	3.71
7	Limehouse Bridge (S-10-20) over the Stono River	2002	Statnamic	72	130.8	30.4	91.4	No	No	4.40[1]
8	Ashley Phosphate Road over I-26	2003	Statnamic	42	75.1	25	32	No	No	2.88
9	US 52 over I-26	2003	Statnamic	48	66.4	25	27.7	No	No	3.11
10	Remount Road/Aviation Avenue over I-26	2008	Statnamic	36	66.5	46	21.5	Yes	No	3.4
11	I-526/Hungryneck Boulevard over US 17	2011	Statnamic	48	120.5	92.8	20.5	Yes	No	3.73
12	Folly Road (SC 171) over Folly Creek	2012	APPLE	48	104.5	56	35.8	Yes	No	3.06
13	US 78 over CSX Railroad	2013	Statnamic	60	117.9	48	64.3	Yes	No	3.67
14	SC 41 over the Wando River	2014	APPLE	72	82.6	17	57.1	Yes	Yes	3.34
15	Cosgrove Avenue (SC 7) over CSX Railroad	2014	Osterberg	60	109.5	43.5	64.8	Yes	No	3.48

1 - Average unit skin resistance where the resistance was fully mobilized.

2 - Observed strain softening of the side shear strength was approximately 50%

4.2 - Construction Information

Each test site was assigned a number from 1 to 15 for this thesis based on the chronological order of the load tests, which were performed between 1991 and 2014. When more than one load test was performed at a given test site, a letter was assigned to differentiate between load tests. The types of load tests performed include static, Osterberg, Statnamic, and APPLE load tests. The diameter of the test shafts ranged from 24 inches to 96 inches, with all load tests performed since 2000 having a minimum diameter of 48 inches. The total length of the constructed test shafts ranged from 66.4 feet to 162.3 feet. The depth to the Cooper Marl at the time of construction ranged from 17 feet to 101 feet below present ground surface. The length of shaft embedment in the Cooper Marl for the test shafts ranged between 10 and 100.8 feet. This data is important for the analysis of the shaft capacity and is also necessary to assess the elevation of the marl tested at each test site. As an example of how these values relate to each other, a schematic of a test shaft from an Osterberg load test is presented in Figure 4.2.

For this shaft, the diameter is 60 in., the total length is 109.5 ft., the depth to marl is 43.3 ft., The cased shaft length is 44.7 ft., the uncased shaft length is 64.8 ft., the top of concrete elevation is 24.4 ft-MSL, the bottom of casing elevation is -20.3 ft-MSL, and the bottom of shaft elevation is -85.1 ft-MSL. In addition, the elevation of each strain gauge level is indicated and, in the case of an Osterberg test, the elevation of the Osterberg load cells is shown. These elevations are listed on the right side of the schematic. On the left side, a generalized soil profile with the elevation of the boundaries of each soil stratum. When used together, this figure allows the soil that corresponds to each strain gauge level to be observed.

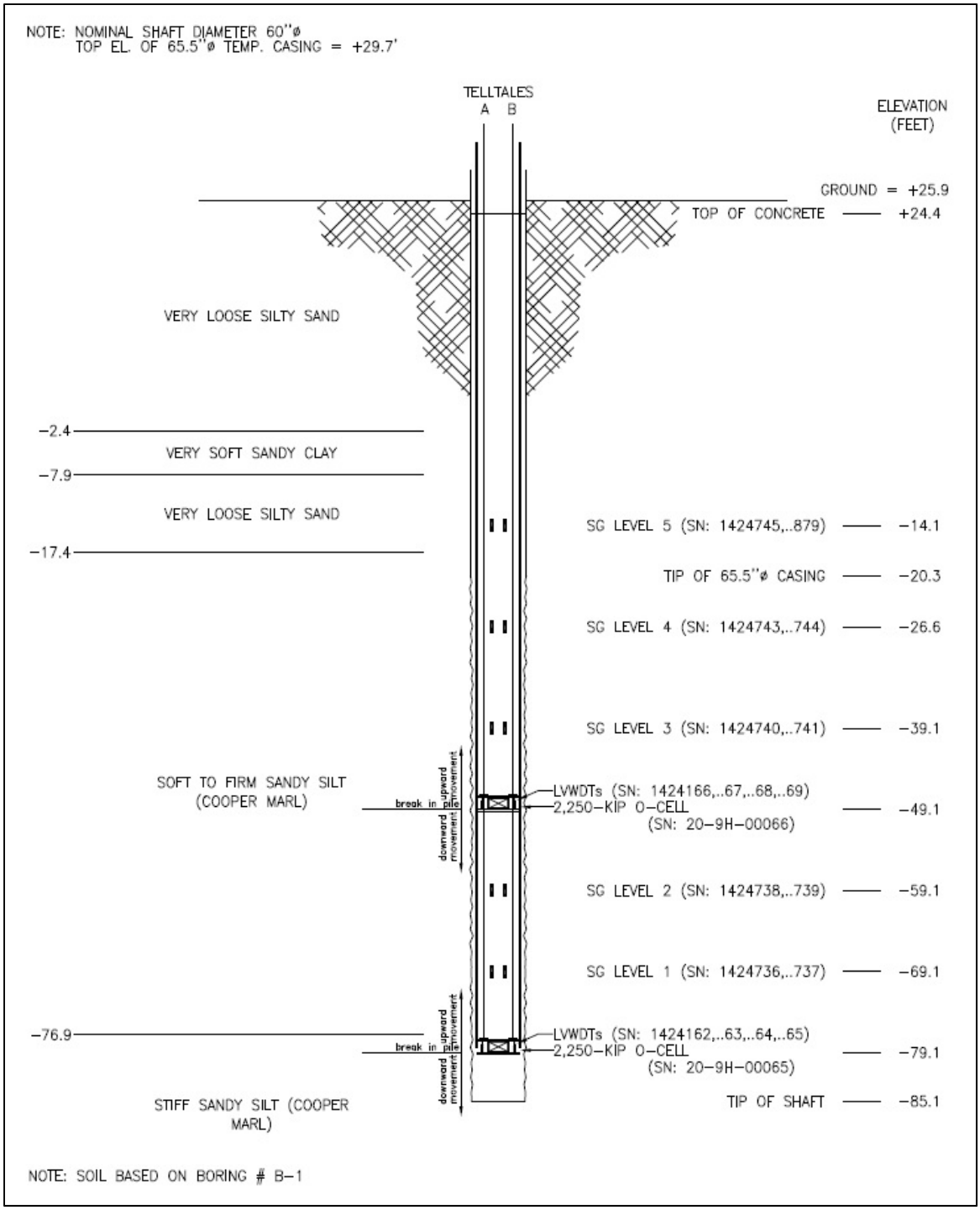

Figure 4.2 – Test Shaft Schematic Drawing (After Loadtest, 2014)

4.3 - SPT Data

For thirteen of the fifteen load test sites, SPT boring logs were available. Figure 4.3 presents the field N-value for each test site for all SPT intervals that are in the Cooper Marl at their approximate elevation. For sites where multiple load tests were performed, only one boring was available for the test site. Additionally, the constructed top of shaft elevation (TOS) has been indicated for each test site.

The N_{60} SPT values corresponding to the field SPT values for the available borings are presented in Figure 4.4. The N_{60} value is the field SPT value normalized to a hammer energy rating of 60%. The purpose of this correction is to allow N-values obtained from hammers with different efficiencies to be compared. For example, if Hammer #1 has a 40% efficiency and records a field N-value of 10 bpf and Hammer #2 has an 80% efficiency and records a field N-value of 10 bpf, once corrected to a N_{60} value, the test with Hammer #1 will have a N_{60} of 8 bpf and the test with Hammer #2 will have a N_{60} of 13 bpf.

In cases where the hammer energy rating was not specified, the energy was assumed based on the hammer type and recommendations provided by the SCDOT GDM. For an automatic trip hammer, the energy is assumed to be 80%. For drop hammers, the energy for a safety hammer is assumed to be 60% and the energy for a donut hammer is assumed to be 45% (SCDOT, 2010). For boring logs where the hammer is specified as a gravity hammer or a drop hammer but the variety is not specified, the hammer energy rating was taken as 53% for borings performed before 2010 and as 60% for borings performed during and after 2010. This year break is based on SCDOT specifically forbidding the use of donut hammers in the 2010 GDM.

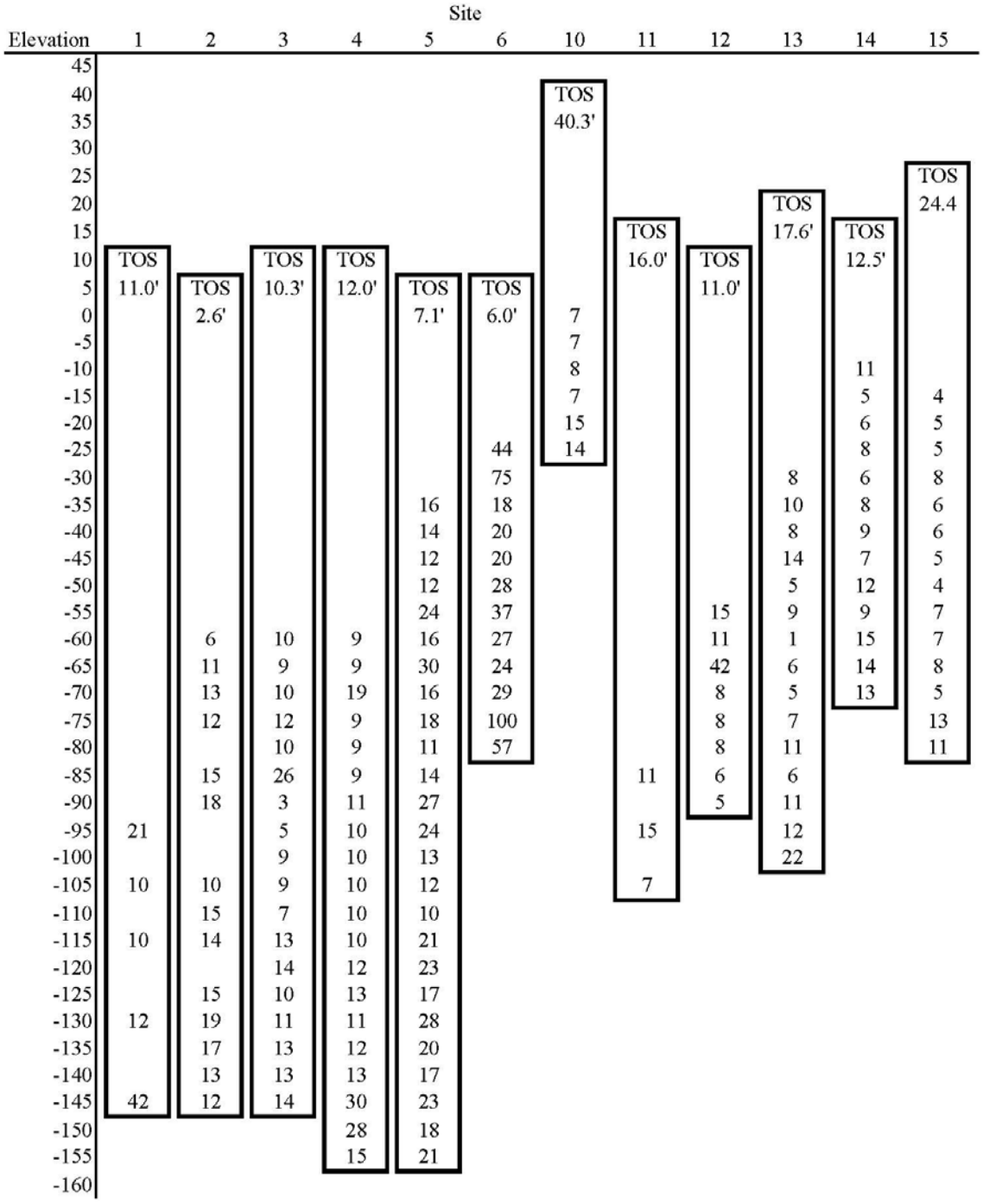

Figure 4.3 – Observed N-Values in Uncased Shaft Lengths Within the Cooper Marl

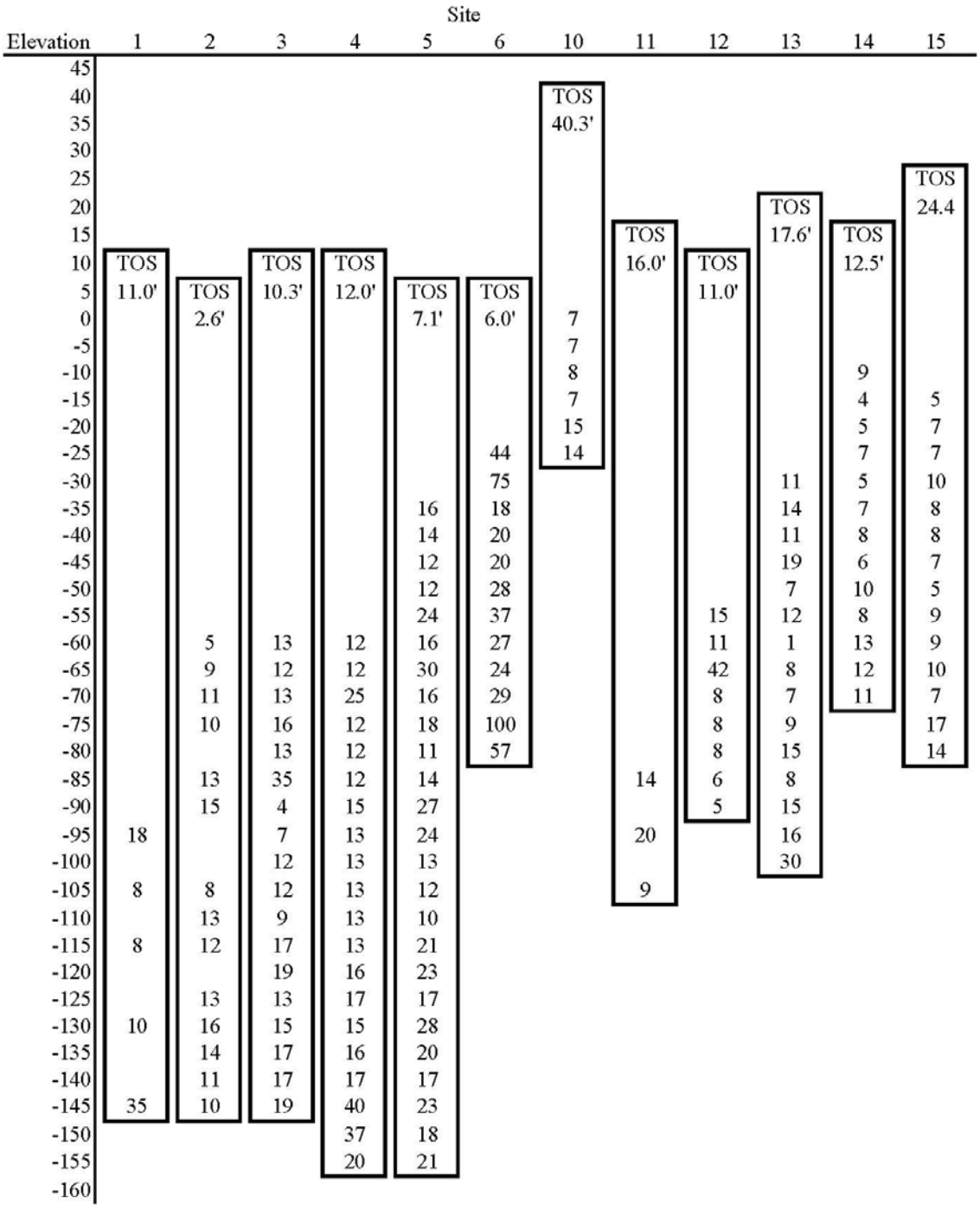

Figure 4.4 – Computed N_{60} Values in Uncased Shaft Lengths Within the Cooper Marl

The SPT values range from 1 to 100 with the majority of the N-values ranging between 5 and 17 with an average N-value of 14 for the sites that had available boring data. The N-values are consistant across the formaton and do not appear to increase or decrease with depth. Test Site 6 exhibited particularly high N-values, which is likely an indication that the test site was in the outcrop of the Parkers Ferry Formation that is located in the vicinity (see Figure 2.2). However, the boring log for this site only indicated that the soils from this site were Cooper Marl (Loadtest, 2001). As such, it is not confirmed if this shaft was in the Ashley Formation or the Parkers Ferry Formation. The N-values that are lower than expected, such as a N-value of 1 at -60 ft-MSL at Test Site 13, do not appear at any particular elevations or depths within the Cooper Marl.

4.4 - Lab Test Data

As shown in Table 4.1, lab test data was available for some of the load test sites. The Cooper Marl characteristics at the Cooper River Bridge have been well defined in the available literature (Camp, 2004), which encompasses three of the six sites where soil lab data is available with the axial load test data. The other three sites are located in the area bounded between the Cooper River and the Atlantic Ocean. This leaves eight test sites with no lab testing performed for the soils at the load test site and no lab data from a load test in the vicinity. For this analysis, the available shear strength test results will be used to investigate the relationship between undrained shear strength and unit skin resistance.

4.5 - Load Test Results

In Table 4.1, the mobilized unit skin resistance presented for each load test is the average skin resistance for all uncased shaft segments in the Cooper Marl for that shaft, to allow for a comparison between sites. The skin resistance values presented are those

reported by the issuer of the load test report. Figure 4.5 is an example unit skin resistance table that would be presented in a load test report. Note that this table includes data from all shaft segments and not just the uncased shaft segments that are in the Cooper Marl.

Load Transfer Zone	Displacement[1]	Net Unit Side Shear [2]
Zero Shear to Strain Gage Level 5	↑ 0.19 in	0.4 ksf
Strain Gage Level 5 to Strain Gage Level 4	↑ 0.20 in	0.5 ksf (0.6 ksf at 2L-12)
Strain Gage Level 4 to Strain Gage Level 3	↑ 0.20 in	2.5 ksf
Strain Gage Level 3 to Upper O-cell	↑ 0.22 in	4.1 ksf
Upper O-cell to Strain Gage Level 2	↓ 0.35 in	3.6 ksf
Strain Gage Level 2 to Strain Gage Level 1	↓ 0.34 in	3.5 ksf
Strain Gage Level 1 to Lower O-cell	↓ 0.34 in	3.4 ksf

[1] Average displacement of load transfer zone.
[2] For upward-loaded shear, the buoyant weight of shaft in each zone has been subtracted from the load shed in the respective zone. Note that net unit shear values derived from the strain gages may not be ultimate values. See Figures 9 & 10 for unit shear vs. displacement (t-z) plots.

Figure 4.5 – Example Load Test Report Skin Resistance Table from Test Site 15 (After Loadtest, 2014)

In tables of this variety, the shaft is broken into segments based on strain gauge bundle location. Then, the unit skin resistance is provided for each shaft segment. For load tests where load versus displacement graphs were available, the presented unit skin resistance values were verified by comparing the unit skin resistance presented in the load test report to the skin resistance values derived from the load versus displacement graphs.

Test shaft segments that were constructed in the Cooper Marl were assessed using the geotechnical soil borings included with the load test reports as well as the test shaft strain gauge location schematics. The unit skin resistance values from test shaft segments that were not fully constructed in the Cooper Marl were not included in the unit skin resistance presented in Table 4.1.

4.5.1 - Skin Resistance Distribution

The skin resistance data presented in Table 4.1 lists the average skin resistance in the uncased portion of the shaft for each load test. These skin resistances came from the average shaft skin resistance reported in the load test reports, an example of which is presented in Figure 4.5. However, as would be expected, there is some variation in the skin resistance along the drilled shaft. Figure 4.6 presents the skin resistance profiles for each of the load tests. These profiles were built by plotting unit skin resistance versus elevation for each of the uncased shaft segments constructed in the Cooper Marl.

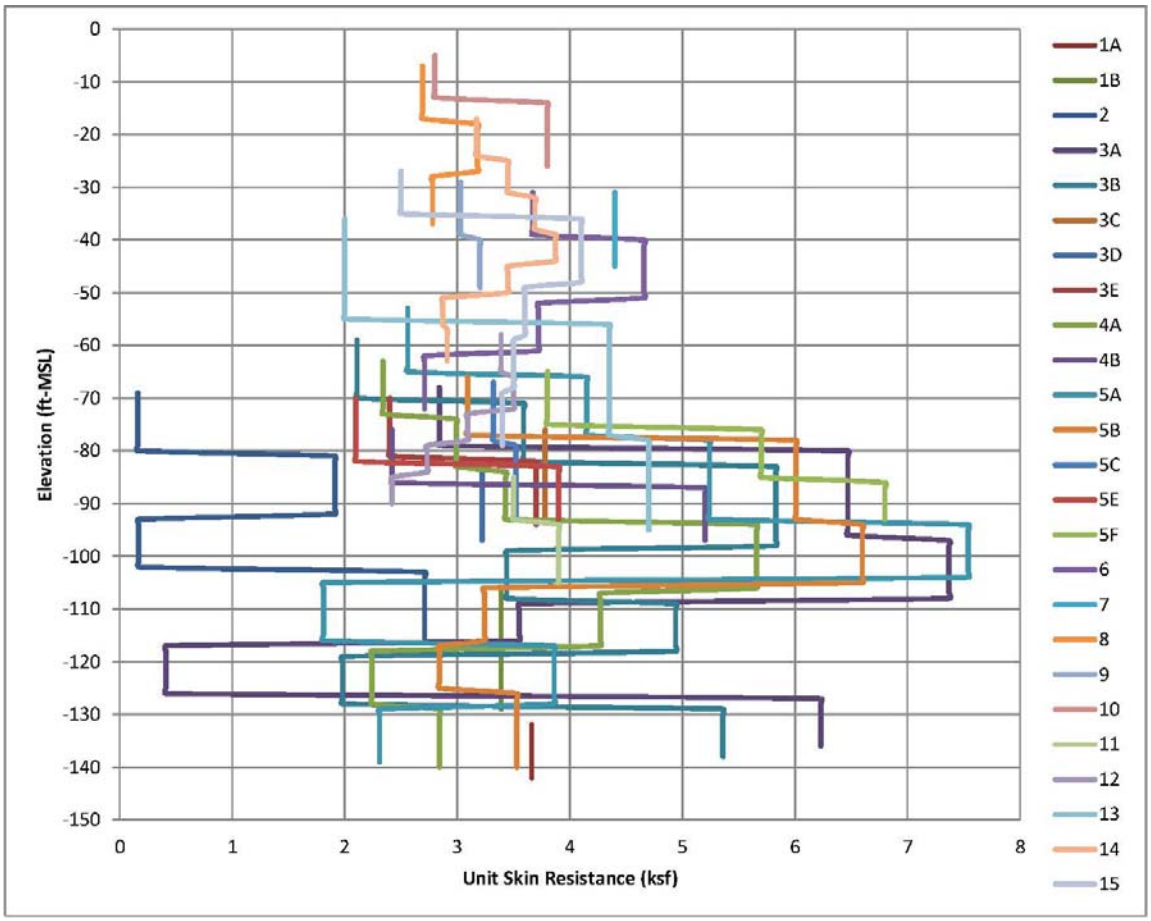

Figure 4.6 – Load Test Skin Resistance Distributions

As can be observed from Figure 4.6, the skin resistance distribution for each load test is not consistent throughout the formation. In general, the unit skin resistance

exhibits a constant with depth distribution to elevation -80 ft-MSL with a general unit skin resistance range of 2 to 4 ksf. From elevation -80 ft-MSL to -105 ft-MSL, there is a noticeable increase in the unit skin resistance for most of the load tests with an increase in the unit skin resistance of 3.5 to 7 ksf. Below elevation -105 ft-MSL, the unit skin resistance returns to a constant with depth distribution of similar magnitude to that above elevation -80 ft-MSL. However, there are outliers, such as Test Site 2 which exhibits a significantly lower resistance, approximately 30% to 50% of the expected unit skin resistance, that do not follow this generalized relationship. Load tests that do not follow the generalized relationship may be due to geological anomalies, construction effects, or other factors.

4.5.2 - Non-Fully Mobilized Test Shafts

Within the load test data, certain data sets indicated that the load test either did not fully mobilize the test shaft or that the load test was designed to primarily test the end bearing of the drilled shaft. In Table 4.1, there is a footnote that mentions that for some of the load tests, the mobilized skin resistance only accounts for the portions of the shaft where the skin resistance was fully mobilized. For these shafts, one of two things occurred during the load test. The first possibility is that the skin resistance was underestimated. One example of this is the test shaft for the Limehouse Bridge over the Stono River (Test Site 7). At this site, based on Figure 2.3 which shows the generalized geology of the Charleston, SC area, the shaft was built in an outcrop of the Parkers Ferry Formation instead of the Ashley Formation. This variation in the geology likely caused the skin friction of the shaft to be underestimated, which in turn caused the load test to be undersized.

The second case is for a load test that was designed to primarily test the end bearing of the drilled shaft. Several of the drilled shafts for the US 17 Bridge over the Cooper River (Test Sites 3 to 5) were set up in this manner. These tests were single cell Osterberg tests with the load cell close to the bottom of the shaft. This caused the load capacity above the cell to be greater than below the cell, which allowed the end bearing to be fully mobilized without needing to take upward motion of the shaft into account. In both the case of a shaft where the load test failed to mobilize the entire shaft and the case where the load test was designed to fail the bottom fully, there is some portion of the shaft that has been fully mobilized and can be used to evaluate a unit skin resistance.

4.6 - Data Sorting for Analysis

For each primary research question in Section 1.2, the data will be filtered three times to form three data sets and then analyzed using two methods. The three primary data sets are:

1. All of the load tests with the exception of 3F and 5D
2. The load tests that are construction in a geologically typical site
3. The portions of the test shafts at geologically typical sites that were constructed above elevation -100 ft-MSL.

Within these data sets, Data Set 2 is a subset of Data Set 1 and Data Set 3 is a subset of Data Set 2.

4.6.1 - Data Set 1

The first data set includes the results of all the load tests in Table 4.1 with the exception of load tests 3F and 5D. These two load tests were performed at two of the

three Cooper River Bridge test sites. They are excluded from the analysis for two reasons. Load test 3F was a Statnamic load test for the Cooper River Bridge. It was performed on a test shaft that had previously been tested using an Osterberg cell. It is excluded from the analysis due to the strain behavior from the shaft being significantly different from other drilled shaft load tests in the Cooper Marl using Statnamic load testing as it pertains to residual skin resistance compared to ultimate skin resistance. Load test 5D was an Osterberg load test that was performed on a test shaft for the Cooper River Bridge. The results from that load test are being excluded because no segments of the drilled shaft had their skin resistance fully mobilized.

As it pertains to the quality of the data for the analysis, the exclusion of these two load tests is not thought to have an effect on data set quality. While these two load tests account for 8% of the total number of load tests, the exclusion of these tests does not exclude any test sites from the analysis nor does it exclude any test shafts from the analysis. Also, the test sites where these load tests were performed had at least two multi-cell Osterberg axial load tests shafts per test site, which will allow for an effective analysis of the test site without including these two load tests data.

4.6.2 - Data Set 2

This data set is a subset of Data Set 1, which excludes load tests 3F and 5D, and includes all of the load tests that were performed at sites which were geologically similar. The geologically typical sites met these three criteria:

- The site was not located in an active tidal zone;
- The site was located either in the Ashley Formation or the Parkers Ferry Formation as defined by Weems and Lewis (2002);

- The site did not have any mention of geologic abnormalities noted in the load test report or the boring log.

While the Cooper Marl is treated as a homogeneous geologic formation, there were some atypical geologic conditions encountered at some of the test sites. These conditions were the dynamic hydraulic conditions at Test Site 2 and the proximity to an outcrop of the Parkers Ferry Formation at Test Sites 6 and 7. Within the Charleston area, this generally encompasses nearly all sites with the exception of sites that are on and between barrier islands. Based on this geological variation, the load test data from Test Site 2 was excluded from geologically typical site data set. It should be noted that the load test at Test Site 2 exhibited significantly lower skin resistance (on the order of a 60% less) than the test sites that were located farther from the Atlantic Ocean. If geotechnical test data were available, the Cooper Marl characterization put forth by Camp (2004) and discussed in Section 2.4 should be used to judge if the marl encountered is typical of the formation by evaluating the engineering properties.

4.6.2.1 – Hydraulic Effects around Barrier Islands

Test Site 2 is located at Breach Inlet, which is the waterway between Sullivan's Island and Isle of Palms. Of the 15 test sites, Test Site 2 was the only one to be located in the direct vicinity of a tidal inlet. As such, the soils at this test site have been exposed to more hydraulically dynamic conditions than the other 14 test sites (Hayes et al., 2013). And, unlike the rest of the test sites, Test Site 2 has been exposed to tidal activity since the Oligocene Epoch. But, the effects on the engineering properties of the Cooper Marl have not been studied to date. Based on these factors, Test Site 2 was excluded from

Data Set 2 due to the possibility of the soil engineering properties being altered due to dynamic hydraulic conditions that were not found at the other tests sites.

4.6.2.2 - Marks Head Formation

When evaluating sites, the presence of the Marks Head Formation must be taken into account. As discussed in Section 2.5, the Marks Head Formation is found on top of the Ashley Formation and has similar visual properties to the Ashley Formation (Cooper Marl), but is not known to have the same engineering properties or unit skin resistance properties. As such, the likely presence of this formation should be taken into account by using the available geologic research. None of the boring logs and load test data for the load tests included in Data Set 2 indicated that Marks Head Formation was encountered or identified. Thus, no sites were excluded based on the presence of the Marks Head Formation.

4.6.2.3 - Parkers Ferry Formation

In their geologic survey of the Charleston, SC area, Weems and Lewis (2002) make note of several outcrops of the Parkers Ferry Formation. The three most notable outcrops are an outcrop between Summerville and Goose Creek, an outcrop north of Huger which tracks along SC Hwy. 41, and an outcrop on Johns Island and James Island running along the Stono River. Two test sites, 6 and 7, are located near the outcrop that runs along the Stono River. Based on the map produced by Weems and Lewis (2002), neither of these sites is directly on the outcrop; however, it is not known how near the surface the Parkers Ferry Formation is at these sites. From an engineering perspective, as stated by Camp (2004), both the Ashley Formation and the Parkers Ferry Formation can be treated as Cooper Marl. Test Sites 6 and 7 were not excluded from Data Set 2 since

the Parkers Ferry Formation is considered to be part of the Cooper Marl for engineering purposes.

4.6.3 - Data Set 3

This data set includes only the skin resistance values for segments of the test shafts that were constructed above elevation -100 ft-MSL at the geologically typical sites. The purpose of using this data set for analysis is to provide a practical application analysis based on the typical length of production drilled shafts. Of the geologically typical test sites, only four have appreciable data below elevation -100 ft-MSL: Sites 1, 3, 4, and 5 with Test Site 1 having all of the skin resistance values in the Cooper Marl recorded below elevation -100 ft-MSL. Test Site 11 had five feet of data recorded below elevation -100 ft-MSL.

4.6.4 - Data Analysis Methods

For each of the three data sets, analysis and observations were drawn using two different methods: incremental analysis and whole site analysis. For the incremental analysis, each discrete one foot portion of the shaft was treated as a single skin resistance point for the analyses. The whole site analysis took the weighted average of the skin resistance at each test site and treated each test site as a data point for the analyses. The purpose of the two separate analyses was to investigate how the soil/shaft interface acts in discrete segments as well as how a drilled shaft acts as a whole.

CHAPTER 5

METHODOLOGY

5.1 - Introduction

This chapter presents the methodologies that were used to answer the three research questions proposed in Chapter 1. Additionally, the data sets that were used will be stated.

5.2 - Relationship between Skin Resistance and Geotechnical Properties

With most geologic formations, relationships between in-situ geotechnical properties and unit skin resistance can be developed. These relationships aid in drilled shaft design without the need for load testing. In the majority of the load test data obtained, SPT information was included in the report. Data Set 1 was used to evaluate a possible relationship between SPT N-values and unit skin resistance. Additionally, the relationship between the effective overburden pressure and the unit skin resistance was evaluated. Other types of data, such as shear strength data, were limited and only available from a few sites.

5.2.1 - Relationship of Skin Resistance to SPT N-Values

As shown in Figure 4.3 and Figure 4.4, SPT N-values were available for twelve of the load test sites. To investigate the relationship between the SPT values and the measured skin resistance, the skin resistance for each N-value increment was found in the drilled shaft report. The data was then plotted on a scatter plot with SPT N-value on the

X-axis and unit skin resistance on the Y-axis. Plots were generated for both the field N-values and the derived N_{60} values. Once the data was plotted, a linear best fit line was determined and the R^2 value was used to evaluate appropriateness of the best fit equation.

To analyze the relationship between the SPT N-values and the unit skin resistance, each SPT value was paired with its related load test measured unit skin resistance. These values were then plotted versus the SPT N-value. This was performed for both the field N-values and the N_{60} values using the load test data groupings listed in Section 4.6. Since Test Sites 7, 8, and 9 did not have SPT data they were not included in these analyses.

5.2.1.1 - Data Exclusions

The data point at elevation -30 ft-MSL for Test Site 6 was excluded from the SPT N-value analysis because the recorded SPT N-value was over twice as large as 97% of the other recorded N-values. This point appears to be an outlier in the overall N-value data. As such, it has been excluded. Since this data point represents less than 1% of the total data points, the exclusion has a small effect on the results of the analysis.

5.2.1.2 - Data Significance

On each graph, a linear trend line was established to assess the linear relationship of the skin resistance and the N-values. To judge the appropriateness of the linear relation to the data, the coefficient of determination (R^2) was evaluated for the linear model. An R^2 value of 1 represents an perfect data correlation between the trend line and the data while a R^2 of 0 indicates there is no relationship between the data and the trend line. As geotechnical data is naturally highly variable, a target R^2 has not been specified

for these analyses to be considered statistically significant, the R^2 was treated more as an indicator, rather than an absolute.

5.2.2 - Relationship of Skin Resistance to Elevation

Although the designated method for the empirical evaluation of drilled shaft unit skin resistance, the α-Method, relies on the undrained soil shear strength, S_u, limited soil shear data is available from the same sites where load test data is also available. Based on the boring logs included with the load test reports, undisturbed samples were obtained at test sites 1 through 5 by means of Shelby Tube sampling. However, the results of shear strength testing, when or if performed, were not presented in the load test reports.

To evaluate the relationship between unit skin resistance and elevation, the data from Figure 4.6 was combined to build a composite unit skin resistance versus elevation plot. Data Set 1 was used in this analysis. The plot was used to look for trends in the unit skin resistance and evaluate the presence of layers in the marl that yield a higher skin resistance or lower skin resistance as well as evaluating trends that would be associated with elevation.

5.2.3 - Relationship of Skin Resistance to Effective Overburden Pressure

Based on the available shaft construction information, the relationship between the effective overburden pressure and the unit skin resistance was evaluated using Data Sets 1, 2, and 3. To investigate this relationship, the effective overburden pressure was calculated for the midpoint of each shaft segment as defined in the drilled shaft load test report. The data was then plotted on a scatter plot with effective overburden pressure on the X-axis and unit skin resistance on the Y-axis. Once the data was plotted, a linear best

fit line was determined and the R^2 value was used to evaluate appropriateness of the best fit equation.

When performing this analysis, a total unit weight of 108 pounds per cubic foot (pcf) was used for the Cooper Marl. This value is based on undisturbed sample densities presented in the Isle of Palms Connector Load Test report (LAW Engineering, 1991). The total unit weight of the overburden soils was assumed to be 105 pcf foot based on the available boring logs.

5.2.4 - Relationship of Skin Resistance to Undrained Shear Strength

In the study by Camp et al. (2002) regarding drilled shaft axial response at the Cooper River Bridge, shear strength data is presented, with the average undrained shear strength across all three test sites being 4.0 ksf. Figure 2.4 presents the full shear strength data set. No other load test sites had available shear strength data. This average undrained shear strength was used in conjunction with the average load test measured skin resistance to estimate an α-value in the Cooper Marl. This α-value was estimated using Data Set 1, Data Set 2, and Data Set 3. The results of this were compared with the results from Camp et al. (2002), which were only based on the Cooper River Bridge test sites.

5.3 - Design Skin Resistance

To evaluate the unit skin resistance data to assess a reasonable design skin resistance for sites with no load test data, two methods were used. The first method used statistical data to evaluate the skin resistance based on the 97.5% confidence interval and the normal distribution. The second approach used the historical load test method as it would be applied in general engineering practice. Additionally, it was necessary to

evaluate which method and data set and skin resistance value best represents a typical construction site.

5.3.1 - Statistical Analysis Method

For evaluation of the design skin resistance, the unit skin resistance was found by dividing the length of the shaft at each test site into one foot increments and taking the unit skin resistance of each increment as a data point. For test sites with multiple load tests, the average unit skin resistance for each one foot increment was used as a single data point to avoid test sites with multiple load tests skewing the data sets. Once the per foot resistance was found for each site, the coefficient of variation was found for six data sets as defined in Section 4.6:

1A. Data Set 1 on a per foot basis

1B. Data Set 1 on a per site basis

2A. Data Set 2 on a per foot basis

2B. Data Set 2 on a per site basis

3A. Data Set 3 on a per foot basis

3B. Data Set 3 on a per site basis

This data was plotted in a bar graph to examine the standard statistical distribution of the unit skin resistance and to determine the mean and standard deviation of the data set. Once the data was aggregated, the expected design unit skin resistance was found by 97.5% confidence interval of the data based on a normal distribution

5.3.2 - Historical Load Test Method

The historical load test method as defined in the SCDOT Geotechnical Design Manual for assessing skin resistance was evaluated. This method is an empirical method

that uses load tests performed at other sites in the same geologic formation to predict unit skin resistance at a site. SCDOT (2010) specified three conditions for using this method:

- More than five load tests shall be used to develop the capacity;
- Load testing shall include static (to include Osterberg), dynamic, and Statnamic load tests;
- The soils at the load test sites shall be compared to the soils at the design location.

To satisfy these requirements, 25 load tests at 15 sites were used in the analysis. These load tests were divided into three data sets. This involved finding the per site average skin resistance and taking the average of the five lowest skin resistances based on the three data sets defined in Section 4.6:

1. Data Set 1 on a per site basis (Test Sites 2, 8, 9, 12, and 14)
2. Data Set 2 on a per site basis (Test Sites 8, 9, 10, 12, and 14)
3. Data Set 3 on a per site basis (Test Sites 8, 9, 10, 12, and 14)

For all three data sets, there were load tests of multiple varieties. For Data Set 2 and Data Set 3, no static or Osterberg load test was included since the dynamic load tests exhibited lower unit skin resistance. The average of the five load tests that showed the lowest unit skin resistance was chosen instead of using the average of all the load tests to prevent the over prediction of unit skin resistance. Taking the average of all of the sites would imply that 50% of the time, the test value would be below the predicted value.

5.4 - Axial Resistance Factor

For this analysis, one of the empirical methods for determining resistance factors presented in Section 3.9.2 was used to find a range of appropriate resistance factors for

drilled shafts in the Cooper Marl. This empirical method used Equation 3-8 as presented by Becker (2005). For utilization of this equation, the geotechnical coefficient of variation was developed by dividing the length of the shaft at each test site into one foot increments and taking the unit skin resistance of each increment as a data point. For test sites with multiple load tests, the average unit skin resistance for each one foot increment was used as a single data point to avoid test sites with multiple load tests skewing the data sets. Once the per foot resistance was found for each site, the coefficient of variation was found for six data subsets:

1A. Data Set 1 on a per foot basis

1B. Data Set 1 on a per site basis

2A. Data Set 2 on a per foot basis

2B. Data Set 2 on a per site basis

3A. Data Set 3 on a per foot basis

3B. Data Set 3 on a per site basis

As summarized in Table 5.1, a reliability index of 2.5 and 3.0 was used, as this is the target range presented by the FHWA (2005). The other constants in Table 5.1, the ratio of mean value to characteristic value, k_r, and the separation coefficient, θ, were taken as presented by Becker (2005). In cases where there are multiple values, the high value and the low value were evaluated.

Table 5.1 – Constants for Becker (2005) Resistance Factor Equation

Value	High	Low
β	3.0	2.5
k_r	1.1	1.0
θ	0.75	

5.5 - Analysis Assumptions

Within these analyses, some assumptions were made regarding the load testing and construction methodologies. The following is a discussion of these design assumptions.

5.5.1 - Osterberg Cell Effects on Statnamic Load Tests

At Test Sites 3 and 5, four test shafts were subject to multiple types of load tests. This was accomplished by using an Osterberg cell mounted in the bottom of the drilled shaft to test the end bearing of the Cooper Marl followed by a Statnamic test to measure the skin resistance of the test shaft. The possible effect on the Statnamic load test data from the Osterberg cells in the test shafts is unknown as it is uncommon for a shaft instrumented with an Osterberg cell to then be retested using a different method. Research performed in Florida by Kim (2001) on shafts that were tested with both Osterberg cells and Statnamic load testing indicated that in general, Statnamic load tests in that geologic area exhibited a higher skin resistance but did not indicate effects on the Statnamic load test results caused by the Osterberg cells. For this analysis, the assumption is made that the Osterberg cells do not affect the Statnamic load test results and that the initial Osterberg test did not alter the skin resistance properties of the shaft.

5.5.2 - Effects of Construction Methodology on Skin Resistance

As discussed in Section 3.3, Camp et al. (2002) investigated the effect of the wet shaft construction method as compared to the dry shaft construction method in the Cooper Marl and concluded that the use of drilling slurry did not have a significant effect on unit skin resistance. As a caveat to this conclusion, the test shafts used for that

assessment all have the same construction method in terms of shaft excavation sidewall roughness, augers used for excavation, concrete placement, and shaft verticality.

The work by Camp et al. (2002) encompassed the test shafts at Test Sites 3, 4, and 5. For the other test sites used herein that were not included in this study, there is not enough information to assess the construction methodology of the drilled shafts. Given that the test shafts were constructed over a 23 year time period by at least three different drilled shaft contractors, it is likely that there are differences in some of the construction methodologies. For this analysis, it was assumed that different construction methodologies are not a significant source of error from site to site in the Cooper Marl. This assumption is based on the research performed by Camp et al. (2002) and that no major changes in construction methods have be implemented since the previous study.

5.5.3 - Unit Skin Resistance Correction for Load Test Type

Within the 27 load tests evaluated for this analysis, all four types of load tests were included. From a design standpoint, the usage of a Statnamic load test or an APPLE load are treated differently than a static load test or an Osterberg load test in terms of the change in the geotechnical resistance factor with the static and Osterberg using a 0.70 resistance factor and the Statnamic and APPLE using a 0.65 resistance factor. However, the effect of the load test type on the unit skin resistance must be addressed in order to weight each load test equally. Table 5.1 summarizes the average unit skin resistance by load test type as well as the number of tests of that type.

Table 5.2 – Unit Skin Resistance by Load Test Type

Load Test Type	Number of Tests	Unit Skin Resistance (ksf)
Static	2	3.52
Osterberg	12	3.60
Statnamic	9	3.61
APPLE	2	3.20

Table 5.1 shows that Statnamic and Osterberg load tests indicate similar unit skin resistance with the APPLE test showing an average of 10% lower unit skin resistance, albeit it with a small sample size (two APPLE tests) and with the static load test showing a 4% lower unit skin resistance from the Statnamic and Osterberg load tests with a similarly small sample size. Based on these results, all of the load test results were equally weighted in the analysis. Additional discussion of the effects of load test type is included in Section 3.7.6.

CHAPTER 6

DATA ANALYSIS

6.1 - Introduction

In this section, the analysis of the data presented in Chapter 4 will be performed. Also, the research questions presented in Chapter 1 will be discussed in depth as well as the statistical significance of the results of this analysis.

6.2 - Skin Resistance Versus SPT N-values

Based on the N-values presented in Figures 4.3 and 4.4 and the load test unit skin resistance values presented in Table 4.1, Figure 6.1 and 6.2 were built to evaluate the data relationship between N-values and unit skin resistance. More detailed skin resistance is included in the Appendix. These figures include the data from all the test sites that had boring logs (see Table 4.1) in Data Set 1. Each test site (TS) is presented as a separate marker type with a trend line for all the sites combined. The trend lines represent the best fit linear equation of all of the data sets.

Using the same sets of N-values, Figure 6.3 and 6.4 were built based on the sites in Data Set 2 that have SPT data. Data Set 3 was evaluated and the results are presented in Figure 6.5 and Figure 6.6. To investigate the effects of load test type on this relationship, Figures 6.7 and 6.8 present the SPT and unit skin resistance sorted by load test type for Data Set 3.

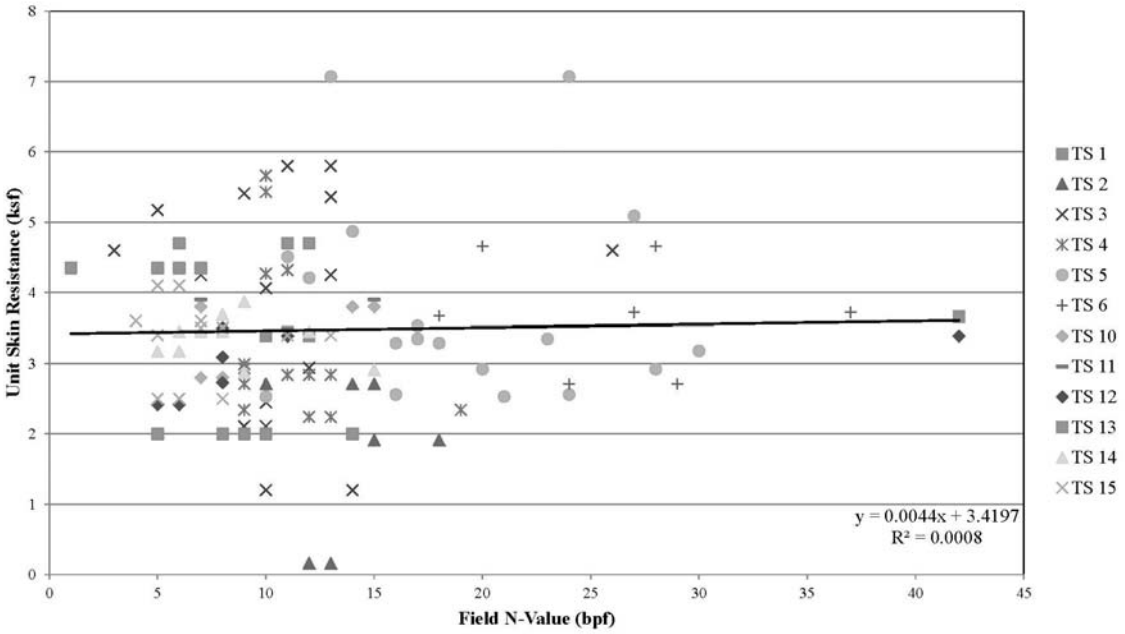

Figure 6.1 – Field N-Values versus Unit Skin Resistance for Data Set 1

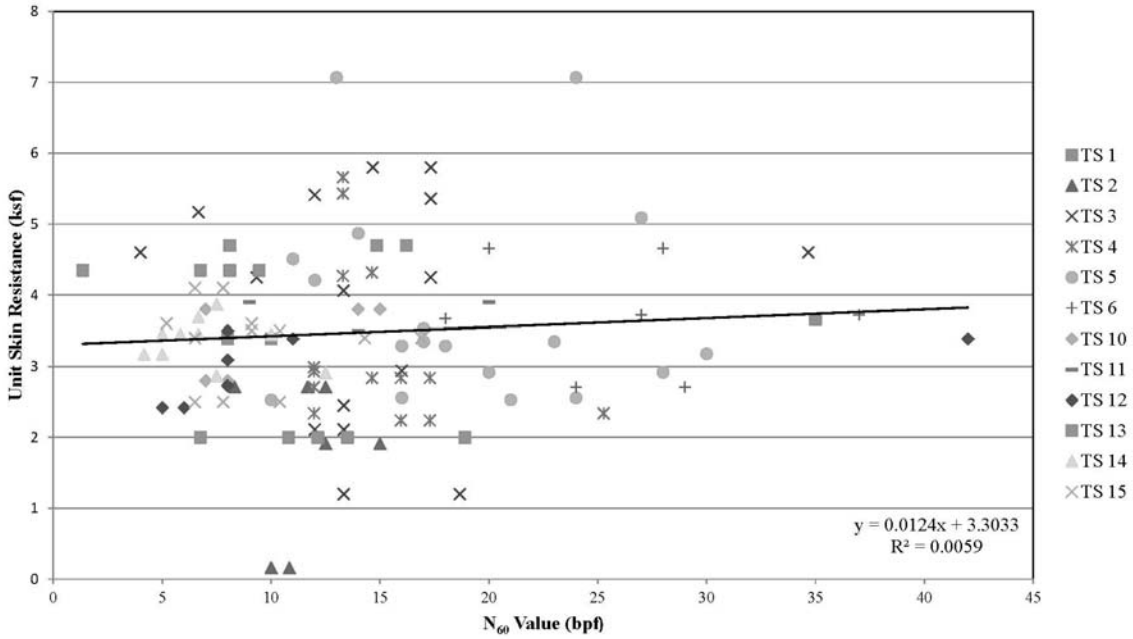

Figure 6.2 – N_{60} Values versus Unit Skin Resistance for Data Set 1

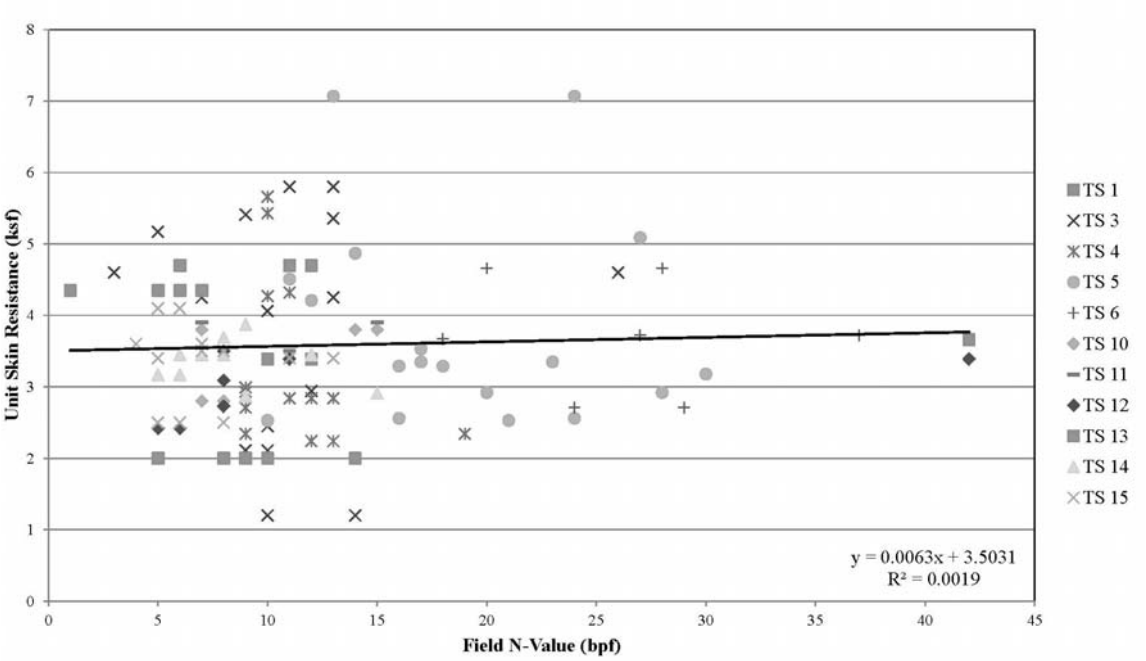

Figure 6.3 – Field N-Values versus Unit Skin Resistance for Data Set 2

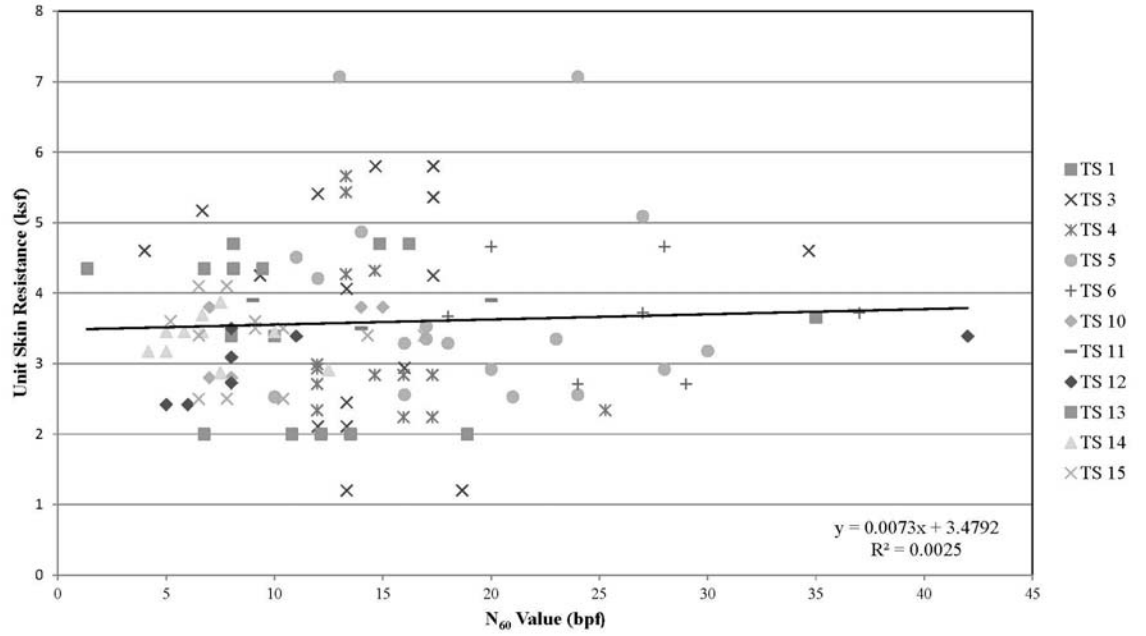

Figure 6.4 – N_{60} Values versus Unit Skin Resistance for Data Set 2

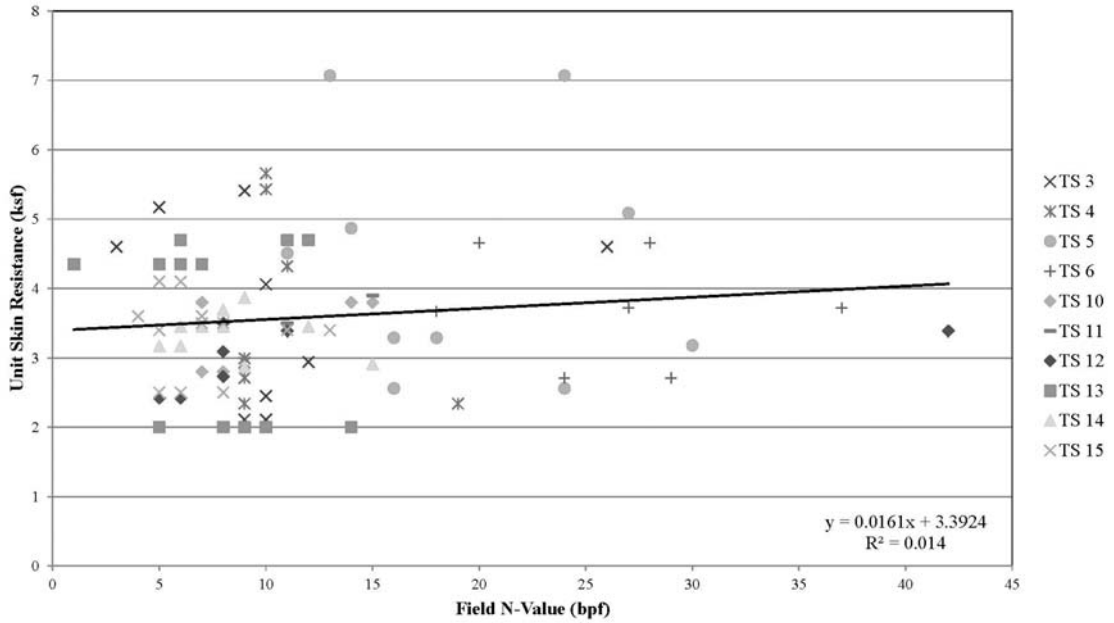

Figure 6.5 – Field N-Values versus Unit Skin Resistance for Data Set 3

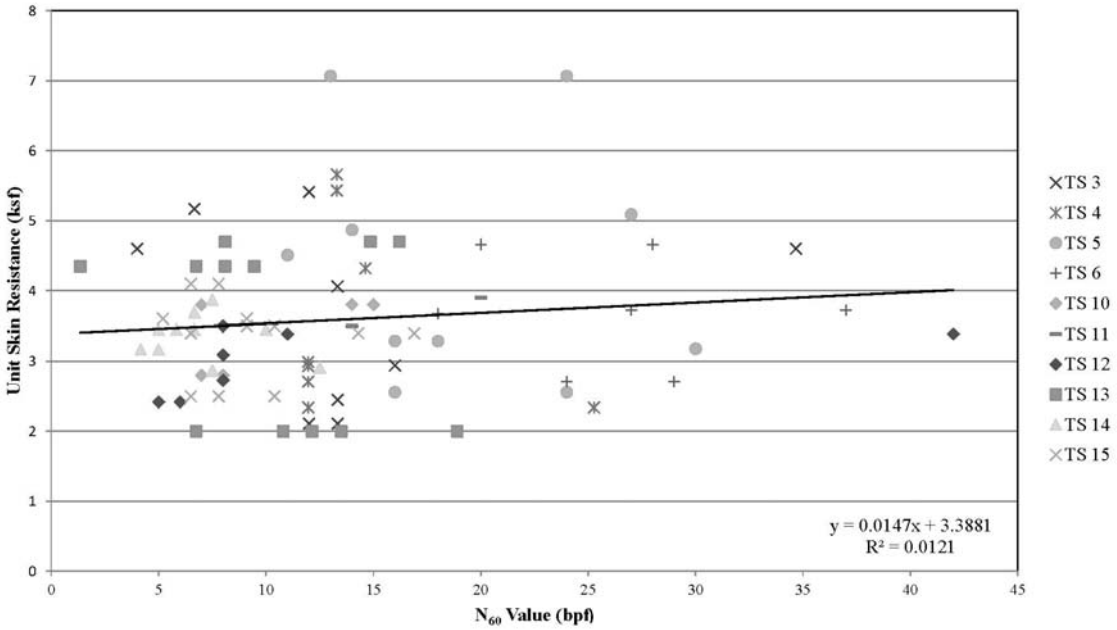

Figure 6.6 – N_{60} Values versus Unit Skin Resistance for Data Set 3

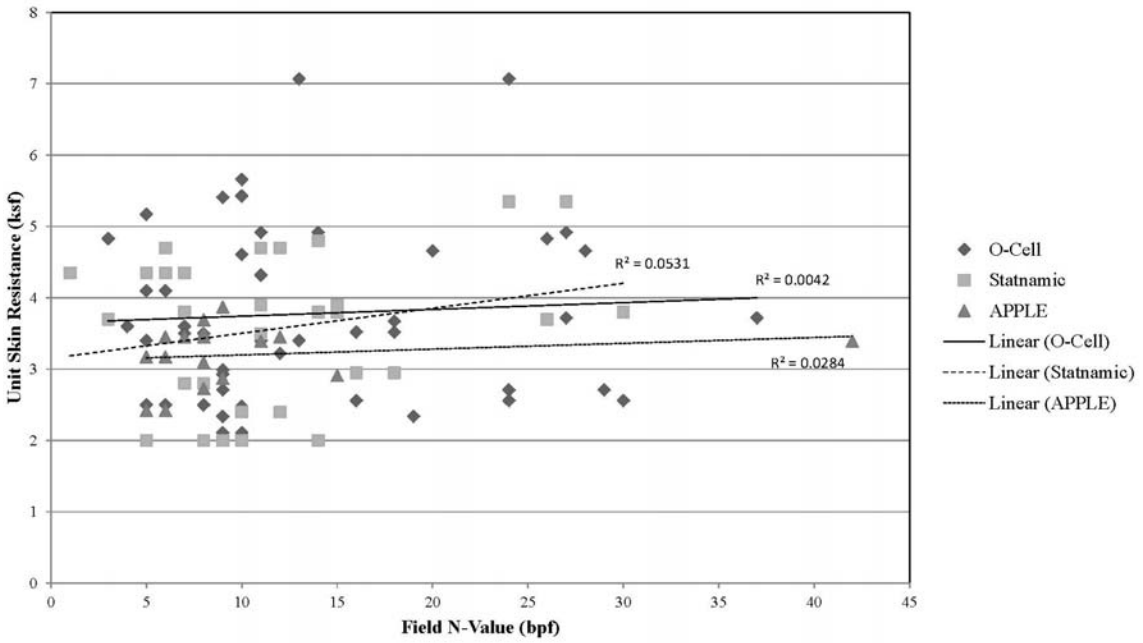

Figure 6.7 – Field N-Values versus Unit Skin Resistance for Data Set 3 Sorted by Load Test Type

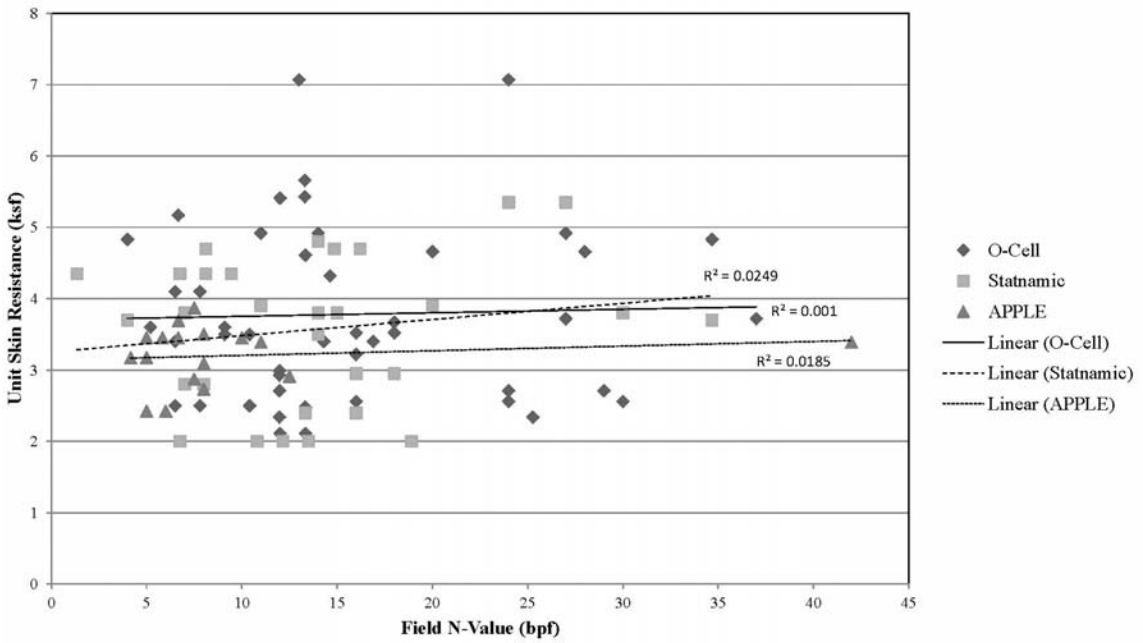

Figure 6.8 – N_{60} Values versus Unit Skin Resistance for Data Set 3 Sorted by Load Test Type

6.2.1 - Analysis of the Relationship between Skin Resistance and SPT N-Values

As can be observed in Figure 6.1 through Figure 6.6, the relationship between the unit skin resistance and the SPT N-values is not linearly correlated. The R^2 values for each of the six cases are presented in Table 6.1.

Table 6.1 - R^2 Values for the SPT to Unit Skin Resistance Relationship

Data Set	**R^2**	
	Field N-Value	N_{60} Value
Data Set 1	0.0008	0.0059
Data Set 2	0.0019	0.0025
Data Set 3	0.014	0.0121

The R^2 values for the six cases support the observation that the unit skin resistance is not linearly correlated with either the field N-values or the N_{60} values. Figure 6.7 and Figure 6.8 verify that this lack of correlation is also true for Osterberg, Statnamic, and APPLE tests when evaluated independently. In addition, based on the data spread and trends, no common mathematical function would reasonably approximate the relationship between the unit skin resistance and the N-values.

6.3 - Relationship of Skin Resistance to Elevation

In Figure 4.6, the unit skin resistance profiles for each load test site were presented. The unit skin resistance distributions are relatively linear in relationship with depth for each load test, with some layers showing higher or lower unit skin resistance. When the distributions for all of the load tests are combined based on elevation, the unit skin resistance trend for the formation can be investigated. Figure 6.9 shows the unit skin resistance based on elevation for all of the load test sites by taking the average unit skin resistance at each elevation for the uncased portion of the test shafts.

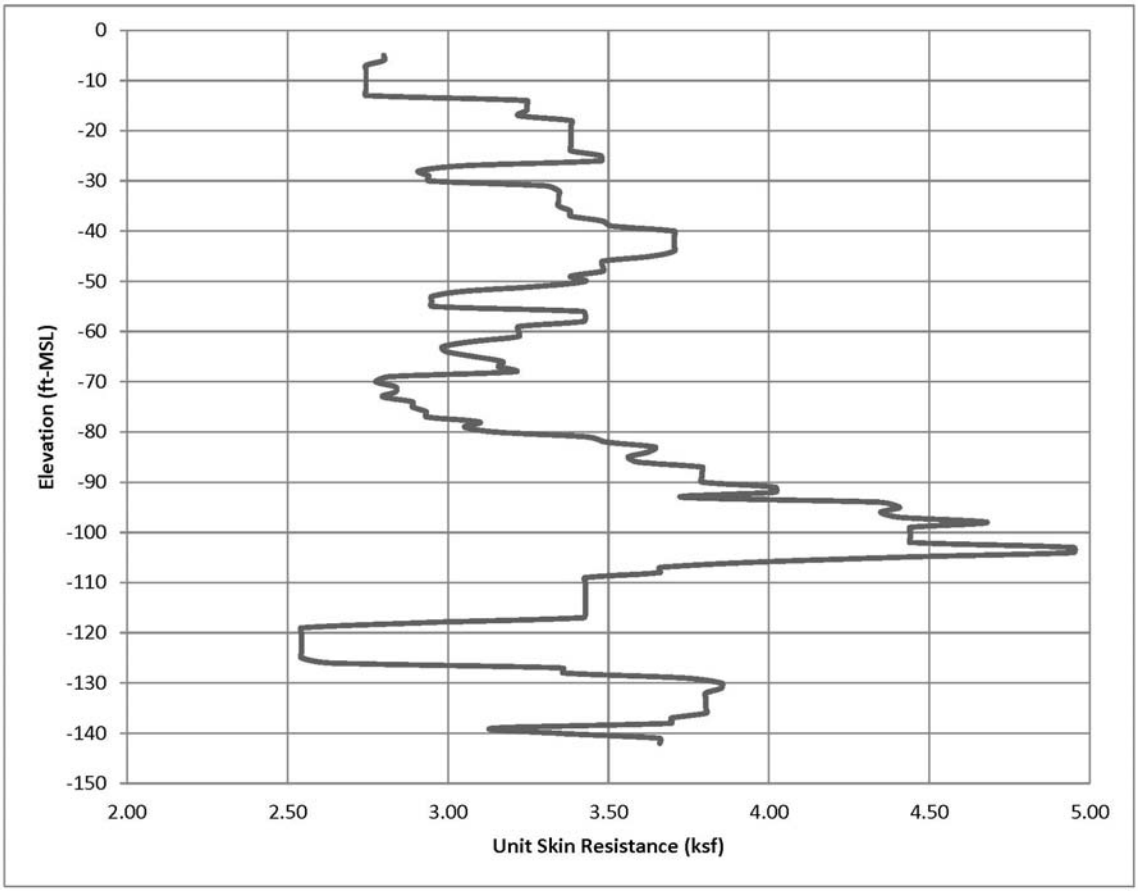

Figure 6.9 – Unit Skin Resistance in the Cooper Marl versus Elevation for All Test Sites

In Figure 6.9, the unit skin resistance from elevation -5 ft-MSL to -90 ft-MSL generally ranges between 2.75 ksf and 3.75 ksf with a linear resistance trend in this range. Below elevation -80 ft-MSL, there is a noted increase in capacity between -80 ft-MSL and -105 ft-MSL before the skin resistance returns to the normally observed range. This increase in unit skin resistance may be caused by a geologic depositional event occurring during the formation of that particular segment of marl, which altered the skin resistance properties since there is no other increase trend in skin resistance with depth, to include no apparent increase in SPT N-values or increase in undrained shear strength (See Figure 2.4). Below elevation -105 ft-MSL, only five of the fifteen load test sites are represented with three of the five sites being the three Cooper River Bridge load test sites.

6.4 - Relationship of Skin Resistance and Effective Overburden Pressure

In Camp's (2004) study regarding drilled shaft axial response at the Cooper River Bridge, the relationship between the effective overburden pressure (also known as the effective vertical stress) and the unit skin resistance was evaluated for the three test sites at the Cooper River Bridge. Camp's study did not indicate any particular relationship between the two values. In extending Camp's work, similar graphs have been built for Data Sets 1, 2, and 3 to include the load tests that Camp used for his analysis. Figures 6.10, 6.11, and 6.12 present the relationship between the effective overburden pressure and the unit skin resistance for the three data sets evaluated. Figure 6.8 also indicates the points that were included in Camp's data set.

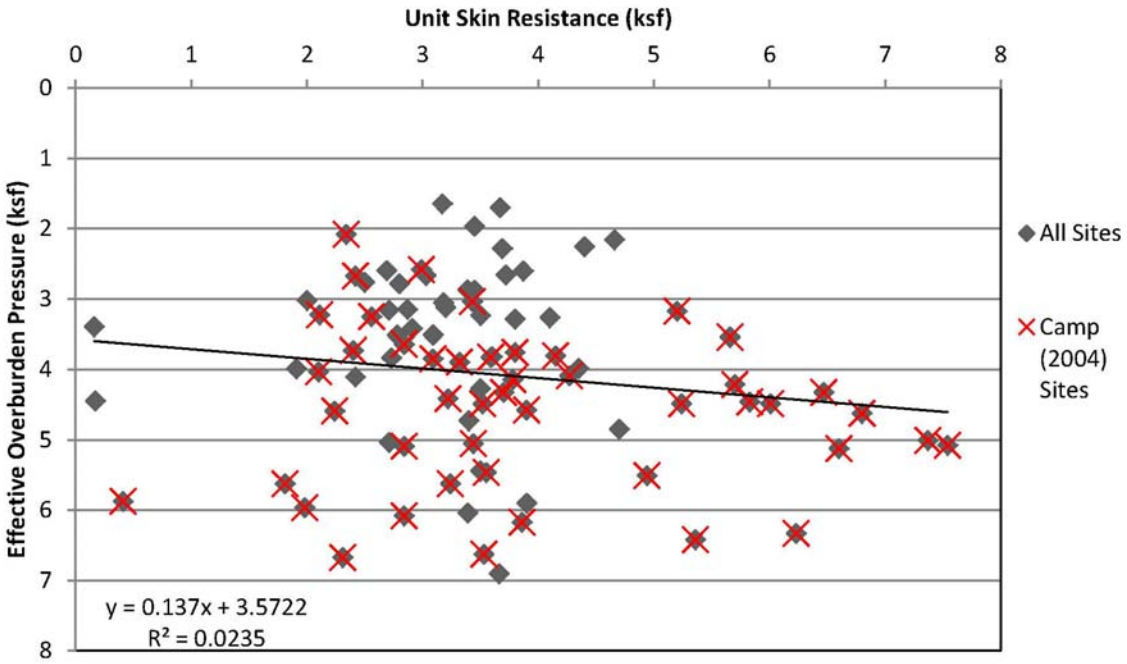

Figure 6.10 – Effective Overburden Pressure versus Unit Skin Resistance for Data Set 1

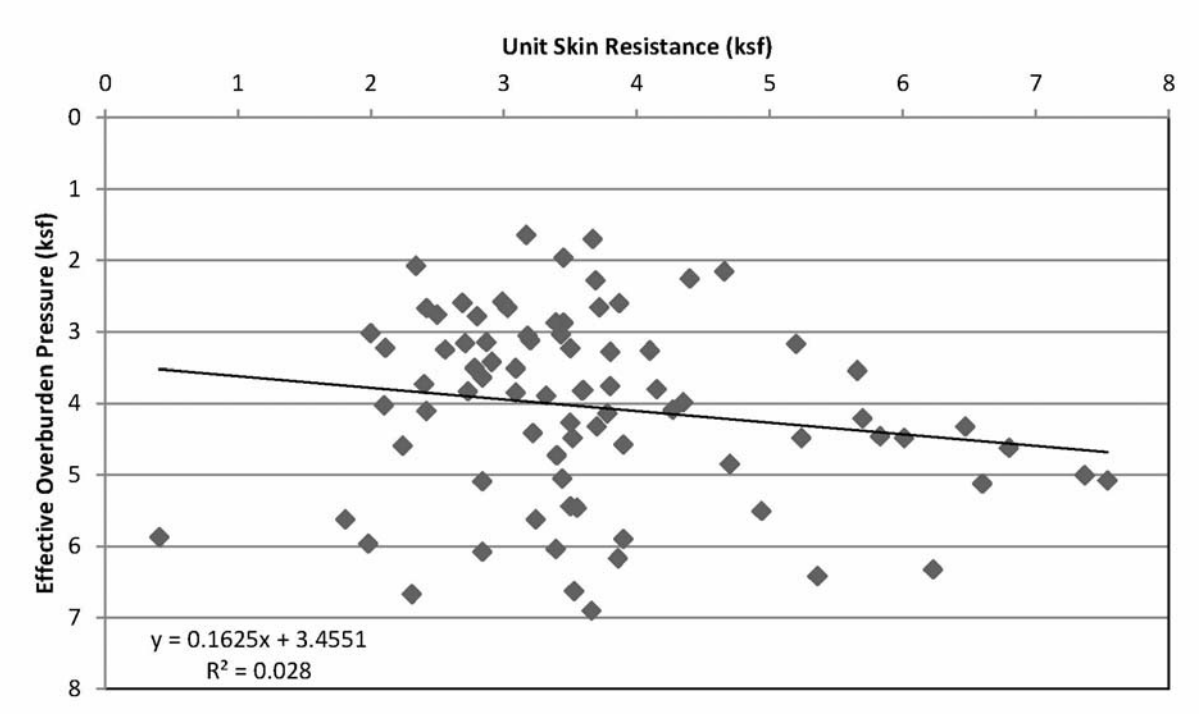

Figure 6.11 – Effective Overburden Pressure versus Unit Skin Resistance Data Set 2

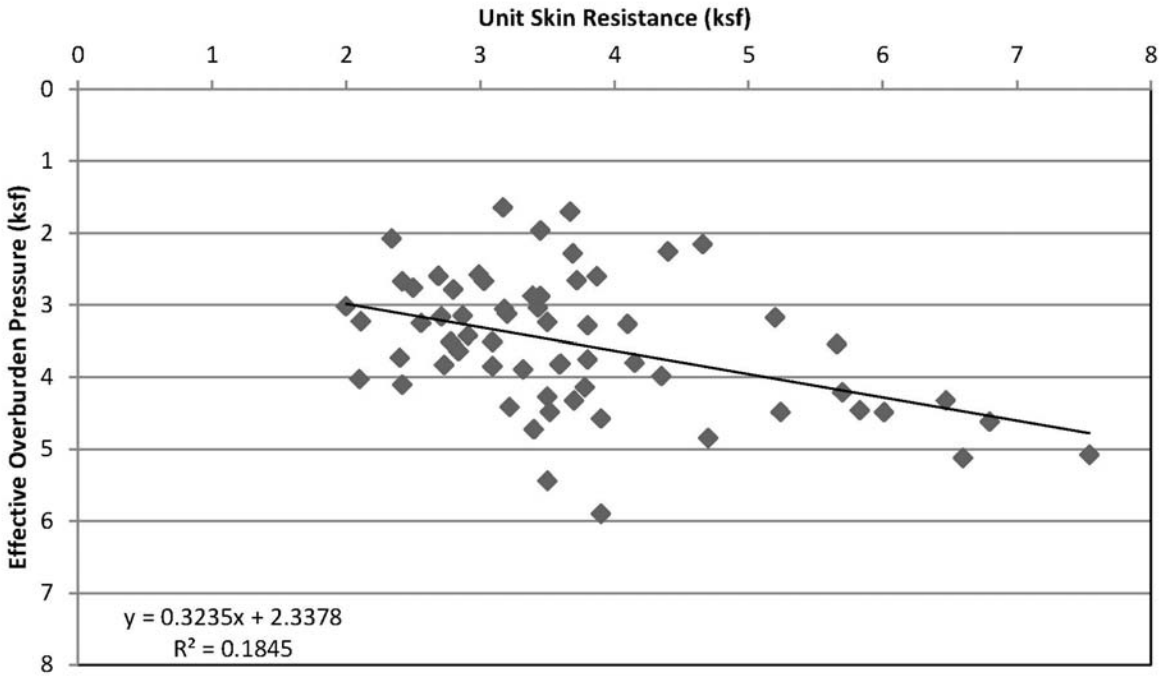

Figure 6.12 – Effective Overburden Pressure versus Unit Skin Resistance for Data Set 3

The relations in Figures 6.10 through 6.12 show an increase in unit skin resistance with an increase in vertical effective stress. However, the R^2 values do not indicate any statistically significant correlation. These results across a larger area of the geologic formation for the relationship between the effective overburden pressure and the unit skin resistance support Camp's findings at the Cooper River Bridge.

6.5 - Relationship of Skin Resistance to Undrained Shear Strength

In the study by Camp et al. (2002) regarding drilled shaft axial response at the Cooper River Bridge, shear strength data is presented, with the average undrained shear strength across all three test sites being 4.0 ksf (See Figure 2.4). Then, Camp used this data to perform five empirical analyses to evaluate the design skin resistance and compared it to the load test measured unit skin resistance. This average shear strength measured at the Cooper River Bridge site can be used in conjunction with the average load test measured skin resistance at the test sites used in this analysis to estimate an α-value in the Cooper Marl. The average unit skin resistances for the three data sets and the corresponding α-values based on using Equation 3-5 and the undrained shear strength values found by Camp et al. (2002) are as summarized in Table 6.2.

Table 6.2 – Average Unit Skin Resistance in the Cooper Marl

Data Set	**Unit Skin Resistance**	**α-Value**
Data Set 1	3.39 ksf	0.85
Data Set 2	3.53 ksf	0.88
Data Set 3	3.54 ksf	0.89

Based on the results presented in Table 6.2, the best fit α-value at the test sites in this analysis is approximately 60% greater than the α-value of 0.45 to 0.50 that would have been predicted by using any of the α-value evaluation methods presented in Table 3.1. These results are also echoed by the conclusion presented by Camp et al. (2002)

regarding the usage of the α-Method in the Cooper Marl, which was that the α-Method using standard α-values would under predict the average unit skin resistance.

6.6 - Load Test Skin Resistance Distribution

For the statistical analyses performed, the load test measured skin resistance has been plotted on a distribution curve to best fit a statistical distribution. This was performed for all three data sets.

6.6.1 - Measured Skin Resistance Distribution – Data Set 1

Figures 6.13 and 6.14 present the frequency distributions of the unit skin resistance as evaluated by the drilled shaft load tests for Data Set 1. Each range bracket is 0.25 ksf, which was chosen based on the standard deviation of Figure 6.8 and represents approximately 20% of a standard deviation. This range bracket was used on all of the frequency distributions to allow for a comparison of results without having to normalize each graph for the standard deviation of each data set.

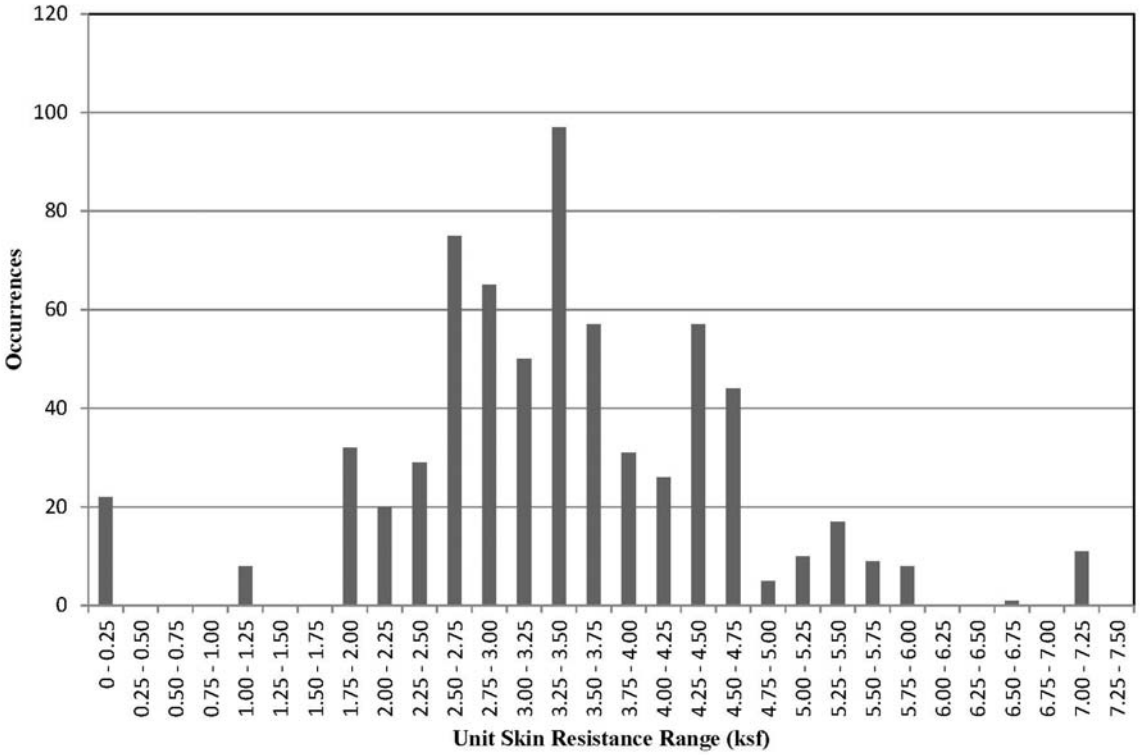

Figure 6.13 – Frequency Distribution of Unit Skin Resistance Based on One Foot Increments for Data Set 1

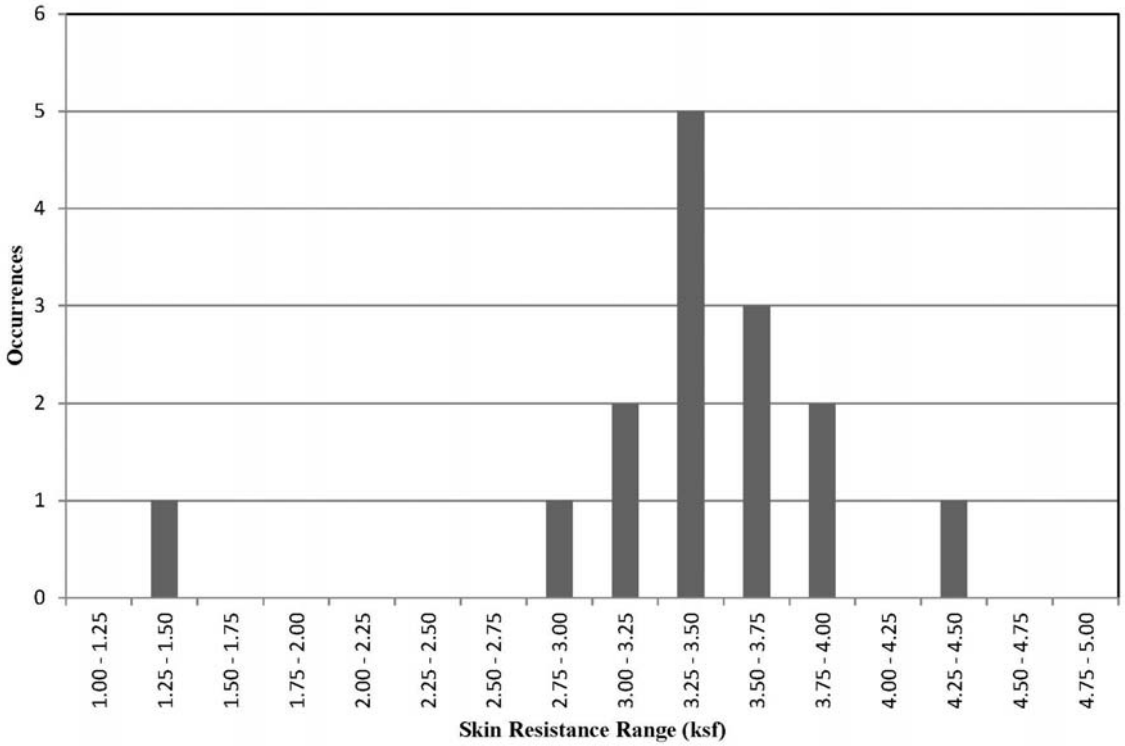

Figure 6.14 – Frequency Distribution of Unit Skin Resistance Based on a Per Site Basis for Data Set 1

For the statistical analysis, the standard distribution is assumed. Table 6.3 contains the statistical information for Figures 6.13 and 6.14 as well as the skin resistance value for which 97.5% of values will exceed based on the normal distribution:

Table 6.3 – Statistical Information of the Unit Skin Resistance Distribution for Data Set 1

Statistical Value	Per Foot	Per Site
Minimum	0.16 ksf	1.34 ksf
Maximum	7.07 ksf	4.4 ksf
Median	3.39 ksf	3.47 ksf
Mean	3.41 ksf	3.39 ksf
Standard Deviation	1.20	0.68
C.O.V.	0.3501	0.2007
97.5% Exceeding	1.06 ksf	2.06 ksf

6.6.2 - Measured Skin Resistance Distribution – Data Set 2

Figures 6.15 and 6.16 present the frequency distributions of the unit skin resistance as evaluated by the drilled shaft load tests for Data Set 2. Each range bracket is 0.25 ksf, which was chosen based on the standard deviation of Figure 6.8 and represents approximately 20% of a standard deviation.

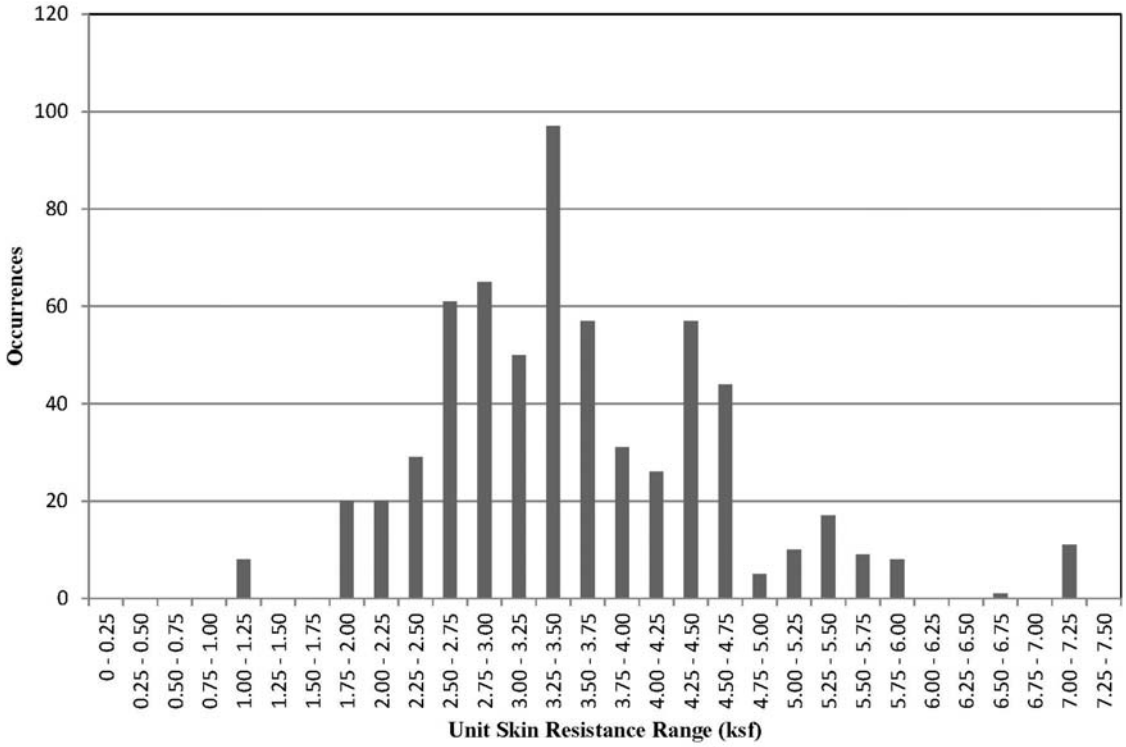

Figure 6.15 – Frequency Distribution of Unit Skin Resistance Based on One Foot Increments for Data Set 2

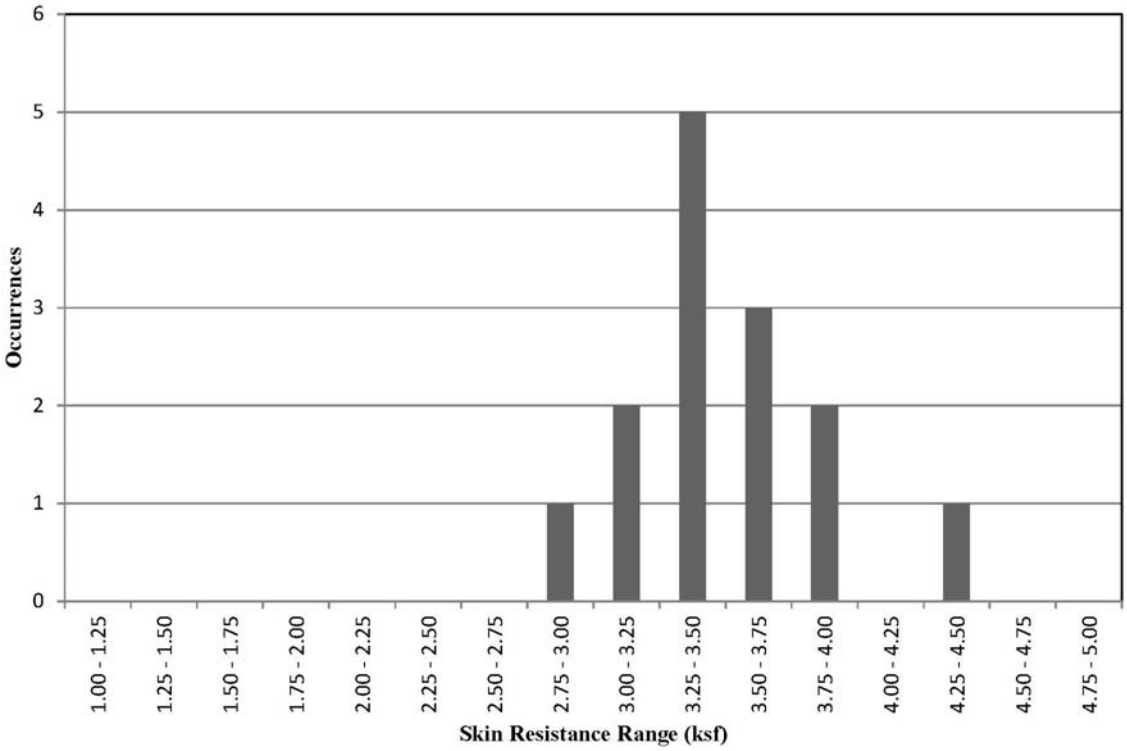

Figure 6.16 – Frequency Distribution of Unit Skin Resistance Based on a Per Site Basis for Data Set 2

For the statistical analysis, the standard distribution is assumed. Table 6.4 contains the statistical information for Figures 6.15 and 6.16 as well as the skin resistance value for which 97.5% of values will exceed based on the normal distribution.

Table 6.4 – Statistical Information of the Unit Skin Resistance Distribution for Data Set 2

Statistical Value	Per Foot	Per Site
Minimum	1.20 ksf	2.88 ksf
Maximum	7.07 ksf	4.4 ksf
Median	3.45 ksf	3.48 ksf
Mean	3.57 ksf	3.53 ksf
Standard Deviation	1.04	0.39
C.O.V.	0.2918	0.1107
97.5% Exceeding	1.53 ksf	2.77 ksf

6.6.3 - Measured Skin Resistance Distribution – Data Set 3

Figures 6.17 and 6.18 present the frequency distributions of the unit skin resistance as evaluated by the drilled shaft load tests for Data Set 3. Each range bracket is 0.25 ksf, which was chosen based on the standard deviation of Figure 6.8 and represents approximately 20% of a standard deviation.

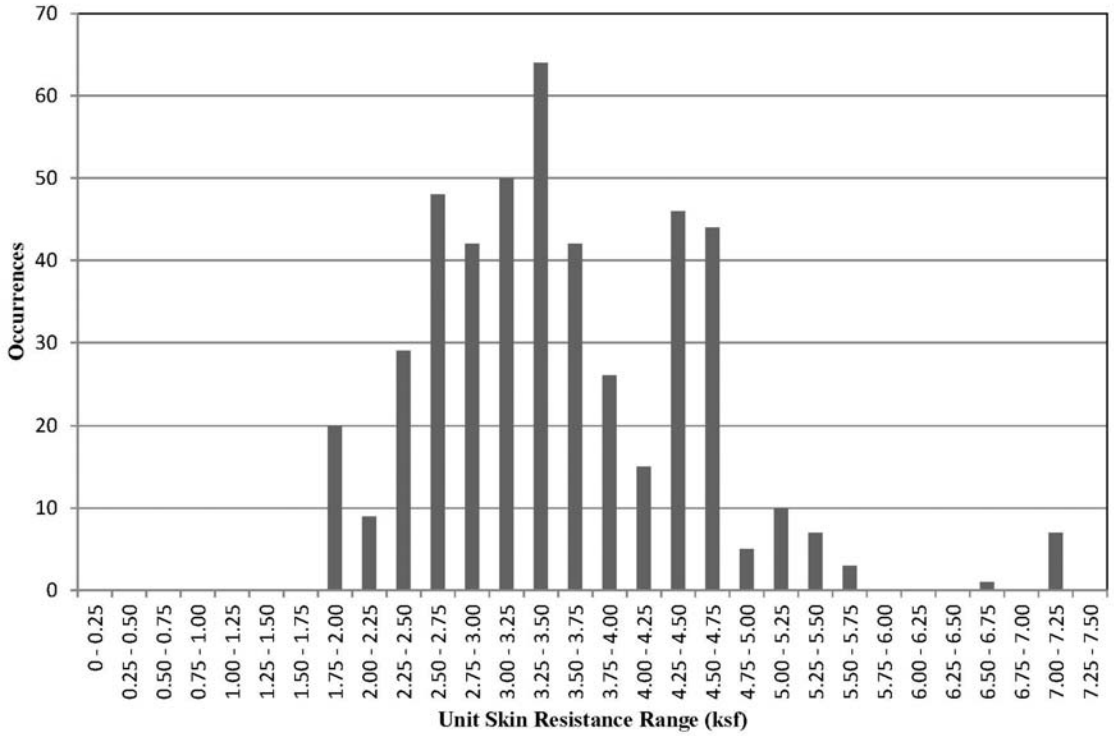

Figure 6.17 – Frequency Distribution of Unit Skin Resistance Based on One Foot Increments for Data Set 3

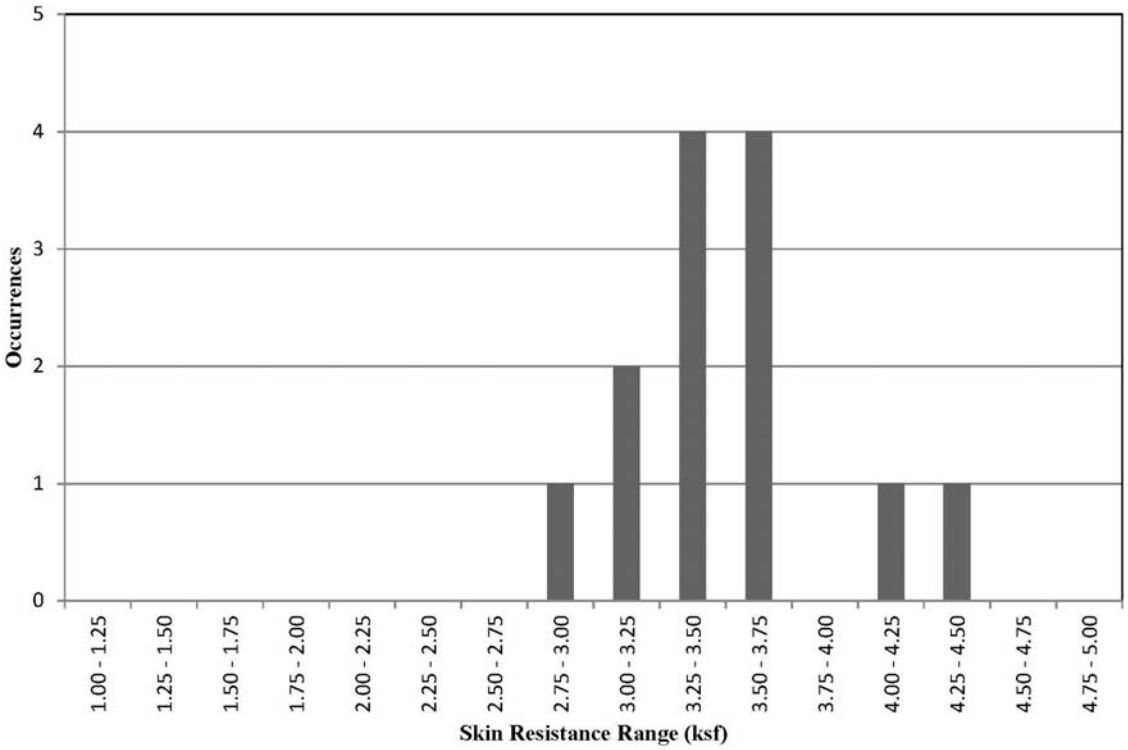

Figure 6.18 – Frequency Distribution of Unit Skin Resistance Based on a Per Site Basis for Data Set 3

For the statistical analysis, the standard distribution is assumed. Table 6.5 contains the statistical information for Figures 6.17 and 6.18 as well as the skin resistance value for which 97.5% of values will exceed based on the normal distribution:

Table 6.5 – Statistical Information of the Unit Skin Resistance Distribution Data Set 3

Statistical Value	**Per Foot**	**Per Site**
Minimum	2.00 ksf	2.88 ksf
Maximum	7.07 ksf	4.4 ksf
Median	3.45 ksf	3.48 ksf
Mean	3.55 ksf	3.54 ksf
Standard Deviation	0.96	0.43
C.O.V.	0.2703	0.1215
97.5% Exceeding	1.67 ksf	2.70 ksf

6.7 - Statistically Based Unit Skin Resistance

As was discussed previously in Section 4.6, all of the skin resistance data for the uncased portion of each shaft in the Cooper Marl was sorted on a per foot basis or a per site basis and then broken out into 3 different data sets. The normal distribution was assumed to be the best statistical fit for the data. From a statistical standpoint, the value for which 97.5% of skin resistance values would be expected to exceed would be used to choose a design skin resistance across the site. However, for half of the data sets, that value is less than the minimum observed skin resistance value. Table 6.6 summarizes these values.

Table 6.6 – Minimum and 97.5% Exceeding Values for All Data Sets

Data Set	**Unit Skin Resistance**	
	97.5% Exceeding	Minimum
Data Set 1 by Foot	1.06 ksf	0.16 ksf
Data Set 1 by Site	2.06 ksf	1.34 ksf
Data Set 2 by Foot	1.53 ksf	1.20 ksf
Data Set 2 by Site	2.77 ksf	2.88 ksf
Data Set 3 by Foot	1.67 ksf	2.00 ksf
Data Set 3 by Site	2.70 ksf	2.88 ksf

This reason that the 97.5% exceeding values are lower than the minimum observed values is likely explained in two different ways. For the data sets that are sorted by site, the data set, 13 to 15 data points is relatively small from a statistical standpoint but large from a load test standpoint. In such, a single high or low value can increase the value of the standard deviation, which in turn will lower the value of the expected skin resistance. For Data Set 3, the data set excluded a cluster of low skin resistance points that were encountered below elevation -100 ft-MSL but did not remove a group of abnormally high skin resistance data points that were approximately 3.5 to 4 standard deviations above both the mean and median. In cases such as these, the minimum observed skin resistance should be substituted for the statistically expected skin resistance that 97.5% of values would be expected to exceed since it was an observed minimum. Table 6.7 summarizes the statistically derived design skin resistances for the six data sets based on the 97.5% confidence level.

Table 6.7 – Statistically Derived Unit Skin Resistance Values for All Data Sets

Data Set	**Unit Skin Resistance**
Data Set 1 by Foot	1.06 ksf
Data Set 1 by Site	2.06 ksf
Data Set 2 by Foot	1.53 ksf
Data Set 2 by Site	2.88 ksf
Data Set 3 by Foot	2.00 ksf
Data Set 3 by Site	2.88 ksf

6.8 - Historical Load Test Method Based Unit Skin Resistance

As summarized in Section 3.9.1.2, the historical load test method is used to evaluate unit skin resistance of drilled shafts in the Cooper Marl when a load test is not performed. Since this method relies on treating the Cooper Marl as a homogeneous layer for design, the average of the unit skin resistance for each available load test would be

used instead of a per foot unit skin resistance analysis. To evaluate the unit skin resistance using this method, the average of unit skin resistance for the five sites with the lowest overall skin resistance was used. The five lowest were chosen to utilize a conservative approach. Table 6.8 contains the average of the five lowest unit skin resistances.

Table 6.8 – Historical Load Test Method Derived Skin Resistance Values

Data Set	**Unit Skin Resistance**
Data Set 1	2.75 ksf
Data Set 2	3.16 ksf
Data Set 3	3.16 ksf

6.9 - Design Unit Skin Resistance Recommendations

While from a statistical standpoint analyzing the unit skin resistance on a per foot basis presents the largest and most comprehensive data set, this method has some flaws. Primarily, shaft segments that exhibit abnormally high or low unit skin resistance will skew the standard deviation while not impacting the average unit skin resistance. For example, at Test Site 5, a segment having a unit skin resistance of 7.07 ksf was followed by a segment with a unit skin resistance of 2.53 ksf. Spreads in the unit skin resistance like this likely accounted for the difference in the magnitude of the standard deviation between the per foot data sets and the per site data sets. Also, it is also important to remember that the goal is to find a reasonable design value for drilled shafts as a whole and not as individual elements in typical geological and construction conditions. As such, the data set used for unit skin resistance recommendations was the geologically typical sites that are above elevation -100 ft-MSL.

For sites that are geologically atypical or sites where drilled shafts are to extend below elevation -100 ft-MSL, load testing is recommended to facilitate proper shaft

design. As such, the recommended design unit skin resistance is 2.88 ksf using the 97.5% confidence interval with the normal distribution and 3.16 ksf using the historical load test method.

6.10 - Geotechnical Resistance Factors in the Cooper Marl

In addition to evaluating the drilled shaft unit skin resistance in the Cooper Marl, evaluating the geotechnical resistance factors for sites when load testing is not performed can improve the drilled shaft design. For this analysis, an empirical method put forth by Becker (2005) was used. This method utilizes Equation 3-8 in conjunction with the constants listed in Table 5.2 and the geotechnical coefficients of variation for the Cooper Marl that were determined using the data sets in Section 6.6. Table 6.9 presents the results of these analyses.

Table 6.9 – Results of Resistance Factor Analysis Using Procedure by Becker (2005)

Data Set	V_r	β for $k_r = 1.0$			β for $k_r = 1.1$		
		2.5	3.0	3.5	2.5	3.0	3.5
Data Set 1 by Foot	0.350	0.52	0.45	0.40	0.57	0.50	0.44
Data Set 1 by Site	0.201	0.69	0.64	0.59	0.76	0.70	0.65
Data Set 2 by Foot	0.292	0.58	0.52	0.46	0.64	0.57	0.51
Data Set 2 by Site	0.111	0.81	0.78	0.75	0.89	0.86	0.82
Data Set 3 by Foot	0.270	0.60	0.54	0.49	0.66	0.60	0.54
Data Set 3 by Site	0.122	0.80	0.76	0.73	0.88	0.84	0.80

As a note, this table is presented in the same format as the results table from Becker (2005). This format presents an overall column for each value of k_r. For each of the k_r values, three different β values were evaluated for each data set using the V_r for that data set to find the resistance factor.

Based on the results from this analysis, the 0.45 resistance factor that is currently in use by SCDOT for drilled shafts in the Cooper Marl is supported by the Becker (2005)

analysis method for all six data sets when a target reliability index of 3.0 (as discussed in Section 3.9.2) is used as none of the computed resistance factors are less than 0.45. However, when only evaluating Data Set 2 and Data Set 3, the current resistance could be increased to 0.52 based on a target reliability index of 3.0 using the Becker (2005) analysis method.

CHAPTER 7

CONCLUSIONS

7.1 - Introduction

This chapter presents the conclusions drawn from research aimed to improve the design process for drilled shafts in the Cooper Marl by addressing the research questions posed in Chapter 1. Load test data obtained from 15 SCDOT projects were collected and reviewed to compile a comprehensive database of unit skin resistance values in the Cooper Marl. The relationship between these values and SPT N-values, effective overburden pressure, and undrained shear strength were explored. The design unit skin resistance was analyzed to find a data supported design unit skin resistance using a statistical method that evaluated the unit skin resistance using the 97.5% confidence interval and an analysis using the historical load test method. Finally, the LRFD resistance factor for the Cooper Marl was empirically calculated using a method presented by Becker (2005). Recommendations and considerations are made for drilled shaft skin resistance design. Future research paths and topics are also put forth.

7.2 - Conclusions

7.2.1 - Relationship between Skin Resistance and SPT Values

The unit skin resistance in the Cooper Marl is not predictable using SPT values.

In this analysis, the relationship between unit skin resistance and SPT N-values and SPT N_{60} values were evaluated across the Cooper Marl. Based on the results of the

analysis, none of these properties are reliable predictors of the drilled shaft unit skin resistance based on the R^2 values of the best fit line. This result was expected based on engineering practice in the area and confirmed the previous research performed by Camp et al. (2002), which was limited to data from 3 test sites.

7.2.2 - Relationship between Skin Resistance and Overburden Pressure

Increased overburden pressure does not correlate with increased unit skin resistance.

The relationship between overburden pressure and unit skin resistance data indicates that the unit skin resistance increases with overburden pressure across the Cooper Marl. But, the R^2 values do not indicate that this relationship is statistically significant. The result found in this analysis was similar to the conclusions drawn by Camp (2004), which was limited to 3 test sites.

7.2.3 - Relationship between Skin Resistance and Elevation

Unit skin resistance exhibits a constant distribution with depth.

The Cooper Marl displayed a relatively uniform unit skin resistance of 2.75 ksf and 3.75 ksf with a layer displaying a higher resistance of 4.0 ksf to 5.0 ksf between elevations -90 ft-MSL and -105 ft-MSL. This increase in unit skin resistance was not related to an increase in undrained shear strength or SPT N-value. After -105 ft-MSL, the unit skin resistance returns to its original range.

7.2.4 - Relationship between Skin Resistance and Undrained Shear Strength

The α-Method underpredicts capacity.

Evaluation of the α-Method using load test data skin resistance data indicated that an α value of 0.85 would be needed to arrive at the load test derived unit skin resistance

based on the undrained shear strength values published by Camp et al. (2002). This value is 65% higher than the suggested design α values summarized in Table 3.1. If one of the suggested design values was chosen, the design unit skin resistance would be under predicted by approximately 55%, which is a similar conclusion to Camp et al. (2002). This also indicates that while the α-Method will give a unit skin resistance that is acceptable for design as is, it will likely not over predict capacity based on the analysis of load test results in the Cooper Marl. As such, the α-Method is overly conservative and other design methods, such as the historical load test method or an effective stress analysis, should be considered.

7.2.5 - Skin Resistance Design

A design unit skin resistance of 3.2 ksf is supported by the historical load test method.

Using the statistical approach detailed in Section 5.3.1, the data supports a design unit skin resistance between 1.53 ksf to 2.00 ksf when a per foot analysis is used, and 2.88 ksf when a per site analysis is used for geologically typical sites. The derivation of these values is based on a 97.5% confidence interval. These values are 5% to 50% lower than what was expected based on the common engineering practice of assuming 3.0 ksf because the standard deviation of the per foot data set is approximately twice the standard deviation of the per site data due to data points that are significantly higher than the average. This causes the per foot analysis to lead to artificially low values as the increased standard deviation caused by skin resistance points on the high end causes a statistical expectation of skin resistance points that are lower than were measured.

Using the historical load test method for evaluating the design unit skin resistance, a unit skin resistance of 3.16 ksf is supported for geologically typical sites.

This is based on using the data from the five load tests that exhibited the lowest average unit skin resistance. This value is a more reasonable design value as it is not influenced by the same high end values that skewed the standard deviation of the statistical method.

7.2.6 - Geotechnical Resistance Factor

The current geotechnical resistance factor of 0.45 is data supported.

Using the method presented by Becker (2005) and the geotechnical coefficients of variation of the load test unit skin resistance data sets, the resistance factors for the Cooper Marl were evaluated. For a reliability index of 3.0, the lowest geotechnical resistance factors found ranged between 0.45 and 0.50. This was based on the analysis from Data Set 1. As the current design resistance factor developed with the adoption of LRFD is 0.45 as specified by FHWA and SCDOT, the analysis concurs with the current design standard which is based on load tests in many soil formations. As other site specific studies as discussed in Section 3.9.2.1 have indicated that the FHWA resistance factors are too high for certain formations, verification of the resistance factor is important to ensure proper foundation design.

7.2.7 – Effect of Load Test Type

Statnamic and Osterberg style load tests produce similar skin resistance results. APPLE style tests showed lower skin resistance values.

The current load test set indicated that Osterberg and Statnamic load tests will mobilize similar unit skin resistance results. The APPLE tests in the data set have shown mobilized skin resistance values that are approximately 10% lower than the Osterberg and Statnamic load test results. However, the sample size for the APPLE test is 15% to 20% of the sample size for Statnamic and Osterberg style load tests.

7.2.1 - Geology Considerations

Although the Cooper Marl is treated as a homogenous formation, there are known discontinuities.

From a geological standpoint, the majority of the load tests were performed in the portion of the Cooper Marl that is classified as the Ashley Formation. The load test that was performed in an outcrop of the underlying Parkers Ferry Formation (Test Site 7), which is also considered part of the Cooper Marl, exhibited 20% higher skin resistance. In addition to the outcrops of the Parkers Ferry Formation, the presence of the Marks Head Formation must also be evaluated during geotechnical investigations. This formation has similar physical characteristics to the Ashley Formation, but the engineering properties are not well defined. As such, soils in the Marks Head Formation should not be treated as Cooper Marl for design.

While care should be taken if a higher design skin resistance is used in these outcrop areas due to the limited amount of data in the Parkers Ferry Formation, the possibility of higher unit skin resistance should be taken into account when designing load tests in these outcrop areas.

In addition, the only load test that was performed on a barrier island (Test Site 2) indicated a significantly lower unit skin resistance. Due to this, significant care should be taken when performing drilled shaft design on these barrier islands and load testing in these cases is recommended.

7.3 - Future Research Paths

7.3.1 - Relationship between Skin Resistance and Other Soil Properties

Future analyses of the relationship between unit skin resistance and CPT data, index test results, or more widespread shear testing may provide a method for relating soil properties and unit skin resistance.

7.3.2 - Statistical Geotechnical Resistance Factor Analysis

To fully evaluate the geotechnical resistance factor to create a geological formation specific resistance factor, a Monte Carlo analysis or similar statistical method should be used. Based on the results of such an analysis, changes to the resistance factor could be made, if needed.

7.3.3 - Extension to Other Formations

Studying of the relationships between the load test skin resistance in the Black Creek and Pee Dee Formations and in-situ geotechnical properties would improve the design process in these formations. While the majority of the engineering research in the South Carolina Coastal Plain is specific to the Cooper Marl, other formations exist where such research could lead to better drilled shaft design. These formations are geologically well defined, can be visually identified during field investigations, and have had drilled shaft load tests performed in them already.

WORKS CITED

Abernethy, Z.W. (2014). "Discussion about Drilled Shaft History in SC.", Personal Interview.

Abu-Farsakh, M.Y., Chen, Q., Haque, M.N. (2013). "Calibration of Resistance Factors for drilled shafts for the New FHWA Design Method." *FHWA/LA.12/495*.

Abu-Hejleh, N., O'Neill, M.W., Hanneman, D., Atwooll, W.J. (2003). "Improvement of the Geotechnical Axial Design Methodology for Colorado's Drilled Shafts Socketed in Weak Rocks." *CDOT-DTD-R-2003-6*.

AFT (2000). "Report of Axial Statnamic Load Tests – US 17 over the Cooper River Charleston Site – Test Shafts C-3 and C-4." Report Submitted to Modern Continental South, Inc., Mount Pleasant, SC.

AFT (2000). "Report of Axial Statnamic Load Tests – US 17 over the Cooper River Mount Pleasant Site – Test Shafts C-3 and C-4." Report Submitted to Modern Continental South, Inc., Mount Pleasant, SC.

AFT (2001). "Report of Axial Statnamic Load Testing – SC 247 over Saluda River." Report Submitted to A.H. Beck Foundation Co., Inc., Asheboro, NC.

AFT (2002). "Statnamic Load Testing Results – Replacement of John F. Limehouse Bridge over Stono River." Report Submitted to Jones Brothers, Inc., Johns Island, SC.

AFT (2003). "Axial Statnamic Load Testing Results – LT-1 – US 52 Bridge over I-26." Report Submitted to Trevi Icos South, Clearwater, FL.

AFT (2003). "Axial Statnamic Load Testing Results – LT-2 – I-26 Interchange at Ashley Phosphate Road." Report Submitted to Trevi Icos South, Clearwater, FL.

AFT (2008). "Final Report of Axial Statnamic Load Testing – Interchange Improvements to I-26 at Remount and Aviation Road." Report Submitted to Case Atlantic Company, Clearwater, FL.

AFT (2011). "Final Report of Axial Statnamic Load Testing – US 17 / I-526 / Hungryneck Boulevard Interchange." Report Submitted to A.H. Beck Foundation Co., Inc., San Antonio, TX.

AFT (2013). "Final Report of Statnamic Load Testing – US 78 (Rivers Ave.) over S-39, NSRR and CSXT Bridge Replacement." Report Submitted to Case Atlantic Company, Clearwater, FL.

AFT (2014). "Statnamic Load Testing Overview." Technical Handout Available Online as of July 2014 at: http://www.testpile.com/PDF/Statnamic%20Testing%20Brief%20Overview%20for%20Web%20Site.pdf

Alvarez, C., Zuckerman, B., Lemke, J. (2006). "Dynamic Pile Analysis Using CAPWAP and Multiple Sensors." *ASCE GEOCongress*: Atlanta, Georgia, February 2006, 1-5.

American Association of State Highway and Transportation Officials (AASHTO) (2012). "AASHTO LRFD Bridge Design Specifications."

Barker, R.M., Duncan, J.M., Rojiani, K.B., Ooi, P.S.K., Tan, C.K., Kim, S.G. (1991). "Manuals for the Design of Bridge Foundations." NCHRP (Final) Report 343, Transportation Research Board, Washington, DC.

Becker, D.E., Devata, M. (2005). "Implementation and Application Issues of Load and Resistance Factor Design (LRFD) for Deep Foundations." *Contemporary Issues in Foundation Engineering,* October 2005, 1-13.

Brown, D.A. (2002). "Effect of Construction on Axial Capacity of Drilled Foundations in Piedmont Soils." *Journal of Geotechnical and Geoenvironmental Engineering,* 128:12(967), 967-973.

Brown, D.A. (1994), "Evaluation of Static Capacity of Deep Foundations from Statnamic Testing" plus discussion, *Geotechnical Testing Journal*, GTJODJ, Vol. 17, No. 4, December 1994, 403-414.

Brown, D.A. (2004). "Zen and the Art of Drilled Shaft Construction: The Pursuit of Quality" Invited keynote lecture and paper, *Geotechnical Special Publication No. 124*, ASCE, pp. 19-33. Geo-Institute International Conference on Drilled Foundations, Orlando.

Brown, D.A. (2012). "Factors Affecting the Selection and Use of Drilled Shafts for Transportation Infrastructure Projects", *ADSC EXPO 2012 Geo-Construction Conference Proceedings*, March 14-17, 2012, San Antonio, TX, 25-35.

Brainard, R., Smith, P., and Drolet, L. (2009) "Daniel Island Surprise – Sand Lens Lurking in Cooper Marl, Charleston, SC." *2009 Rapid Excavations and Tunneling Conference Proceeding*, 185-194.

Bustamante, M., Gianeselli, L. (1982). "Pile Bearing Capacity Prediction by Means of Static Penetrometer CPT." *Proceedings of the 2nd European Symposium on Penetration Testing*, ESOPT-II, Amsterdam, 2, 493-500, Rotterdam.

Camp, W.M., Brown, D.A., and Mayne, P.W. (2002) "Drilled Shaft Axial Design Values: Predicted Versus Measured Response in a Calcareous Clay" *Deep Foundations 2002*, Geotechnical Special Publication No. 116, 1518-1532.

Camp, W.M., Brown, D.A., and Mayne, P.W. (2002) "Construction Methods Effects on Drilled Shaft Axial Performance." *Deep Foundations 2002*, Geotechnical Special Publication No. 116, 193-208.

Camp W.M. (2004). "Site Characterization and Subsurface Conditions for the Cooper River Bridge." *Geotechnical Engineering for Transportation Projects.* Geotechnical Special Publication No. 126, 347-360.

Camp, W.M. (2004). "Drilled and Driven Foundation Behavior in a Calcareous Clay." *GeoSupport 2004*. 1-18.

Castelli, R.J. (2004). "Design of Drilled Shaft Foundations for the Cooper River Bridge." *Geotechnical Engineering for Transportation Projects.,* Geotechnical Special Publication No. 126, 334-346.

Chakraborty, T., Salgado, R., Basu, P., and Prezzi, M. (2013). "Shaft Resistance of Drilled Shafts in Clay." *Journal of Geotechnical and Geoenvironmental Engineering,* 2013.139:548-563, 548-563.

Conroy, R., Mondello, B., Hussein, M.H., Gissal, R. (2010). "Drilled Shaft Load Testing: Made Easy and Inexpensive." *Foundation Drilling Magazine*, June/July 2010; 53-57.

Cooke, C.W. (1936). "Geology of the Coastal Plain of South Carolina.", U.S. Geologic Survey Bulletin 867.

Drayton, J. (1802). A View of South Carolina, as Respects Her Natural and Civil Concerns., W.P. Young, Charleston, SC.

Duncan, D.A., Colquhoun, D.J. (1983)., "Surface and Subsurface Stratigraphy, Structure and Aquifers of the South Carolina Coastal Plain.", University of South Carolina, Department of Geology.

Eslami, A., Fellenius, B.H. (1997). "Pile Capacity by Direct CPT and CPTu Methods Applied to 102 Case Histories", *Canadian Geotechnical Journal*, 34, 866-904.

F&ME Consultants, Inc. (2001). “Drilled Shaft Rehabilitation Procedure and Statnamic Load Testing (Revised) – SC Route 247 over Saluda River.”, Report Submitted to SCDOT, Columbia, SC.

F&ME Consultants, Inc. (2001). “SC 247 over Saluda River, Bent #4-Shafts #1, #2, and #3 – Drilled Shaft Acceptances Recommendation.”, Report Submitted to SCDOT, Columbia, SC.

F&ME Consultants, Inc. (2013). “Final Bridge Geotechnical Engineering Report – S-10-967 (Bryans Dairy Rd.) Replacement Bridge over Abbapoola Creek, Charleston County, South Carolina”, Report Submitted to Infrastructure Consulting and Engineering, Columbia, SC.

F&ME Consultants, Inc. (2008). “SCE&G Limestone Investigation, Dorchester County, South Carolina”, Report Submitted to South Carolina Electric and Gas, Columbia, SC.

Farr, S. (1983). “Recent Load Tests in South Carolina.” Load Testing Report; Recipient Unknown.

FHWA (1993). “Drilled Shafts for Bridge Foundations.” *FHWA-RD-92-004*. U.S. Department of Transportation, Federal Highway Administration, Washington, DC.

FHWA (2005). “Development of Geotechnical Resistance Factors and Downdrag Load Factors of LRFD Foundation Strength Limit State Design.” *FHWA-NHI-05-052*. U.S. Department of Transportation, Federal Highway Administration, Washington, DC.

FHWA (2010). “Drilled Shafts: Construction Procedures and LRFD Design Methods.” *FHWA-NHI-10-016*, Geotechnical Engineering Circular No. 10, NHI Course NO. 132014.

FHWA (2012). “National Bridge Inventory for S-8-35 over Lake Moultrie Rediversion Canal (NBI Structure 000870003500200) and SC 45 over Lake Moultrie Rediversion Canal (NBI Structure 000840004500105)”.

FPS (2006). “Federation of Pile Specialists – Handbook on Pile Load Testing.” Federation of Pile Specialists, 83 Copers Cope Road, Beckenham, Kent, February 2009, 1-29.

Golder, H.Q., Leonard, M.W. (1954). “Some Tests on Bored Piles in London Clay”, *Géotechnique*, vol 4. 32-41.

GRL Engineers, Inc. (2001). “Crosshole Sonic Logging Summary Report #1 – SC Route 247 over Saluda River.” Report Submitted to SCDOT, Columbia, SC.

GRL Engineers, Inc. (2012). "Folly Road over Folly Creek – APPLE Testing Results." Report Submitted to Cape Romain Contractors, Inc., Wando, SC.

GRL Engineers, Inc. (2014). "High Strain Dynamic Testing Results – SC 41 RBO Wando River." Report Submitted to PCL Civil Constructors, Inc., Raleigh, NC.

Hayes, J.A. (2012). "The Landmark Osterberg Cell Test." *Deep Foundations,* Nov/Dec 2012, 45-49.

Hayes, M.O., FitzGerald, D.M. (2013). "Origin, Evolution, and Classification of Tidal Inlets." *Journal of Coastal Research*, 69(sp1), 14-33.

Heron, S.D. (1962), "Limestone Resources of the Coastal Plain of South Carolina." Bulletin No. 28, Division of Geology, State Development Board, Columbia, SC.

Holmes, F.S. (1870). Phosphate Rocks of South Carolina and the Great Carolina Marl Bed., Holmes Book House, Charleston, SC.

Horvath, R.G., Kenney, T.C., Trow, W.A. (1980). "Results of Tests to Determine Shaft Resistance of Rock-Socketed Drilled Piers." *International Conference on Structural Foundations on Rock*, Sydney, May 7-9, 349-361.

Hussein, M.H., Townsend, F., Rausche, F., Likins, G. E. (1992). "Dynamic Testing of Drilled Shafts." *Transportation Research Record*, No. 1336; Foundation Engineering: Seismic Design, Drilled Shafts, and Other Issues: Washington, D.C., January 1992, 65-69.

ICA Engineering (2014). "Preliminary Geotechnical Bridge Report – Replacement of SC 41 over Wando River", Report Submitted to SCDOT, Columbia, SC.

Kim, M.H. (2001). "Analysis of Osterberg and Statnamic Axial Load Testing and Conventional Lateral Load Testing." Thesis for Master of Engineering – University of Florida.

Kulhawy, F.H., Trantmann, C.H., Beech, J.F., O'Rourke, T.D., McGuire, W. (1983). "Transmission Line Structure Foundations for Uplift-Compression Loading." Final Report, Project 1493-1, EPRI EL-2870, Geotechnical Engineering Group, Cornell University, Ithaca, NY.

LAW Engineering (1991). "Report of Test Shaft Program – Isle of Palms Connector – Contractor No. 1." Report Submitted to The LPA Group, Columbia, SC.

Likins, G.E., Webster, S., Saavedra, M. (2004). "Evaluations of Defects and Tomography for CSL." *Proceedings of the Seventh International Conference on the Application of Stresswave Theory to Piles* 2004: Petaling Jaya, Selangor, Malaysia; 381-386.

Likins, G.E., Robinson, B., Piscsalko, G. (2012). "A Brief Overview of Testing of Deep Foundations *(Keynote Lecture)*." *Proceedings from Testing and Design Methods for Deep Foundations;* IS-Kanazawa: Kanazawa, Japan; 3-11.

Loadtest (2000). "Data Report on Drilled Shaft Load Testing (Osterberg Method) – Bent 10 Test Shaft – SC 703 Bridge over Breach Inlet." Report Submitted to Case Atlantic Company, Clearwater, FL.

Loadtest (2000). "Data Report on Drilled Shaft Load Testing (Osterberg Method) Test Shaft C-1 – Cooper River Bridge." Report Submitted to Trevi Icos Corporation, Boston, MA.

Loadtest (2000). "Data Report on Drilled Shaft Load Testing (Osterberg Method) Test Shaft C-2 – Cooper River Bridge." Report Submitted to Trevi Icos Corporation, Boston, MA.

Loadtest (2000). "Data Report on Drilled Shaft Load Testing (Osterberg Method) Test Shaft C-3 – Cooper River Bridge." Report Submitted to Trevi Icos Corporation, Boston, MA.

Loadtest (2000). "Data Report on Drilled Shaft Load Testing (Osterberg Method) Test Shaft C-3 – Cooper River Bridge." Report Submitted to Trevi Icos Corporation, Boston, MA.

Loadtest (2000). "Data Report on Drilled Shaft Load Testing (Osterberg Method) Test Shaft DI-1 – Cooper River Bridge." Report Submitted to Trevi Icos Corporation, Boston, MA.

Loadtest (2000). "Data Report on Drilled Shaft Load Testing (Osterberg Method) Test Shaft DI-2 – Cooper River Bridge." Report Submitted to Trevi Icos Corporation, Boston, MA.

Loadtest (2000). "Data Report on Drilled Shaft Load Testing (Osterberg Method) Test Shaft MP-1 – Cooper River Bridge." Report Submitted to Trevi Icos Corporation, Boston, MA.

Loadtest (2000). "Data Report on Drilled Shaft Load Testing (Osterberg Method) Test Shaft MP-2 – Cooper River Bridge." Report Submitted to Trevi Icos Corporation, Boston, MA.

Loadtest (2000). "Data Report on Drilled Shaft Load Testing (Osterberg Method) Test Shaft MP-3 – Cooper River Bridge." Report Submitted to Trevi Icos Corporation, Boston, MA.

Loadtest (2000). "Data Report on Drilled Shaft Load Testing (Osterberg Method) Test Shaft MP-4 – Cooper River Bridge." Report Submitted to Trevi Icos Corporation, Boston, MA.

Loadtest (2001). "Report on Drilled Shaft Load Testing (Osterberg Method) – TS-1 – Cosgrove Avenue Bridge Replacement." Report Submitted to Case Atlantic Company, Clearwater, FL.

Loadtest (2014). "Report on Drilled Shaft Load Testing (Osterberg Method) – Test Shaft #1 – Maybank Highway Bridge Replacement." Report Submitted to Case Atlantic Company, Clearwater, FL.

Mackiewicz, S. and Lehman-Svoboda, J. (2012). "Measured versus Predicted Side Resistance of Drilled Shafts in a Heterogeneous Soil Profile." *GeoCongress* 2012, 2412-2421.

Malde, H.E. (1959). "Geology of the Charleston Phosphate Area, South Carolina.", U.S. Geologic Survey Bulletin 1079.

McCullough, D.G. (1972), "The Great Bridge". Simon and Schuster, New York, 636.

Meyerhof, G.G. (1951). "The Ultimate Bearing Capacity of Foundations", *Géotechnique*, vol 2. 301-332.

Meyerhof, G.G., Murdock, L.J. (1953). "An Investigation of the Bearing Capacity of Some Bored and Driven Piles in London Clay", *Géotechnique*, vol 3. 267-282.

Middendorp, P., Bermingham, P. & Kuiper, B. (1992). "Statnamic Load Testing of Foundation Piles." *4th Int. Conf. on the Application of Stresswave Theory to Piles*, The Hague 21–24 September 1992, 265–272.

Mullins, A.G. (2010). "Thermal Integrity Profiling of Drilled Shafts." *DFI Journal* Volume 4 No. 2, Hawthorne , NJ, pp. 54-64.

O'Neill, M.W. and Reese, L.C. (1999). "Drilled shafts: Construction Procedures and Design Methods." *Publication No. FHWA-IF-99-025*, U.S. Department of Transportation, Federal Highway Administration, Washington, DC.

O'Neill, M., Tabsh, S.W., Sarhan, H. (2003). "Response of Drilled Shafts with Minor Flaws to Axial and Lateral Loads." *Engineering Structures*, 25 (2003), 47-56.

Osterberg, J. O. (1998) ''The Osterberg Load Test Method for Bored and Driven Piles – The First Ten Years." *Presented at 7th International Conference & Exhibition on Piling and Deep Foundations*, Deep Foundations Institute, Vienna, Austria, June 1998.

Paikowsky, S. G., with contributions from Birgisson, B., McVay, M., Nguyen, T., Kuo, C., Baecher, G., Ayyab, B., Stenersen, K., O'Malley, K., Chernauskas, L., and O'Neill, M. (2004). "Load and Resistance Factor Design (LRFD) for Deep Foundations." *NCHRP (Final) Report 507*, Transportation Research Board, Washington, DC.

Piscsalko, G., Likins, G. E., White, B. (2013). "Non-Destructive Testing of Drilled Shafts – Current Practice and New Method." *Proceedings from the International Bridge Conference*: 2013, Pittsburg, PA.

Pizzi, J.F. (2007). "Case History: Capacity of a Drilled Shaft in the Atlantic Coastal Plain." *Journal of Geotechnical and Geoenvironmental Engineering,* 133:5(522), 522-530.

Rausche, F., Seidel, J. (1984). "Design and Performance of Dynamic Tests of Large Diameter Drilled Shafts." *Second International Conference on the Application of Stress Wave Theory on Piles*: Stockholm, Sweden, May 1984; 9-16.

Rausche, F., Robinson, B. (2010). "Advances in the Evaluation of Pile and Shaft Quality." *Proceedings of the Symposium on the Application of Geophysics to Environmental and Engineering Problems* (SAGEEP): Keystone, CO; 325-334.

Roberts, L.A., Fick, D., and Misra, A. (2011). "Performance-Based Design of Drilled Shaft Bridge Foundations." *Journal of Bridge Engineering,* 2011.16:749-758, 749-758.

Robinson, B., Rausche, F., Likins, G. E., Ealy, C. (2002). "Dynamic Load Testing of Drilled Shafts at National Geotechnical Experimentation Sites." *Deep Foundations* 2002, An International Perspective on Theory, Design, Construction, and Performance, Geotechnical Special Publication No. 116, O'Neill M. W., and Townsend, F. C. Eds., American Society of Civil Engineers: Orlando, FL February 2002.

Rogers, G.S. (1913). "The Phosphate Deposits of South Carolina.", U.S. Geologic Survey Bulletin 580, Part 1. 183-220.

Rollins, K.M., Clayton, R.J., Mikesell, R.C., and Blaise, B.C. (2005). "Drilled Shaft Side Friction in Gravelly Soils." *Journal of Geotechnical and Geoenvironmental Engineering,* 131:8(987), 987-1003.

Ruffin, E. (1843). "Report of the Commencement and Progress of the Agricultural Survey of South Carolina for 1843.", Columbia.

S&ME (1988). "Drilled Shaft Load Test – Dredge Disposal Island – I-526 Bridge over Cooper River and Clouter Creek", Report Submitted to Howard, Needles, Tammen & Bergendoff, Wando, SC.

S&ME (2001). “Summary Report of Load Test Program – Cooper River Bridge Replacement Project”, Report Submitted to Sverdrup Civil, Inc., New York, NY.

Salgado, R. (2006). “The role of analysis in non-displacement pile design.” *Modern Trends in Geomechanics*, W. Wu and H.-S. Yu, eds., Springer, New York, 521–540.

SCDOT (2007). “2007 Standard Specifications for Highway Construction” South Carolina Department of Transportation, Columbia, SC.

SCDOT (2008). “SCDOT Seismic Design Specifications for Highway Bridges, Version 2.0” South Carolina Department of Transportation, Columbia, SC.

SCDOT (2010). “Geotechnical Design Manual Version, 1.1” South Carolina Department of Transportation, Columbia, SC.

Seidel, J., Rausche, F. (1984). “Correlation of Static and Dynamic Pile Tests on Large Diameter Drilled Shafts.” *Second International Conference on the Application of Stress Wave Theory on Piles*: Stockholm, Sweden, May 1984; 313-318.

Sellountou, A., Alvarez, C., Rausche, F. (2013). “Thermal Integrity Profiling: A Recent Technological Advancement in Integrity Evaluation of Concrete Piles.” *Proceedings from the First International Conference, Seminar on Deep Foundations*: Santa Cruz, Bolivia.

Shen, L. and Bittner, R.B. (2013). “Design of the drilled Shaft Foundations for the Cooper River Bridge.” *Deep Marine Foundations – A Perspective on the Design and Construction of Deep Marine Foundations*. 1-14.

Skempton, A.W. (1959). “Cast In-situ Bored Piles in London Clay”, *Géotechnique*, vol 9. 153-173.

Takesue, K., Sasao, H., Matsumoto, T. (1998). “Correlation Between Ultimate Pile Skin Friction and CPT Data”, *Geotechnical Site Characterization*, Vol. 2, Rotterdam, 1177-1182

USBM (1996). Dictionary of Mining, Mineral, and Related Terms., US Bureau of Mines.

Weems, R.E., Lemon, E.M. (1985). “Detailed Sections from Auger Holes and Outcrops in the Cainhoy, Charleston, and Fort Moultrie Quadrangles, South Carolina.”, U.S. Geologic Survey Open-File Report Number 85-378.

Weems, R.E., Lewis, W.C. (2002). “Structural and Tectonic Setting of the Charleston, SC Region: Evidence from the Tertiary Stratigraphic Record,” *Geological Society of America Bulletin.,* January 2002, 24-42.

APPENDIX A – LOAD TEST DATA

DRILLED SHAFT LOG

Project:	Isle of Palms Connector (SC 517)		
Data Source / Testing Firm:	Law Engineering		
County:	Charleston	**Load Test Type:**	Static
Load Test Number:	1A	**Year Tested:**	1991

Shaft Part	Elevation (ft)	Diagram	Elevation (ft)	Unit Skin Resisance
TOS/TOC	11			
TOG	8		8	0.24 ksf
WL	0		-32	
SG	-32		-32	0.25 ksf
SG	-64		-64	0.30 ksf
TOM/SG	-93		-93	0.43 ksf
BOC/SG	-132		-132	3.66 ksf
BOS	-142		-142	

Top of Casing Elevation (ft):	11
Bottom of Casing Elevation (ft):	-132
Diameter of Shaft (in):	24
Mud-line/Surface Elev. (ft):	8
Constructed Shaft Length (ft):	153
Top of Shaft Elevation (ft):	11
Tip Elevation (ft):	-142

Legend	Meaning
TOC	Top of Casing
TOG	Top of Ground
TOS	Top of Shaft
BOC	Bottom of Casing
BOS	Bottom of Shaft
TOM	Top of Marl
WL	Water Level
SG	Strain Gage
OC	Osterberg Cell

DRILLED SHAFT LOG

Project:	Isle of Palms Connector (SC 517)		
Data Source / Testing Firm:	Law Engineering		
County:	Charleston	**Load Test Type:**	Static
Load Test Number:	1B	**Year Tested:**	1991

Shaft Part	Elevation (ft)	Diagram	Elevation (ft)	Unit Skin Resisance
TOS/TOC	11			
TOG	8		8	0.62 ksf
WL	0		-24	
SG	-24		-24	0.06 ksf
SG	-64		-64	0.81 ksf
TOM/SG	-93		-93	0.0 ksf
BOC/SG	-106		-106	3.39 ksf
SG	-114		-114	3.39 ksf
BOS	-129		-129	

Top of Casing Elevation (ft):	11
Bottom of Casing Elevation (ft):	-106
Diameter of Shaft (in):	24
Mud-line/Surface Elev. (ft):	8
Constructed Shaft Length (ft):	140
Top of Shaft Elevation (ft):	11
Tip Elevation (ft):	-129

Legend	Meaning
TOC	Top of Casing
TOG	Top of Ground
TOS	Top of Shaft
BOC	Bottom of Casing
BOS	Bottom of Shaft
TOM	Top of Marl
WL	Water Level
SG	Strain Gage
OC	Osterberg Cell

DRILLED SHAFT LOG

Project:	SC 703 over Breach Inlet		
Data Source / Testing Firm:	Loadtest		
County:	Charleston	**Load Test Type:**	Single Cell Osterberg
Load Test Number:	2	**Year Tested:**	2000

Shaft Part	Elevation (ft)	Diagram	Elevation (ft)	Unit Skin Resisance
TOC	2.6			
TOG/TOS	2.2		2.2	1.10 ksf
WL	2			
			-54.8	
SG 5	-54.8		-54.8	0.25 ksf
TOM	-57.4			
BOC	-64.6			
			-68.8	
SG 4	-68.8		-68.8	0.16 ksf
			-80.4	
SG 3	-80.4		-80.4	1.91 ksf
			-91.8	
SG 2	-91.8		-91.8	0.17 ksf
			-103.3	
SG 1	-103.3		-103.3	2.79 ksf
OC	-115.3		-115.3	
BOS	-142.2			

Top of Casing Elevation (ft):	2.6
Bottom of Casing Elevation (ft):	-64.6
Diameter of Shaft (in):	48
Mud-line/Surface Elev. (ft):	2.2
Constructed Shaft Length (ft):	144.4
Top of Shaft Elevation (ft):	2.2
Tip Elevation (ft):	-142.2

Legend	Meaning
TOC	Top of Casing
TOG	Top of Ground
TOS	Top of Shaft
BOC	Bottom of Casing
BOS	Bottom of Shaft
TOM	Top of Marl
WL	Water Level
SG	Strain Gage
OC	Osterberg Cell

DRILLED SHAFT LOG

Project:	US 17 over the Cooper River		
Data Source / Testing Firm:	Loadtest		
County:	Charleston	**Load Test Type:**	Two Cell Osterberg
Load Test Number:	3A	**Year Tested:**	2000

Shaft Part	Elevation (ft)	Diagram	Elevation (ft)	Unit Skin Resisance
TOC/TOS	9.1			
TOG	4.1		4.1	
WL	1.1			
				0.0 ksf
			-32.2	
SG 8	-32.2		-32.2	
				0.0 ksf
			-44.2	
SG 7	-44.2		-44.2	
				0.0 ksf
BOC	-49.9			
			-56.2	
SG 6	-56.2		-56.2	
TOM	-59			4.07 ksf
			-68.2	
SG 5	-68.2		-68.2	
				2.84 ksf
			-80.2	
SG 4	-80.2		-80.2	
				6.47 ksf
			-96.2	
OC	-96.2		-96.2	
				7.37 ksf
			-106.2	
SG 3	-106.2		-106.2	
				3.55 ksf
			-116.2	
SG 2	-116.2		-116.2	
				0.41 ksf
			-126.2	
SG 1	-126.2		-126.2	
				6.23 ksf
OC	-136.2		-136.2	
BOS	-148.2			

Top of Casing Elevation (ft):	9.1
Bottom of Casing Elevation (ft):	-49.9
Diameter of Shaft (in):	96
Mud-line/Surface Elev. (ft):	4.1
Constructed Shaft Length (ft):	157.3
Top of Shaft Elevation (ft):	9.1
Tip Elevation (ft):	-148.2

Legend	Meaning
TOC	Top of Casing
TOG	Top of Ground
TOS	Top of Shaft
BOC	Bottom of Casing
BOS	Bottom of Shaft
TOM	Top of Marl
WL	Water Level
SG	Strain Gage
OC	Osterberg Cell

DRILLED SHAFT LOG

Project:	US 17 over the Cooper River		
Data Source / Testing Firm:	Loadtest		
County:	Charleston	**Load Test Type:**	Two Cell Osterberg
Load Test Number:	3B	**Year Tested:**	2000

Shaft Part	Elevation (ft)	Diagram	Elevation (ft)	Unit Skin Resisance
TOC/TOS	10.3			
TOG	4.4			
WL	1.1			
				0.0 ksf
			-34.6	
SG 8	-34.6		-34.6	
				0.0 ksf
			-46.6	
SG 7	-46.6		-46.6	
BOC	-47.7			0.0 ksf
			-58.6	
SG 6	-58.6		-58.6	
TOM	-59			2.11 ksf
			-70.6	
SG 5	-70.6		-70.6	
				3.59 ksf
			-82.6	
SG 4	-82.6		-82.6	
				5.83 ksf
			-98.6	
OC	-98.6		-98.6	
				3.44 ksf
			-108.6	
SG 3	-108.6		-108.6	
				4.94 ksf
			-118.6	
SG 2	-118.6		-118.6	
				1.98 ksf
			-128.6	
SG 1	-128.6		-128.6	
				5.36 ksf
OC	-138.6		-138.6	
BOS	-147.2			

Top of Casing Elevation (ft):	10.3
Bottom of Casing Elevation (ft):	-47.7
Diameter of Shaft (in):	96
Mud-line/Surface Elev. (ft):	4.4
Constructed Shaft Length (ft):	157.5
Top of Shaft Elevation (ft):	10.3
Tip Elevation (ft):	-147.2

Legend	Meaning
TOC	Top of Casing
TOG	Top of Ground
TOS	Top of Shaft
BOC	Bottom of Casing
BOS	Bottom of Shaft
TOM	Top of Marl
WL	Water Level
SG	Strain Gage
OC	Osterberg Cell

DRILLED SHAFT LOG

Project:	US 17 over the Cooper River		
Data Source / Testing Firm:	Loadtest		
County:	Charleston	**Load Test Type:**	Single Cell Osterberg
Load Test Number:	3C	**Year Tested:**	2000

Shaft Part	Elevation (ft)	Diagram	Elevation (ft)	Unit Skin Resisance
TOC	11.1			
TOS	10.1		10.1	0.0 ksf
TOG	4.89			
WL	1.1			
			-27.8	
SG 5	-27.8		-27.8	0.0 ksf
			-39.8	
SG 4	-39.8		-39.8	0.11 ksf
TOM	-50		-51.8	
SG 3	-51.8		-51.8	0.75 ksf
BOC	-57.9		-63.8	
SG 2	-63.8		-63.8	2.14 ksf
			-75.8	
SG 1	-75.8		-75.8	3.78 ksf
OC	-93.3		-93.3	
BOS	-101.2			

Top of Casing Elevation (ft):	11.1
Bottom of Casing Elevation (ft):	-57.9
Diameter of Shaft (in):	96
Mud-line/Surface Elev. (ft):	4.89
Constructed Shaft Length (ft):	111.3
Top of Shaft Elevation (ft):	10.1
Tip Elevation (ft):	-101.2

Legend	Meaning
TOC	Top of Casing
TOG	Top of Ground
TOS	Top of Shaft
BOC	Bottom of Casing
BOS	Bottom of Shaft
TOM	Top of Marl
WL	Water Level
SG	Strain Gage
OC	Osterberg Cell

DRILLED SHAFT LOG

Project:	US 17 over the Cooper River		
Data Source / Testing Firm:	Loadtest		
County:	Charleston	**Load Test Type:**	Single Cell Osterberg
Load Test Number:	3D	**Year Tested:**	2000

Shaft Part	Elevation (ft)	Diagram	Elevation (ft)	Unit Skin Resisance
TOC/TOS	11.1		11.1	
TOG	4.1			
WL	1.1			
				0.0 ksf
			-35.9	
SG 5	-35.9		-35.9	
				0.0 ksf
			-47.9	
SG 4	-47.9		-47.9	
				0.0 ksf
BOC	-58.9		-59.9	
SG 3	-59.9		-59.9	
TOM	-63			
				0.89 ksf
			-71.9	
SG 2	-71.9		-71.9	
				1.75 ksf
			-83.9	
SG 1	-83.9		-83.9	
				3.22 ksf
OC	-97.0		-97.0	
BOS	-100.0			

Top of Casing Elevation (ft):	10.1
Bottom of Casing Elevation (ft):	-58.9
Diameter of Shaft (in):	72
Mud-line/Surface Elev. (ft):	4.1
Constructed Shaft Length (ft):	110.1
Top of Shaft Elevation (ft):	10.1
Tip Elevation (ft):	-100

Legend	Meaning
TOC	Top of Casing
TOG	Top of Ground
TOS	Top of Shaft
BOC	Bottom of Casing
BOS	Bottom of Shaft
TOM	Top of Marl
WL	Water Level
SG	Strain Gage
OC	Osterberg Cell

DRILLED SHAFT LOG

Project:	US 17 over the Cooper River		
Data Source / Testing Firm:	Applied Foundation Testing		
County:	Charleston	**Load Test Type:**	Statnamic
Load Test Number:	3E	**Year Tested:**	2000

Shaft Part	Elevation (ft)	Diagram	Elevation (ft)	Unit Skin Resisance
TOC / TOS	6.0		6.0	
TOG	0			
				1.2 ksf
			-36.2	
SG	-36.2		-36.2	
				1.3 ksf
TOM	-56.5			
BOC	-62.8			
			-70.2	
SG	-70.2		-70.2	
				2.4 ksf
			-82.2	
SG	-82.2		-82.2	
				3.7 ksf
			-97.4	
SG	-97.4			
BOS	-106.2			

Top of Casing Elevation (ft):	6.0
Bottom of Casing Elevation (ft):	-62.8
Diameter of Shaft (in):	96
Mud-line/Surface Elev. (ft):	0
Constructed Shaft Length (ft):	112.2
Top of Shaft Elevation (ft):	6.0
Tip Elevation (ft):	-106.2

Legend	Meaning
TOC	Top of Casing
TOG	Top of Ground
TOS	Top of Shaft
BOC	Bottom of Casing
BOS	Bottom of Shaft
TOM	Top of Marl
WL	Water Level
SG	Strain Gage
OC	Osterberg Cell

DRILLED SHAFT LOG

Project:	US 17 over the Cooper River		
Data Source / Testing Firm:	Applied Foundation Testing		
County:	Charleston	**Load Test Type:**	Statnamic
Load Test Number:	3F	**Year Tested:**	2000

Shaft Part	Elevation (ft)	Diagram	Elevation (ft)	Unit Skin Resisance
TOC / TOS	6.0		6.0	
TOG	0			
				1.9 ksf
TOM	-50.5			
BOC	-63.0			
			-70.1	
SG	-70.1		-70.1	
				8.2 ksf
			-82.0	
SG	-82.0		-82.0	
				8.9 ksf
			-93.0	
SG	-93.0			
BOS	-102.7			

Top of Casing Elevation (ft):	6.0
Bottom of Casing Elevation (ft):	-63.0
Diameter of Shaft (in):	72
Mud-line/Surface Elev. (ft):	0
Constructed Shaft Length (ft):	112.2
Top of Shaft Elevation (ft):	6.0
Tip Elevation (ft):	-106.2

Legend	Meaning
TOC	Top of Casing
TOG	Top of Ground
TOS	Top of Shaft
BOC	Bottom of Casing
BOS	Bottom of Shaft
TOM	Top of Marl
WL	Water Level
SG	Strain Gage
OC	Osterberg Cell

DRILLED SHAFT LOG

Project:	US 17 over the Cooper River		
Data Source / Testing Firm:	Loadtest		
County:	Charleston	**Load Test Type:**	Two Cell Osterberg
Load Test Number:	4A	**Year Tested:**	2000

Shaft Part	Elevation (ft)	Diagram	Elevation (ft)	Unit Skin Resisance
TOC/TOS	12.0		0.0	
WL	0.0			
				0.0 ksf
			-21.0	
TOG	-21.0		-21.0	
				0.53 ksf
			-52.5	
SG 7	-52.5		-52.5	
				0.05 ksf
TOM	-57			
BOC	-61		-62.5	
SG 6	-62.5		-62.5	
				2.34 ksf
			-72.5	
SG 5	-72.5		-72.5	
				2.99 ksf
			-82.5	
SG 4	-82.5		-82.5	
				3.43 ksf
			-92.5	
SG 3	-92.5		-92.5	
				5.66 ksf
			-107.0	
OC	-107.0		-107.0	
				4.27 ksf
			-118.0	
SG 2	-118.0		-118.0	
				2.24 ksf
			-129.0	
SG 1	-129.0		-129.0	
				2.84 ksf
OC	-140.2		-140.2	
BOS	-146.5			

Top of Casing Elevation (ft):	12.0
Bottom of Casing Elevation (ft):	-61.0
Diameter of Shaft (in):	96
Mud-line/Surface Elev. (ft):	-21.0
Constructed Shaft Length (ft):	158.5
Top of Shaft Elevation (ft):	12.0
Tip Elevation (ft):	-146.5

Legend	Meaning
TOC	Top of Casing
TOG	Top of Ground
TOS	Top of Shaft
BOC	Bottom of Casing
BOS	Bottom of Shaft
TOM	Top of Marl
WL	Water Level
SG	Strain Gage
OC	Osterberg Cell

DRILLED SHAFT LOG

Project:	US 17 over the Cooper River		
Data Source / Testing Firm:	Loadtest		
County:	Charleston	**Load Test Type:**	Single Cell Osterberg
Load Test Number:	4B	**Year Tested:**	2000

Shaft Part	Elevation (ft)	Diagram	Elevation (ft)	Unit Skin Resisance
TOC/TOS	11.9		11.9	
WL	0			
TOG	-21.6			0.02 ksf
			-55.8	
SG 4	-55.8		-55.8	
TOM	-57			0.38 ksf
BOC	-60.1			
			-65.8	
SG 3	-65.8		-65.8	
				1.91 ksf
			-75.8	
SG 2	-75.8		-75.8	
				2.42 ksf
			-85.8	
SG 1	-85.8		-85.8	
				5.20 ksf
OC	-96.7		-96.7	
BOS	-101.2			

Top of Casing Elevation (ft):	11.9
Bottom of Casing Elevation (ft):	-60.1
Diameter of Shaft (in):	72
Mud-line/Surface Elev. (ft):	-21.6
Constructed Shaft Length (ft):	115.1
Top of Shaft Elevation (ft):	11.1
Tip Elevation (ft):	-103.2

Legend	Meaning
TOC	Top of Casing
TOG	Top of Ground
TOS	Top of Shaft
BOC	Bottom of Casing
BOS	Bottom of Shaft
TOM	Top of Marl
WL	Water Level
SG	Strain Gage
OC	Osterberg Cell

DRILLED SHAFT LOG

Project:	US 17 over the Cooper River		
Data Source / Testing Firm:	Loadtest		
County:	Charleston	**Load Test Type:**	Two Cell Osterberg
Load Test Number:	5A	**Year Tested:**	2000

Shaft Part	Elevation (ft)	Diagram	Elevation (ft)	Unit Skin Resisance
TOC	11.3			
TOS	10.6			
TOG	7.1		7.1	
WL	2.1			
				0.07 ksf
			-29.2	
SG 8	-29.2		-29.2	
TOM	-30			0.19 ksf
			-41.2	
SG 7	-41.2		-41.2	
				2.09 ksf
BOC	-46.7			
			-53.2	
SG 6	-53.2		-53.2	
				2.56 ksf
			-65.2	
SG 5	-65.2		-65.2	
				4.15 ksf
			-77.2	
SG 4	-77.2		-77.2	
				5.24 ksf
			-93.2	
OC	-93.2	X	-93.2	
				7.54 ksf
			-104.2	
SG 3	-104.2		-104.2	
				1.81 ksf
			-116.2	
SG 2	-116.2		-116.2	
				3.86 ksf
			-127.7	
SG 1	-127.7		-127.7	
				2.31 ksf
OC	-139.2	X	-139.2	
BOS	-147.5			

Top of Casing Elevation (ft):	11.3
Bottom of Casing Elevation (ft):	-46.7
Diameter of Shaft (in):	96
Mud-line/Surface Elev. (ft):	7.1
Constructed Shaft Length (ft):	158.1
Top of Shaft Elevation (ft):	10.6
Tip Elevation (ft):	-147.5

Legend	Meaning
TOC	Top of Casing
TOG	Top of Ground
TOS	Top of Shaft
BOC	Bottom of Casing
BOS	Bottom of Shaft
TOM	Top of Marl
WL	Water Level
SG	Strain Gage
OC	Osterberg Cell

DRILLED SHAFT LOG

Project:	US 17 over the Cooper River		
Data Source / Testing Firm:	Loadtest		
County:	Charleston	**Load Test Type:**	Two Cell Osterberg
Load Test Number:	5B	**Year Tested:**	2000

Shaft Part	Elevation (ft)	Diagram	Elevation (ft)	Unit Skin Resisance
TOC/TOS	12.8			
TOG	7.1		7.1	
WL	2.1			
				0.01 ksf
TOM	-30		-30.2	
SG 8	-30.2		-30.2	
				2.47 ksf
			-42.2	
SG 7	-42.2		-42.2	
				1.28 ksf
			-54.2	
SG 6	-54.2		-54.2	
				2.79 ksf
BOC	-60.2			
			-66.2	
SG 5	-66.2		-66.2	
				3.09 ksf
			-78.2	
SG 4	-78.2		-78.2	
				6.01 ksf
			-94.2	
OC	-94.2		-94.2	
				6.60 ksf
			-105.7	
SG 3	-105.7		-105.7	
				3.24 ksf
			-117.2	
SG 2	-117.2		-117.2	
				2.84 ksf
			-128.7	
SG 1	-128.7		-128.7	
				3.53 ksf
OC	-140.2		-140.2	
BOS	-144.2			

Top of Casing Elevation (ft):	12.8
Bottom of Casing Elevation (ft):	-60.2
Diameter of Shaft (in):	96
Mud-line/Surface Elev. (ft):	7.1
Constructed Shaft Length (ft):	157
Top of Shaft Elevation (ft):	12.8
Tip Elevation (ft):	-144.2

Legend	Meaning
TOC	Top of Casing
TOG	Top of Ground
TOS	Top of Shaft
BOC	Bottom of Casing
BOS	Bottom of Shaft
TOM	Top of Marl
WL	Water Level
SG	Strain Gage
OC	Osterberg Cell

DRILLED SHAFT LOG

Project:	US 17 over the Cooper River		
Data Source / Testing Firm:	Loadtest		
County:	Charleston	**Load Test Type:**	Single Cell Osterberg
Load Test Number:	5C	**Year Tested:**	2000

Shaft Part	Elevation (ft)	Diagram	Elevation (ft)	Unit Skin Resisance
TOC	12.6			
TOS	12.1		12.1	0.13 ksf
TOG	6.6			
WL	2.1			
TOM	-31		-31.4	
SG 5	-31.4		-31.4	0.13 ksf
SG 4	-43.4		-43.4	0.13 ksf
SG 3	-55.4		-55.4	0.30 ksf
BOC	-59.4			
SG 2	-67.4		-67.4	3.32 ksf
SG 1	-79.4		-79.4	3.52 ksf
OC	-92.6		-92.6	
BOS	-96.9			

Top of Casing Elevation (ft):	12.6
Bottom of Casing Elevation (ft):	-59.4
Diameter of Shaft (in):	96
Mud-line/Surface Elev. (ft):	6.6
Constructed Shaft Length (ft):	109
Top of Shaft Elevation (ft):	12.1
Tip Elevation (ft):	-96.9

Legend	Meaning
TOC	Top of Casing
TOG	Top of Ground
TOS	Top of Shaft
BOC	Bottom of Casing
BOS	Bottom of Shaft
TOM	Top of Marl
WL	Water Level
SG	Strain Gage
OC	Osterberg Cell

DRILLED SHAFT LOG

Project:	US 17 over the Cooper River		
Data Source / Testing Firm:	Loadtest		
County:	Charleston	**Load Test Type:**	Single Cell Osterberg
Load Test Number:	5D	**Year Tested:**	2000

Shaft Part	Elevation (ft)	Diagram	Elevation (ft)	Unit Skin Resisance
TOC	11.5			
TOS	11.1		11.1	
TOG	7.5			
WL	2.1			
				0.0 ksf
			-28.5	
SG 5	-28.5		-28.5	
TOM	-31			0.37 ksf
			-40.5	
SG 4	-40.5		-40.5	
				0.21 ksf
			-52.5	
SG 3	-52.2		-52.5	
				0.32 ksf
BOC	-57.5			
			-64.5	
SG 2	-64.5		-64.5	
				1.23 ksf
			-76.5	
SG 1	-76.5		-76.5	
				2.97 ksf
OC	-90.8		-90.8	
BOS	-96.9			

Top of Casing Elevation (ft):	11.5
Bottom of Casing Elevation (ft):	-57.5
Diameter of Shaft (in):	72
Mud-line/Surface Elev. (ft):	7.5
Constructed Shaft Length (ft):	106.4
Top of Shaft Elevation (ft):	11.1
Tip Elevation (ft):	-95.3

Legend	Meaning
TOC	Top of Casing
TOG	Top of Ground
TOS	Top of Shaft
BOC	Bottom of Casing
BOS	Bottom of Shaft
TOM	Top of Marl
WL	Water Level
SG	Strain Gage
OC	Osterberg Cell

DRILLED SHAFT LOG

Project:	US 17 over the Cooper River		
Data Source / Testing Firm:	Applied Foundation Testing		
County:	Charleston	**Load Test Type:**	Statnamic
Load Test Number:	5E	**Year Tested:**	2000

Shaft Part	Elevation (ft)	Diagram	Elevation (ft)	Unit Skin Resisance
TOC / TOS	6.0		6.0	
TOG	0			
				1.6 ksf
TOM	-41			
			-43.9	
SG	-43.9		-43.9	
				1.6 ksf
BOC	-66.0			
			-69.8	
SG	-69.8		-69.8	
				2.1 ksf
			-81.9	
SG	-81.9		-81.9	
				3.9 ksf
			-93.2	
SG	-93.2			
BOS	-104.0			

Top of Casing Elevation (ft):	6.0
Bottom of Casing Elevation (ft):	-66.0
Diameter of Shaft (in):	96
Mud-line/Surface Elev. (ft):	0
Constructed Shaft Length (ft):	110.0
Top of Shaft Elevation (ft):	6.0
Tip Elevation (ft):	-104

Legend	Meaning
TOC	Top of Casing
TOG	Top of Ground
TOS	Top of Shaft
BOC	Bottom of Casing
BOS	Bottom of Shaft
TOM	Top of Marl
WL	Water Level
SG	Strain Gage
OC	Osterberg Cell

DRILLED SHAFT LOG

Project:	US 17 over the Cooper River		
Data Source / Testing Firm:	Applied Foundation Testing		
County:	Charleston	**Load Test Type:**	Statnamic
Load Test Number:	5F	**Year Tested:**	2000

Shaft Part	Elevation (ft)	Diagram	Elevation (ft)	Unit Skin Resisance
TOC / TOS	4.0		4.0	
TOG	0			
				2.0 ksf
			-30.0	
SG	-30		-30.0	
TOM	-40			
				1.1 ksf
			-65.0	
BOC/SG	-65.0		-65.0	
				3.8 ksf
			-75.0	
SG	-75.0		-75.0	
				5.7 ksf
			-85.0	
SG	-85.0		-85.0	
				6.8 ksf
			-93.0	
SG	-93.0			
BOS	-102.8			

Top of Casing Elevation (ft):	4.0
Bottom of Casing Elevation (ft):	-65.0
Diameter of Shaft (in):	72
Mud-line/Surface Elev. (ft):	0
Constructed Shaft Length (ft):	106.8
Top of Shaft Elevation (ft):	4.0
Tip Elevation (ft):	-102.8

Legend	Meaning
TOC	Top of Casing
TOG	Top of Ground
TOS	Top of Shaft
BOC	Bottom of Casing
BOS	Bottom of Shaft
TOM	Top of Marl
WL	Water Level
SG	Strain Gage
OC	Osterberg Cell

DRILLED SHAFT LOG

Project:	Maybank Highway (SC 700) over the Stono River		
Data Source / Testing Firm:	Loadtest		
County:	Charleston	**Load Test Type:**	Two Cell Osterberg
Load Test Number:	6	**Year Tested:**	2001

Shaft Part	Elevation (ft)	Diagram	Elevation (ft)	Unit Skin Resisance
TOC	6.3		6.3	
TOS	6.0			
TOG/WL	3.3			
				0.15 ksf
TOM	-20.7		-23.0	
SG 4	-23.0		-23.0	
				1.06 ksf
			-31.2	
SG 3	-31.2		-31.2	
				3.67 ksf
			-39.4	
SG 2	-39.4		-39.4	
				4.66 ksf
			-50.5	
OC	-50.5		-50.5	
				3.72 ksf
			-60.7	
SG 1	-60.7		-60.7	
				2.71 ksf
OC	-71.5		-71.5	
BOS	-78.9			

Top of Casing Elevation (ft):	6.3
Bottom of Casing Elevation (ft):	-28.7
Diameter of Shaft (in):	78
Mud-line/Surface Elev. (ft):	3.3
Constructed Shaft Length (ft):	84.9
Top of Shaft Elevation (ft):	6.0
Tip Elevation (ft):	-78.9

Legend	Meaning
TOC	Top of Casing
TOG	Top of Ground
TOS	Top of Shaft
BOC	Bottom of Casing
BOS	Bottom of Shaft
TOM	Top of Marl
WL	Water Level
SG	Strain Gage
OC	Osterberg Cell

DRILLED SHAFT LOG

Project:	Limehouse Bridge (S-10-20) over the Stono River		
Data Source / Testing Firm:	Applied Foundation Testing		
County:	Charleston	**Load Test Type:**	Statnamic
Load Test Number:	7	**Year Tested:**	2002

Shaft Part	Elevation (ft)	Diagram	Elevation (ft)	Unit Skin Resisance
TOC/TOS	7.6			
TOG	0			
TOM	-22.7		-22.7	
SG	-22.8		-22.7	
				4.40 ksf
BOC	-30.4			
			-37.8	
SG	-37.8		-37.8	
				1.73 ksf
			-77.8	
SG	-77.8		-77.8	
				1.87 ksf
SG	-121.8		-121.8	
BOS	-123.2			

Top of Casing Elevation (ft):	7.6
Bottom of Casing Elevation (ft):	-30.4
Diameter of Shaft (in):	72
Mud-line/Surface Elev. (ft):	0
Constructed Shaft Length (ft):	130.8
Top of Shaft Elevation (ft):	7.6
Tip Elevation (ft):	-123.2

Legend	Meaning
TOC	Top of Casing
TOG	Top of Ground
TOS	Top of Shaft
BOC	Bottom of Casing
BOS	Bottom of Shaft
TOM	Top of Marl
WL	Water Level
SG	Strain Gage
OC	Osterberg Cell

DRILLED SHAFT LOG

Project:	Ashley Phosphate Road over I-26		
Data Source / Testing Firm:	Applied Foundation Testing		
County:	Charleston	**Load Test Type:**	Statnamic
Load Test Number:	8	**Year Tested:**	2003

Shaft Part	Elevation (ft)	Diagram	Elevation (ft)	Unit Skin Resisance
TOC/TOS	35.5		35.5	
TOG	34.0			
				0.37 ksf
			12.9	
SG	12.9		12.9	
TOM	10.4			
				3.11 ksf
			2.9	
SG	2.9		2.9	
				3.62 ksf
			-7.1	
SG	-7.1		-7.1	
BOC	-7.6			
				2.69 ksf
			-17.1	
SG	-17.1		-17.1	
				3.18 ksf
			-27.1	
SG	-27.1		-27.1	
				2.78 ksf
SG	-37.0		-37.0	
BOS	-39.6			

Top of Casing Elevation (ft):	35.5
Bottom of Casing Elevation (ft):	-7.6
Diameter of Shaft (in):	42
Mud-line/Surface Elev. (ft):	34.0
Constructed Shaft Length (ft):	75.1
Top of Shaft Elevation (ft):	35.5
Tip Elevation (ft):	-39.6

Legend	Meaning
TOC	Top of Casing
TOG	Top of Ground
TOS	Top of Shaft
BOC	Bottom of Casing
BOS	Bottom of Shaft
TOM	Top of Marl
WL	Water Level
SG	Strain Gage
OC	Osterberg Cell

DRILLED SHAFT LOG

Project:	US 52 over I-26		
Data Source / Testing Firm:	Applied Foundation Testing		
County:	Charleston	**Load Test Type:**	Statnamic
Load Test Number:	9	**Year Tested:**	2003

Shaft Part	Elevation (ft)	Diagram	Elevation (ft)	Unit Skin Resisance
TOC/TOS	15.3		15.3	
TOG	13.0			
				0.33 ksf
			-8.7	
SG	-8.7		-8.7	
TOM	-12.0			
				2.92 ksf
			-18.7	
SG	-18.7		-18.7	
BOC	-23.4			3.89 ksf
			-28.7	
SG	-28.7		-28.7	
				3.03 ksf
			-38.7	
SG	-38.7		-38.7	
				3.20 ksf
SG	-48.7		-48.7	
BOS	-51.1			

Top of Casing Elevation (ft):	15.3
Bottom of Casing Elevation (ft):	-23.4
Diameter of Shaft (in):	48
Mud-line/Surface Elev. (ft):	36.0
Constructed Shaft Length (ft):	66.4
Top of Shaft Elevation (ft):	15.3
Tip Elevation (ft):	-51.1

Legend	Meaning
TOC	Top of Casing
TOG	Top of Ground
TOS	Top of Shaft
BOC	Bottom of Casing
BOS	Bottom of Shaft
TOM	Top of Marl
WL	Water Level
SG	Strain Gage
OC	Osterberg Cell

DRILLED SHAFT LOG

Project:	Remount Road / Aviation Avenue over I-26		
Data Source / Testing Firm:	Applied Foundation Testing		
County:	Charleston	**Load Test Type:**	Statnamic
Load Test Number:	10	**Year Tested:**	2008

Shaft Part	Elevation (ft)	Diagram	Elevation (ft)	Unit Skin Resisance
TOC/TOS	40.3		40.3	
TOG	39.1			
WL	28.0			1.3 ksf
			16.1	
SG	16.1		16.1	
				2.0 ksf
TOM	1.5			
			-3.9	
SG	-3.9		-3.9	
BOC	-4.7			
				3.8 ksf
			-13.9	
SG	-13.9		-13.9	
				3.8 ksf
BOS	-26.2		-26.2	

Top of Casing Elevation (ft):	40.3
Bottom of Casing Elevation (ft):	-4.7
Diameter of Shaft (in):	36
Mud-line/Surface Elev. (ft):	39.1
Constructed Shaft Length (ft):	66.5
Top of Shaft Elevation (ft):	40.3
Tip Elevation (ft):	-26.2

Legend	Meaning
TOC	Top of Casing
TOG	Top of Ground
TOS	Top of Shaft
BOC	Bottom of Casing
BOS	Bottom of Shaft
TOM	Top of Marl
WL	Water Level
SG	Strain Gage
OC	Osterberg Cell

DRILLED SHAFT LOG

Project:	I-526 / Hungryneck Bouevard over US 17		
Data Source / Testing Firm:	Applied Foundation Testing		
County:	Charleston	**Load Test Type:**	Statnamic
Load Test Number:	11	**Year Tested:**	2011

Shaft Part	Elevation (ft)	Diagram	Elevation (ft)	Unit Skin Resisance
TOC/TOS	16.0		16.0	
TOG	14.8			
WL	9.0			
				0.3 ksf
			-24.5	
SG	-24.5		-24.5	
				1.3 ksf
			-54.5	
SG	-54.5		-54.5	
				0.7 ksf
TOM	-78.0			
BOC	-84.0		-84.5	
SG	-84.5		-84.5	3.8 ksf
			-92.5	
SG	-92.5		-92.5	3.9 ksf
			-102.5	
SG	-102.5		-102.5	3.9 ksf
BOS	-104.5		-104.5	

Top of Casing Elevation (ft):	16
Bottom of Casing Elevation (ft):	-84.0
Diameter of Shaft (in):	48
Mud-line/Surface Elev. (ft):	14.8
Constructed Shaft Length (ft):	120.5
Top of Shaft Elevation (ft):	16
Tip Elevation (ft):	-104.5

Legend	Meaning
TOC	Top of Casing
TOG	Top of Ground
TOS	Top of Shaft
BOC	Bottom of Casing
BOS	Bottom of Shaft
TOM	Top of Marl
WL	Water Level
SG	Strain Gage
OC	Osterberg Cell

DRILLED SHAFT LOG

Project: Folly Road (SC 171) over Folly Creek
Data Source / Testing Firm: GRL Engineers
County: Charleston **Load Test Type:** APPLE
Load Test Number: 12 **Year Tested:** 2012

Shaft Part	Elevation (ft)	Diagram	Elevation (ft)	Unit Skin Resisance
TOC/TOS	11.0			
TOG	1.6			
WL	0.0			
TOM	-57.2			
			-58.0	
BOC	-62.5			3.39 ksf
			-65.0	
			-65.0	
				3.5 ksf
			-72.0	
			-72.0	
				3.09 ksf
			-78.0	
			-78.0	
				2.73 ksf
			-84.0	
			-84.0	
				2.42 ksf
			-90.0	
BOS	-93.0			

Top of Casing Elevation (ft):	11
Bottom of Casing Elevation (ft):	-62.5
Diameter of Shaft (in):	48
Mud-line/Surface Elev. (ft):	1.6
Constructed Shaft Length (ft):	104
Top of Shaft Elevation (ft):	11
Tip Elevation (ft):	-93

Legend	Meaning
TOC	Top of Casing
TOG	Top of Ground
TOS	Top of Shaft
BOC	Bottom of Casing
BOS	Bottom of Shaft
TOM	Top of Marl
WL	Water Level
SG	Strain Gage
OC	Osterberg Cell

DRILLED SHAFT LOG

Project:	US 78 over CSX Railroad		
Data Source / Testing Firm:	Applied Foundation Testing		
County:	Charleston	**Load Test Type:**	Statnamic
Load Test Number:	13	**Year Tested:**	2013

Shaft Part	Elevation (ft)	Diagram	Elevation (ft)	Unit Skin Resisance
TOC/TOS	17.6			
GL	17.0			
WL	13.5			
SG	9.7		9.7	
				1.08 ksf
			-27.2	
SG	-27.2		-27.2	
				3.45 ksf
TOM	-35.7			
BOC	-35.9		-36.2	
SG	-36.2		-36.2	
				2.0 ksf
			-56.2	
SG	-56.2		-56.2	
				4.35 ksf
			-76.2	
SG	-76.2		-76.2	
				4.7 ksf
SG	-95.2		-95.2	
BOS	-100.2			

Top of Casing Elevation (ft):	17.6
Bottom of Casing Elevation (ft):	-35.9
Diameter of Shaft (in):	60
Mud-line/Surface Elev. (ft):	17.0
Constructed Shaft Length (ft):	117.8
Top of Shaft Elevation (ft):	17.6
Tip Elevation (ft):	-100.2

Legend	Meaning
TOC	Top of Casing
TOG	Top of Ground
TOS	Top of Shaft
BOC	Bottom of Casing
BOS	Bottom of Shaft
TOM	Top of Marl
WL	Water Level
SG	Strain Gage
OC	Osterberg Cell

DRILLED SHAFT LOG

Project:	SC 41 over the Wando River		
Data Source / Testing Firm:	GRL Engineers		
County:	Berkeley	**Load Test Type:**	APPLE
Load Test Number:	14	**Year Tested:**	2014

Shaft Part	Elevation (ft)	Diagram	Elevation (ft)	Unit Skin Resisance
TOC	14.0			
TOS	12.5			
TOG	7.0			
WL	2.5			
TOM	-10.0			
BOC	-13.0			
			-17.0	
				3.17 ksf
			-24.0	
			-24.0	
				3.45 ksf
			-31.0	
			-31.0	
				3.69 ksf
			-38.0	
			-38.0	
				3.87 ksf
			-44.0	
			-44.0	
				3.45 ksf
			-50.0	
			-50.0	
				2.87 ksf
			-56.0	
			-56.0	
				2.91 ksf
			-63.0	
BOS	-70.1			

Top of Casing Elevation (ft):	14.0
Bottom of Casing Elevation (ft):	-13.0
Diameter of Shaft (in):	72
Mud-line/Surface Elev. (ft):	7.0
Constructed Shaft Length (ft):	82.6
Top of Shaft Elevation (ft):	12.5
Tip Elevation (ft):	-70.1

Legend	Meaning
TOC	Top of Casing
TOG	Top of Ground
TOS	Top of Shaft
BOC	Bottom of Casing
BOS	Bottom of Shaft
TOM	Top of Marl
WL	Water Level
SG	Strain Gage
OC	Osterberg Cell

DRILLED SHAFT LOG

Project: SC 7 (Cosgrove Ave.) Replacement Bridge over CSX Railroad
Data Source / Testing Firm: Loadtest
County: Charleston
Load Test Type: Two Cell Osterberg
Load Test Number: 15
Year Tested: 2014

Shaft Part	Elevation (ft)	Diagram	Elevation (ft)	Unit Skin Resisance
TOG/TOC	25.9			
TOS	24.4		24.4	
WL	20.1			
				0.4 ksf
			-14.1	
SG 5	-14.1		-14.1	
TOM	-17.4			
BOC	-20.3			0.5 ksf
			-26.6	
SG 4	-26.6		-26.6	
				2.5 ksf
			-39.1	
SG 3	-39.1		-39.1	
				4.1 ksf
			-49.1	
OC	-49.1		-49.1	
				3.6 ksf
			-59.1	
SG 2	-59.1		-59.1	
				3.5 ksf
			-69.1	
SG 1	-69.1		-69.1	
				3.4 ksf
OC	-79.1		-79.1	
BOS	-85.1			

Top of Casing Elevation (ft):	25.9
Bottom of Casing Elevation (ft):	-20.3
Diameter of Shaft (in):	60
Mud-line/Surface Elev. (ft):	25.9
Constructed Shaft Length (ft):	109.5
Top of Shaft Elevation (ft):	24.4
Tip Elevation (ft):	-85.1

Legend	Meaning
TOC	Top of Casing
TOG	Top of Ground
TOS	Top of Shaft
BOC	Bottom of Casing
BOS	Bottom of Shaft
TOM	Top of Marl
WL	Water Level
SG	Strain Gage
OC	Osterberg Cell